2020

# Characterization of Naturally Derived Polymer by Oxidative, Thermal, and Spectrometric Methods

Ranen Roy
*South Dakota State University*

# CHRACTERIZATION OF NATURALLY DERIVED POLYMER BY OXIDATIVE, THERMAL, AND SPECTROMETRIC METHODS

BY

RANEN ROY

A dissertation submitted in partial fulfillment of the requirements for the

Doctor of Philosophy

Major in Chemistry

South Dakota State University

2020

DISSERTATION ACCEPTANCE PAGE

Ranen Roy

This dissertation is approved as a creditable and independent investigation by a candidate for the Doctor of Philosophy degree and is acceptable for meeting the dissertation requirements for this degree. Acceptance of this does not imply that the conclusions reached by the candidate are necessarily the conclusions of the major department.

Douglas Raynie
Advisor Date

Douglas Raynie
Department Head Date

Nicole Lounsbery, PhD
Director, Graduate School Date

THIS DISSERTATION IS DEDICATED TO MY FATHER AND MOTHER

# ACKNOWLEDGEMENT

The God is very glorious and mysterious. I am literally thankful for so many things in my life, but without God I would have nothing else to be thankful for. I am expressed my gratitude to God whatever he has done for me so far. After God, I am very much thankful for many peoples to fulfill my dissertation work successfully. I would like to put some nice word to acknowledge those people and their valuable contribution.

I would like to express my gratitude to my academic advisor, Dr. Douglas E. Raynie for his continuous support, guidance, training, mentorship, sharing his vast knowledge in the field of analytical chemistry, and encouragement all through. Without his unconditional support, and continuous enthusiasm, it would not be possible to finish my dissertation. I am also very much grateful to my committee members, Dr. Fathi Halaweish, Dr. Cheng Zhang, and Dr. Fereidoon Delfanian. I am very much thankful to them for their continuous support, guidance, motivation, feedbacks, and reviews.

I am eternally indebted to my parents Rakhal Chandra Roy and Manju Roy for their inspirations, encouragement, and prayers throughout my education. I am thankful to my brother Ramani Roy, my sisters Shefali Roy, Manorama Roy, and Erani Roy. I find no words to express my special thanks to my lovely wife Mukta Biswas and wonderful son Ervin Roy for their outstanding support me through my tough times. I also very grateful to my nephew's Amit Halder, Rudra Roy, Ankan Madhu, and Ritesh Roy. It would not be possible to finish my journey without their unconditional encouragement, support, and affection.

I like to express my special thanks to my all graduate lab mates for their help, support, and motivation. I am also very much grateful to the Department of Chemistry

and Biochemistry, SDSU for giving me the opportunity to pursue my higher education and financially supporting me throughout my education. I also like to thank to the Department of Pharmacy, Agricultural Engineering for granting me access to use their facilities and instruments. I also thankful to my all graduate friends for their support and help during my education.

This study was supported by the National Science Foundation EPSCoR Track II Dakota BioCon project for the North and South Dakota (Grant Nos. IIA-1355466 and IIA-1330842). The views and conclusions contained in this document are those of the authors and should not be interpreted as representing the official policies, either expressed or implied, of the National Science Foundation. National Science Foundation is authorized to reproduce and distribute reprints for their purposes notwithstanding any copyright notation herein.

CONTENTS

LIST OF FIGURES

# LIST OF TABLES

# LIST OF ABBREVIATIONS

$^{1}$H NMR …….Proton Nuclear Magnetic Spectroscopy

α …….Hydrogen Bond Donating Acidity Parameter

β ……..Hydrogen Bond Accepting Basicity Parameter

µg ……Microgram

µL ……..Microliter

µU ……..Micro Units

$\Delta T_f$ ……...Freezing Point Difference

°C …….....Degree Centigrade

% …….....Percentage

Acetone-d6…….Deuterated Acetone

AcChCl ……Acetylcholine Chloride

$cm^{-1}$…….……Per Centimeter

$CO_2$ …….....Carbon Dioxide

DCM ……..Dichloromethane

DES ……...…Deep Eutectic Solvent

DESs ……Deep Eutectic Solvents

$d_6$-DMSO ……Deuterated Dimethyl Sulfoxide

$D_2O$ ……....Deuterium Oxide

EBS……..EMIM Benzene Sulfonate

EEBS……..EMIM Labs

e.g. ……...Example

EHS ……..Environmental Health and Safety

EMIM …….....1-Ethyl-3-methylimidazolium

EMIMAc ……..1-Ethyl-3-methylimidazolium Acetate

ETS …….....EMIM Toluene Sulfonate

EtOH ...……..Ethanol

EXS …….....EMIM Xylene Sulfonate

FBS ...……Fetal Bovine Serum

FTIR ……Fourier Transform Infrared Spectroscopy

GC-MS…….Gas Chromatography Mass Spectrometry

G ……..Glycerol

g ……...Gram

HBA ……...Hydrogen Bond Accepting

HBD …….Hydrogen Bond Donor

HBDs ……..….Hydrogen Bond Donors

Hr …….…….Hour

IL ….…….....Ionic Liquid

ILs ….……...Ionic Liquids

PLA……. Poly Lactic Acid

kGy…….Kilo Gray

kcal mole$^{-1}$ ….……..Kilocalorie per Mole

kg ….…….....Kilogram

kj mole$^{-1}$ ….……...Kilojoules per Mole

M ……Molar

MeOH ……Methanol

mg …….Milligram

mg $g^{-1}$…….Milligram per Gram

MHz …….Megahertz

mL ……...Milliliter

mm ……...Millimeter

GPC……Gel Permeation Chromatography

NaOH...……Sodium Hydroxide

NMR ……Nuclear Magnetic Resonance Spectroscopy

OSHA ……...Occupational Safety and Health Administration

PCG ……...Prairie Cordgrass

Pet. Ether …….Petroleum Ether

RI …….....Refractive Index

RPM ……...Rounds Per Minute

$T_d$ ……Decomposition Temperature

$T_f$ ……Freezing Temperature

$T_g$……Glass Transition Temperature

$T_m$ ……Melting Temperature

THF …….Tetrahydrofuran

UV ……..……..Ultraviolet

UV-Vis …….…...Ultraviolet-Visible

VOC ……...Volatile Organic Carbon

Wt % …….....Percentage by Weight

# ABSTRACT

CHRACTERIZATION OF NATURALLY DERIVED POLYMER BY OXIDATIVE, THERMAL, AND SPECTROMETRIC METHODS

RANEN ROY

2020

Extensive use of fossil fuel for different purposes has resulted in significant depletion of it at an alarming rate. Therefore, a potential and sustainable alternative source are badly needed at this moment. Nowadays, lignocellulose biomass is appealing to much interest by the researchers because of its potential nature as a renewable carbon source. It is the most abundant renewable source which is composed of cellulose, hemicellulose, and lignin. Among them, lignin is considered the 2$^{nd}$ most abundantly natural polymer after cellulose which comprises 10-30 % of biomass depending on the source and the environment. Lignin is a three-dimensional cross-linked organic polymer, composed of three different phenylpropanoid units such as coniferyl, sinapyl, and p-coumaryl alcohols. Being a renewable and polyaromatic by nature, lignin is being considered as a potential source of a wide range of chemicals and renewable energy. But it is very important to understand the comprehensive structure of lignin before convert into value-added products. Therefore, our main aim is to characterize the naturally derived lignin by thermal, spectrometric, oxidative, and chromatographic techniques to understand the comprehensive structure and macromolecular features of lignin. To accomplish the goal, the objectives of this work are: 1. Optimize the processing conditions for the extraction of lignin from the non-wood source. 2. To investigate the

thermal stability and functional groups of lignin and its residue by thermal and spectrometric methods. 3. To study the molecular weight distribution, and monomeric structure of lignin and its residue by chromatography. 4. Oxidative degradation of lignin into monomers and to optimize the reaction conditions for conversion.

In **chapter II**, thermal behaviors of lignin and its residue after catalytic hydrodeoxygenation reaction were characterized by TGA and DSC. TGA results indicated that both lignin and its residue showed variable weight loss in different temperature ranges, different percentages of residual carbon, and different $DTG_{max}$ of the sample. Results showed that the weight loss of residue was lower than the lignin throughout different temperature ranges. But a higher percentage of residual carbon (45.85 %) was observed for residue than lignin (25.89 %). On the other hand, the maximum rate of weight loss ($DTG_{max}$) for residue was observed at a lower temperature at 420 °C than lignin at 480 °C. DSC results showed a lower melting point for residue(150.48 °C) than lignin (174.40 °C). Moreover, the lignin-residue decomposed at 370 °C, whereas no visible change was observed in lignin around this temperature. So, DSC and TGA analysis revealed that lignin residue was thermally less stable compared to lignin. Additionally, lower melting point with higher residual carbon for residue showed that both thermally stable and unstable compounds were produced during the hydrodeoxygenation reaction.

In **chapter III**, chemical structure, functional groups, and molecular weight of lignin and residue were investigated by FTIR, NMR, and GPC analysis. FTIR study, showed both lignin and residue contain the same functional group, and no further new band was noticed, which suggests residue still contains unreacted lignin or smaller

breakdown products with similar chemical properties of lignin. NMR analysis also showed the same chemical functional group present in both lignin and residue. But the quantitative study of NMR showed a different amount of the functional groups. It was shown that lignin is higher in aromatic proton where the residue is higher in the aliphatic proton. Results also showed, aliphatic/aromatic ratio of the residue is 3 times greater than the lignin. The higher aliphatic/aromatic ratio of residue demonstrated that the significant number of aromatic moieties of the lignin have gone with the reaction mixture leaving the aliphatic moiety in the residue. On the other hand, GPC analysis found three distinct peaks for lignin and two for residue. The greater molecular weight distribution and polydispersity were observed which indicated the formation of C-C bonds during the catalytic reaction. The study showed that this kind of bond formation is related to the guaiacol units which are connected to each other at elevated temperature.

In **chapter IV,** lignin and its residue were depolymerized by cupric oxide oxidation and monomeric products were identified and quantified by GC-MS analysis. A chromatographic study showed that lignin produced four monomers and residue produced two monomers, respectively where all of them are characterized as a G moiety. Among the phenolic monomers, vanillin was the major product for both samples. Additionally, the results showed residue contains less amount of vanillin and acetovanillone than lignin and no peaks for guaiacol and homovanillic acid. Oxidative depolymerization of lignin was also carried out at different temperatures and times to optimize the reaction conditions for better yield. The chromatographic study showed four monomers produced in each condition. Among them, vanillin was found as a major product and production of vanillin increased with the increase of both temperatures and times. The production of

guaiacol and acetovanillone increased when the temperature reached 150 °C and time at 2 hours then slightly decreased with the increase of both temperature and time. But the production of homovanillic acid significantly decreased when the temperature reached 175 °C but slightly decreased when time reached 2.5 hours. Therefore, our oxidative study found 150 °C and 2.5 hours as an optimization conditions for the better production of phenolic monomers from lignin.

In **chapter V,** lignin was extracted from wheat straw using an accelerated solvent extraction technique. To optimize the extraction conditions, extraction was carried at three different temperatures such as 140 °C, 170 °C, and 200 °C and two different acidic conditions 0.05% and 0.1% for 60 minutes. Then the extracted lignin was characterized by TGA, FTIR, and subcritical water. The study showed that extraction of lignin increased from 13.89 % to 28.69 % when the temperatures increase from 140 °C to 200 °C. But acid concentration showed very little impact on extraction of lignin. It was shown, extraction of lignin increased slightly with the increases of acid concentration at a specific temperature. On the other hand, characterization of lignin with TGA, FT-IR, and liquefaction showed the similar result with the commercial lignin, indicated lignin was successfully extracted from wheat straw. Liquefaction of lignin followed by GC-MS analysis showed 9 phenolic monomeric products with 86% total relative amount.

# CHAPTER ONE

# INDRODUCTION

## 1.1.Background

In our everyday life, we are using different types of value-added products such as materials, chemicals, and fuels and energy where most of them are produced from fossil fuel resources such as oil, natural gas, and coal[1-2]. Fossil fuels are nonrenewable and the production of various materials from petroleum sources has increased every day. According to "British Petroleum Statistical Review of World Energy 2019" the present reserve of oil is 1688 billion barrels, natural gas is186 trillion cubic meters and coal is 892 billion tons were shown in **Figure 1.1**[3]. At present, the yearly consumption of these fossil fuels is about 1%. Therefore, the coal will be finished by 114 years, the natural gas will be finished by 53 years and the last drop oil will be finished by 51 years[3]. The depletion of fossil fuels at an alarming rate has increased the global concern throughout the world community which pushes the community to find out a suitable replacement. Therefore, the gradual depletion of fossil fuels has created research opportunities throughout the world on sustainable energy and the development of different types of chemical resources[4]. Nowadays many countries are looking towards different biofuels, biomaterial, renewable feedstock, and sustainable green energy sources such as hydropower, wind energy, solar energy, and different types of lignocellulose biomass including corn, sugarcane, wood, and different types of grasses[5].

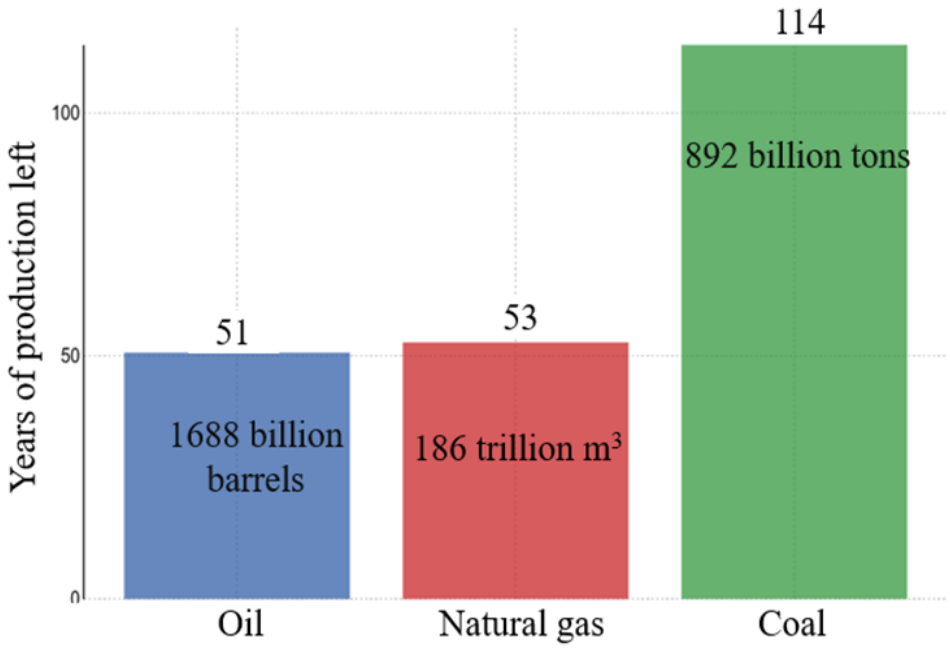


**Figure 1.1.** Years of fossil fuels left worldwide based on "BP Statistical Review of World Energy 2019"

Among these, Lignocellulose biomass is considering one of the very important sustainable resources which are now appealing more interest by the researchers because of its potential as a renewable carbon source. Lignocellulose is a complex biopolymer which is mainly available on plant cells, composed of three different polymer, such as cellulose, hemicellulose, and lignin[6]. Percent quantities of lignocellulose compounds is depending on the age of plants, environment, and harvest season, etc.[7]. Every year about 200 billion tons of lignocellulose are being produced throughout the world[7-8]. The lignocellulose biomass already has been proven as a significant raw material for its conversion into different types of biofuel as well as value-added products. It offers many possibilities to produce energy as a form of biofuel as well as different types of value-added products due to its potential chemical composition[9]. The conversion of lignocellulose into value-added products usually goes through various pretreatment process to separate them into its components such as

cellulose, hemicellulose, lignin, and protein and oils[10]. The biorefineries industry and pulping industry are producing different types of liquid biofuel by using the sugar part like cellulose, hemicellulose, or oil part where lignin is considered as a waste material in biorefineries industry. Every year about 70 million tons of lignin are being produced by those industries and among them, only 1-2% is used for different purposes[11-12]. Therefore, lignin is being considered as a low value product nowadays. But being a polyaromatic in nature, lignin is chemically like petroleum which makes it a promising source of various sustainable products and chemicals.

Lignin is a complex, cross-linked, highly branched aromatic polymer which is formed by the polymerization of three different phenylpropanoid units through ether and carbon-carbon linkages. Therefore, it is very hard to elucidate the complete structure of lignin by a single method. In recent years, numerous studies have been performed on lignin-blended and lignin materials, still, its complete structure and chemical nature have not been explored properly[13]. In this research works, different types of thermal and structural degradative and nondegradative methods are used to elucidate the comprehensive structure of lignin. Thermal analysis is a well-proven degradative technique which is widely used to determine the physical and chemical properties[14] of lignin as a function of temperature. But this method has some sort of limitations which provide only partial chemical information of complete polymer structure leading to artifacts the complicated data analysis. On the other hand, infrared spectroscopy along with nuclear magnetic spectroscopy techniques reveal the complete structure of lignin. Nuclear magnetic spectroscopy provides quantifiable data based on the lignin structure to determine the functional groups and interlinkages present in the lignin. Additionally, catalytic

degradation methods selectively break down the ether linkages of the lignin polymer and produce various types of monomers which determine the quantitative amount of each monomers present in the lignin. In our present work, we have performed thermal, structural, chromatographic, catalytical liquefaction along with oxidative techniques on lignin and the residue to understand the comprehensive macromolecule structure of naturally derived lignin as well as poly lactic acid.

**1.2.Lignin**

Lignin is a class of organic polymer, which is a very complex, crosslinked, and highly branched aromatic polymer. Lignin is an amorphous irregular biopolymer that is a major structural component of the secondary cell wall of vascular plant cells mixed with cellulose and hemicellulos[15-17]. In vascular plant cells, lignin occupies the free space among cellulose and hemicellulose and crosslinked with them which form a rigid structure. It plays an important biological role by conducting water and nutrient materials in plant stems.

Lignin is the 2$^{nd}$ most abundantly natural polymer after cellulose and its proportion varies from 15-35% of the total of biomass depending on the age, environment, and sources of the biomass. It does not have any repetitive monomeric unit which makes it distinct from other polymer likes cellulose and hemicellulose. Lignin has a helical structure which is polymerization by three different phenyl propane monomeric units namely p-coumaryl alcohol (H), coniferyl alcohol (G), and synapyl alcohol (S). The phenolic monomers are interconnected with each other by different types of ether and C-C linkages such as β-O-4 (45%-60%), 4-O-5 (2%-10%), 5-5 (5%-25%), β-5 (5%-25%), β-1 (2%-10%), β-β (2%-10%) bonds which is depend on their botanical source[13, 18-20].

A French scientist named Anselme Payen who was the first person to attempt to bring out lignin materials from the woods. In 1838, he treated the wood with concentrated nitic acid and sodium hydroxide and obtained one soluble portion and another insoluble solid portion. The insoluble solid materials was named as a "cellulose"[21-22]. He also pointed out that soluble portion is rich in carbon than cellulose and named as "incrusting materials"[22]. F. Schulze who supported Payen's "incrustation hypothesis" which also supported by Konig, Wislicenus and very recently by Freundenburg. Payen, in 1865 named the richer carbon "incrusting materials" as a lignin. The word "lignin" was coming from the Latin word "lignum" which meaning is wood. After 30 years, in 1897 Swedish Chemist named Johan Peter klason studied the lignin structure and pointed out that lignin is constituted by coniferyl alcohol monomers. After that early of 1900's, he proposed that lignin is a macromolecule compound which is constitutes by coniferyl alcohol moieties linked through ether linkages[21].

### 1.3.Monomers of Lignin

Lignin compound is composed of three different monomers where the basic units have randomly combined each other through a wide range of ether and carbon-carbon bonds. The name of three monomers is p-coumeryl alcohol (H-moiety), coniferyl alcohol (G-moiety) and sinapyl alcohol (S-moiety)[23] which are shown in **Figure 1.2**. The monomers are aromatic in nature and called phenylpropanoid monomeric units. In lignin structure, they link by each other through the propane side chain where the monomers differ from each other by methoxy groups. H moiety does not have any methoxy groups, but G and S moiety has one and two, respectively. During polymerization of lignin, the three

monomers connect each other through free radical reaction and form a three-dimensional complex compound. The combination and the composition of monomers in lignin are depending on the nature of soil, weather conditions, plant age, and extraction and isolation methods[11, 24]. In hardwood species lignin, G, and S moieties are present in different quantities, although S units tend to be the plentiful. On the other hand, in softwood species lignin, G units are the most abundant ones while, in grass lignin, all three are usually present [25].

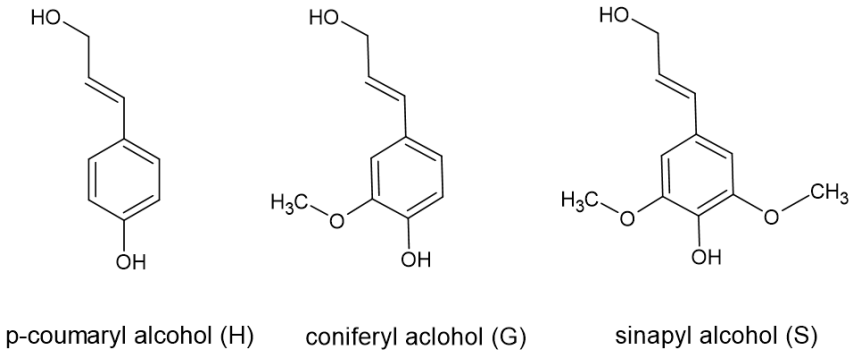


**Figure 1.2.** Structure of lignin monomers.

The structural information of lignin monomers is described using two different nomenclature. The nomenclatures are shown in **Figure 1.3,** where (A) shows the IUPAC nomenclature of lignin and (B) shows wood chemistry nomenclature of lignin. Both nomenclatures are based on C9 unit part of the aliphatic side chain, which represents the phenylpropanoid monomeric units. The phenylpropanoid unit is differed by the methoxy group substitutions at C-3 and C-5 position of aromatic ring where the aliphatic side chain always attached to the C-1 position of aromatic ring. The main difference between the two

nomenclature is IUPAC naming uses the numbers 7, 8, and 9 and uses α, β, and γ for the wood chemistry nomenclature for the positions of side-chain carbons.

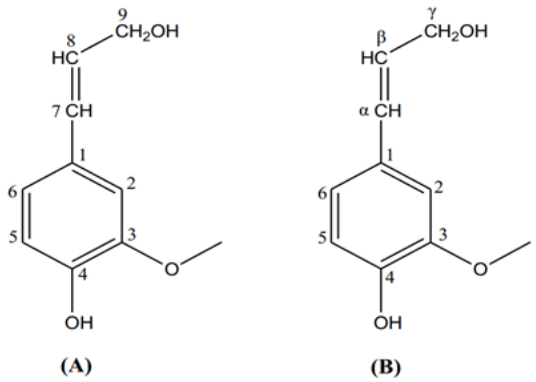


**Figure 1.3.** (A) IUPAC nomenclature and (B) Wood chemistry nomenclature of lignin monomers.

### 1.4.Polymerization of monomers and linkages

Lignin is a generic term for a large group of aromatic polymers which is synthesized through oxidative coupling reaction of its monomers[23]. Lignin polymers mainly produce in the cell walls plant and covalently bonded to cellulose and hemicellulose making the wall rigid and impermeable. At first, Erdtmann proposed the idea that macromolecular lignin is produced from the oxidative coupling reaction of phenoxy radicals where the radicals are come from coniferyl alcohols[26]. After Erdtmann, Freudenberg established coupling reaction is initiated by peroxidase/$H_2O_2$ or laccase/$O_2$ which leads to the formation of phenoxy radical[27]. Phenoxy radical generates from the phenolic hydroxyl group of coniferyl alcohol by the oxidation reaction. The reaction starts by the abstraction of an electron from the phenolic group and then the unpaired electron of phenoxy radical delocalizes among five different resonance positions O-4, C-1, C-3, C-5, and C-β shown in **Figure 1.4**[28]. This phenoxy radical further initiates the formation of lignin.

The five different radicals combine each other through different types of linkages and form lignin macromolecular structures where the linkages depend on different types of factors such as solvation, steric, and electronic effects. The formation of the macromolecular structure of lignin can be initiated by a dimer formation through the coupling reaction, then trimer by adding another radical and finally the lignin structure through a continuous process.

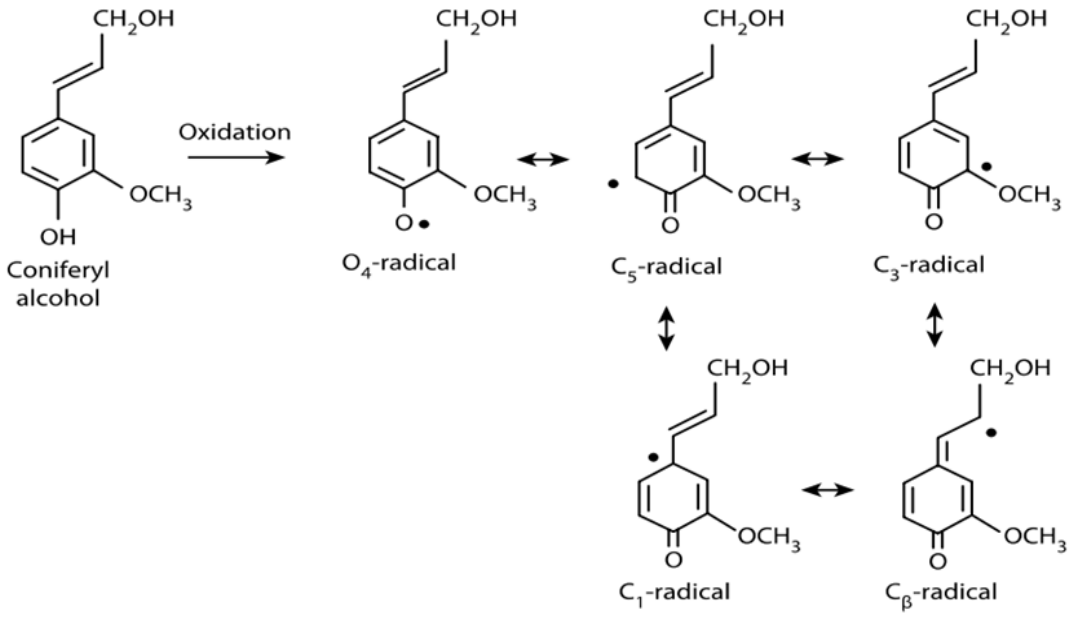


**Figure 1.4.** Resonance structure of coniferyl alcohol formation during polymerization of lignin[28]

Among the five radicals, C-β is considered the most reactive phenoxy radicals which leads to the formation of different linkages among the monomer's unit such as *β*-O-4, *β*-5, *β*-1, and β-β linkages. The linkages *β*-O-4 is called arylglycerol-β-aryl ether linkages which is the most abundant linkages in lignin, and the percentage is more than 50 percent in terms of relative amount. Following **Figure 1.5** is showing the stepwise formation of *β*-

O-4 linkage. Besides *β*-O-4 linkage, lignin structure also contains some other linkages in a different amount such as α-O-4, 4-O-5, *β*-5, *β*-1, and β-β linkages shown in **Figure 1.6**

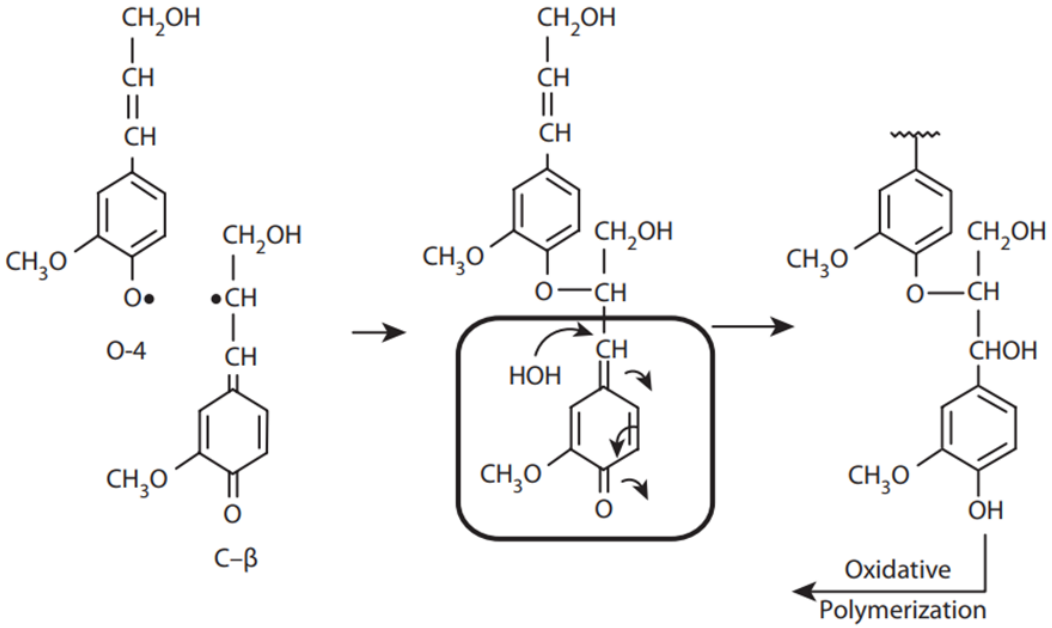


**Figure 1.5.** *β*-O-4 bond formation through coupling reaction.

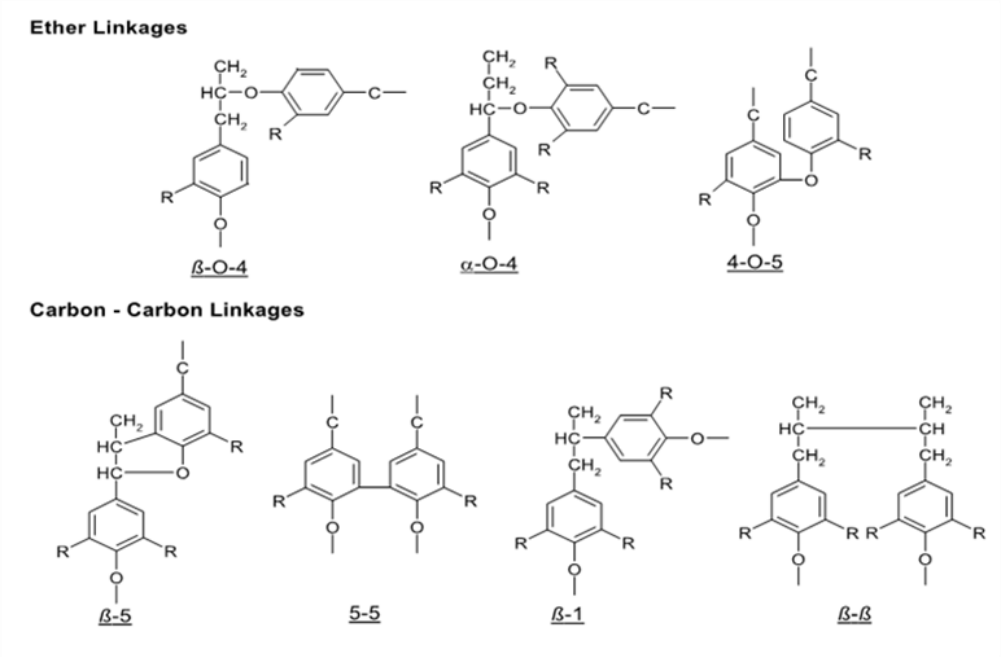


**Figure 1.6.** Structure of linkages present in Lignin.

### 1.5. Subcritical water based hydrotreatment of Lignin

Like cellulose and hemicellulose, Lignin is one of the major components in lignocellulose biomass. Being a crosslinked polymer lignin interferes with the hydrolysis reaction of polysaccharides. The biorefinery, paper and pulp industries mainly focus on easily convertible cellulose and hemicellulose to produce different types of value-added products. Therefore, lignin has been isolated in large quantities in the biorefinery, paper, and pulp industries to produce their target products. Isolated lignin is underutilized because it is very difficult to convert into useful biochemicals. But lignin is polyaromatic in nature and chemically like petroleum rather than other biomass[29]. Therefore, proper handling of lignin would be a great source of phenolic compounds which potentially could replace the use of petroleum products.

In recent years, several methods such as oxidation, pyrolysis, hydrolysis, hydrothermal gasification, and hydrothermal depolymerization have been used to depolymerize the lignin to produce different types of value-added products such as resins, coatings and the phenolic additives for food and pharmaceuticals[30].

Hydrothermal depolymerization is a hydrogenolysis method carries out in the presence of subcritical water and catalyst. Subcritical water is a special form of water that exists between the normal boiling point 100 °C, and the critical temperature of 374 °C indicated in **Figure 1.7.**[31]. Hydrotreatment usually performs at a temperature range of 200 °C - 374 °C and pressure range 10 - 25 MPa. Subcritical and supercritical water shows a unique property e.g. ionic product, and dielectric constant[32]. The density of subcritical water compare to normal water decreases from 1000 kg/m$^3$ at room temperature to 820 kg/m$^3$ at 250 °C and 25 MPa[33]. The decreases of density result in, to decrease the viscosity and increase the solubility of hydrophobic compounds. As a result, the solubility of hydrophobic lignin increases at temperature 250 °C which helps to transform the lignin into its useful products. Though a significant change of water density has been observed at high temperature and pressure, high temperature e.g. 250 °C or above leads to the formation of char/carbon, increase the corrosion of the reaction vessel, salt precipitation, damage of the catalyst, and increase the chance of repolymerization[34]. Therefore, this method requires expensive alloy in the reactors and the high operating makes (pressure and temperature) makes the process expensive. But the conversion of lignin subcritical water along with optimized procession conditions could make this process more viable and economically feasible.

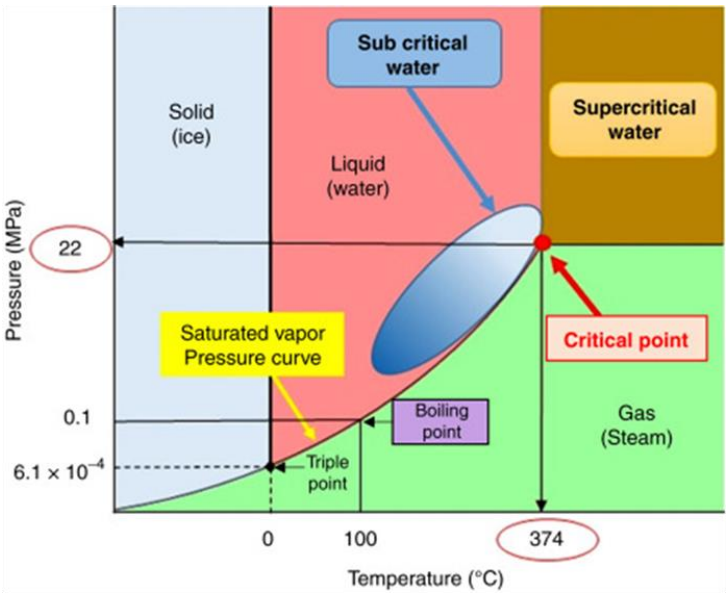


**Figure 1.7.** Change of water properties under different temperatures and pressures[31].

### 1.6.Polymer of Lactic Acid (PLA)

Polylactic acid is a polymer of lactic acid. It is biodegradable and biocompatible which is derived from renewable sources such as corn starch, cassava roots, and sugarcane[35]. Therefore, it has been received much attention from researchers as an alternative biodegradable polymer because of its wide range of applications in biomedical, food packaging, and agricultural fields[35-36].

Poly Lactic Acid is a linear aliphatic thermoplastic polymer that is produced by ring-opening polymerization of two main monomers lactides and lactic acid obtained by the fermentation of sugar feed stocks[35]. Ring-opening polymerization is considered the most common route where lactide reacts with the different metal catalysts in solution or as a suspension. The metal-catalyzed reaction goes through racemization of PLA which reducing the stereoregularity than initial starting materials[37]. On the other hand, PLA is

also produced by the condensation of lactic acid monomers. In this reaction, one mole of water is produced for every condensation (esterification) step. This condensation reaction is reversible which means the removal water is required to generate high molecular weight species[38].

Commercially produced polylactic acid are copolymers of poly (L-lactic acid) (PLLA) and poly (D,L-lactic acid (PDLLA), which are produced from L-lactides and D,L-lactides, respectively. The physical properties of PLA such as melting temperature and crystallinity influenced by the ratio of L- and D,L- enantiomers. PLA also can show classical crystallization property during both heating and cooling which mainly depends on its molecular weight[39-40].

Polylactic is thermally unstable and show rapid loss of molecular weight because of thermal treatment with the increase of temperatures. PLA tends to degrade during thermal treatment because the ester linkage is unstable at high temperatures. Degradation of PLA starts at a lower temperature than the melting point but above the melting point, degradation increases rapidly. It has been postulated that thermal degradation mainly occurs by the random breakdown of main chain but several reactions such as hydrolysis, depolymerization, and oxidation are also responsible for the degradation of polymer during thermal treatment[41-42]. In addition, other factors such as moisture content, crystallinity, molecular weight, and molecular weight distribution are responsible for the degradation of polymer[43].

### 1.7.Pretreatment of lignocellulose biomass

The cell of a plant is mainly the source of biomass which is composed of three major polymers such as cellulose, hemicellulose, and lignin along with a small amount of fat, wax, salt, minerals, etc. The percentage of major components depends on the source, environment, and the age of the plant[44-45]. Cellulose is a polymer of glucose and hemicellulose is a polymer of pentose sugars, therefore cellulose and hemicellulose are considered the potential source of fermentable sugars and biofuels. On the other hand, lignin is a crosslinked complex polymer which is rich in phenolic compounds. But due to the complex structure, it is very difficult to ferment during the process of paper from wood. Therefore, lignin is considered as waste materials or underutilized materials.

Pretreatment prior to the conversion of lignin plays an important role to produce different types of value-added products. Different types of pretreatment methods are being used to breakdown the crosslinkages between lignocellulose materials to separate into carbohydrate and lignin[46]. These methods include physical, mechanical, chemical, biological, and thermochemical which are used to increase the surface area of materials for sufficient contact to the enzymes, reduction of the degrees of polymerization, and crystallization of polymers[47].

In our study, we are using the organosolv chemical pretreatment method to separate the lignin from the lignocellulose biomass. In this method, we used sulfuric acid which acts as catalyst responsible to break down the linkages between lignin and carbohydrate and improve the extraction efficiency. On the other hand, a mixture of organic solvents is used to dissolve the lignin.

### 1.8.Purposes of this study

The aim of this study is to characterize the naturally derived polymers such as lignin and polylactic acid. Lignin is a very complex organic polymer and very difficult to understand its structure by a single method. Therefore, in this study lignin was characterized by using thermal, oxidative, chromatographic, and spectrometric methods to develop a comprehensive picture of lignin structure for better understanding. In thermal methods, lignin samples were subjected to a control temperature program. In these techniques, sample temperature is increased or decreased at a constant rate and physical and chemical changes of the substances are monitored as a function of temperature. In spectrometric techniques, samples were subjected to magnetic resonance and spectra. The magnetic resonance and spectra confirm the identity and estimation of various functional groups and interunit linkages present in the samples. On the other hand, in oxidative techniques, cupric oxide (CuO) was used as oxidant. Cupric oxide selectively cleaves the ether linkages and degrades the samples into its monomeric products and gas chromatography of the product mixture helps to identify and determine the structural moieties present in the samples. In addition, gel permeation chromatography (GPC) is one of the highly useful techniques which helps to investigate the molecular weight distribution of polymers e.g. lignin[48].

Poly lactic acid (PLA) is also another type of naturally derived polymer. In this research, thermal performance of PLA was examined after subjected to different kiloGray of gamma radiation from a Cobalt-60 irradiator.

Thus, the hypothesis for our research is that a combination of thermal, oxidative, Chromatographic, and spectrometric techniques will be helpful for

understanding comprehensive structure of lignin, its type of moieties, and interunit linkages between the monomers as well as the thermal properties of polylactic acid after subjected to different kilo Gray of gamma radiation from a Cobalt-60 irradiator. So, the specific objectives for the proposed study are:

1. Investigation and better understand the catalytic hydrodeoxygenation reaction of lignin by comparative structural characterization of its residue using thermal, spectrometric, oxidative, and chromatographic techniques.

   To fulfill the first objectives there are sub-objectives which are:

   I. To determine the thermal performance like glass transition temperature, melting temperature, decomposition temperature, percent weight loss of lignin samples by using thermogravimetric analysis (TGA), and differential scanning calorimetric (DSC) analysis.

   II. Analysis of functional groups, interunit linkages present in lignin samples by instrumental techniques such as Fourier transforms infrared (FTIR) spectroscopy, nuclear magnetic resonance (NMR) spectroscopy.

   III. Quantitative monomeric and molecular weight distribution studies by chromatography.

   IV. Investigation of molecular weight distribution of lignin by gel permeation chromatography (GPC)

2. To identify the glass transition, melting, decomposition, and crystallization temperatures, range of peak temperature, and percent of weight loss of

samples after different gamma irradiation using thermogravimetric analysis (TGA) and differential scanning calorimetric (DSC) analysis.

3. Optimize the reaction conditions for cupric oxide oxidation of lignin at different temperatures and times followed by GC-MS analysis.
4. Characterization of the lignin extracted from wheat straw biomass under optimized reaction conditions using thermal, spectrometric, and hydrothermal treatment

# CHAPTER TWO

# THERMAL CHARACTERIZATION OF POLYMER

## 2.1.Thermogravimetry Analysis (TGA)

### 2.1.1. Introduction

With the change of heat, materials undergo several types of physical and chemical changes. These changes represent diverse types of data which help to identify and characterize those materials. Several types of thermal analysis are widely used to determine the physical and chemical properties of polymer. Thermogravimetry analysis (TGA) is a well-proven widely used technique to determine the physical and chemical properties of the polymers as a function of time where the samples are subjected to an isothermal or a predetermined temperature program in an inert atmosphere[14]. With the change of temperature, the polymer sample undergoes various physical and chemical changes and the instrument measures the amount of weight loss and rate of weight loss as a function of time or temperature[49]. This instrument is especially useful for the study of polymeric materials, including thermoplastics, thermosets, elastomers, composites, films, fibers, coatings, and paints. On the other hand, it is used to measure the thermal/oxidative stability, reaction mechanism, compositional properties, and phase transformation during the heating[50]. Besides that, this technique also able to monitor the exact temperature where diverse types of heterogeneous reactions have occurred.

Thermogravimetry analysis gives two different types of thermogram like TG and DTG. The TG thermogram denotes % weight loss of the sample as a function of temperature, whereas the DTG thermogram is the $1^{st}$ derivative of TG thermogram

denoting the rate of weight loss as a function of temperature. The maximum peak of the DTG thermogram is denoted as a $DTG_{max}$ can be expressed as a single thermal decomposition temperature which can be used to compare the thermal stability of different materials[18].

In recent years, many researchers had done the thermal characterization of various categories of lignin to understand the thermal behavior at various temperatures. Up to now, there are lots of data are available on the study of thermal behavior of various lignocellulose materials[51-52] and lignin blended materials[53-55]. In several studies thermal and decomposition behavior of different natural sources such as paddy straw, rich husk, oil palm shell, lignin, different types of cellulose mixture, poplar, and pine were studied by thermogravimetry analysis[56-58]. Till date, there is only limited data on the thermal behavior of pure lignin. But, to the best of my knowledge, the comparative thermal study of lignin and its residue after hydrothermal treatment has not been studied widely. Consequently, the thermal study of the residue after the hydrothermal reaction is very important. Therefore, the key objectives of our study are 1. To understand the inclusive knowledge about the thermal degradation of lignin residue and lignin, 2. To compare the % weight loss as a function of temperature at different thermal degradation stage, 3. To determine the maximum rate of weight loss temperature, 4. To compare the thermal stability of lignin-residue with the lignin itself.

### 2.1.2. Materials

In our study alkali lignin, from Sigma-Aldrich (St. Louis, MO) and lignin residue after catalytic hydrothermal reaction at 240 °C were used as a sample and Tzero aluminum pans, from TA instruments (New Castle, DE) was used.

### 2.1.3. Method

The thermogravimetry analysis of lignin samples was carried out by using TG/DTA 220 from Seiko Instruments (Tokyo, Japan) with an aluminum reference pan. About 10 mg of samples were taken in a TGA pan for analysis. The oven temperature was performed from room temperature to 575°C at a constant heating rate of 10 °C/min. Nitrogen gas was used as a carrier gas at a flow rate of 20 mL/min to maintain an inert atmosphere and to avoid the samples to contact with the air and helps to sweep the pyrolysis gas such as $H_2$, $CO_2$, CO, $CH_4$, $C_2H_2$ and water vapor from the system which is responsible for the vapor phase interaction with the samples[59].

### 2.1.4. Results and Discussion

Thermal decomposition behavior of the lignin and its residue was measured from 25°C to 560°C at a heating rate of 10°C/min in a nitrogen atmosphere. **Figure 2.1.** shows the TGA curves of lignin and its residue. **Figure 2.2.** shows the DTG curve of lignin and its residue on the other hand, **Table 2.1.** and **Table 2.2.** show the various degradation stages at different temperature range, its corresponding peak and weight loss, maximum thermal decomposition temperature, and residual carbon at 560 °C for pure lignin and its residue, respectively.

The DTG curves of both samples show four peaks. The 1st peak in the temperature range of 25-175˚C is mainly due to the evaporation of free and bound water in the samples[14]. Therefore, the initial weight loss for lignin and residue is almost similar which are 1.35% and 1.82%, respectively. A very small DTG peak is shown in this region because of very slow weight loss during the drying stage.

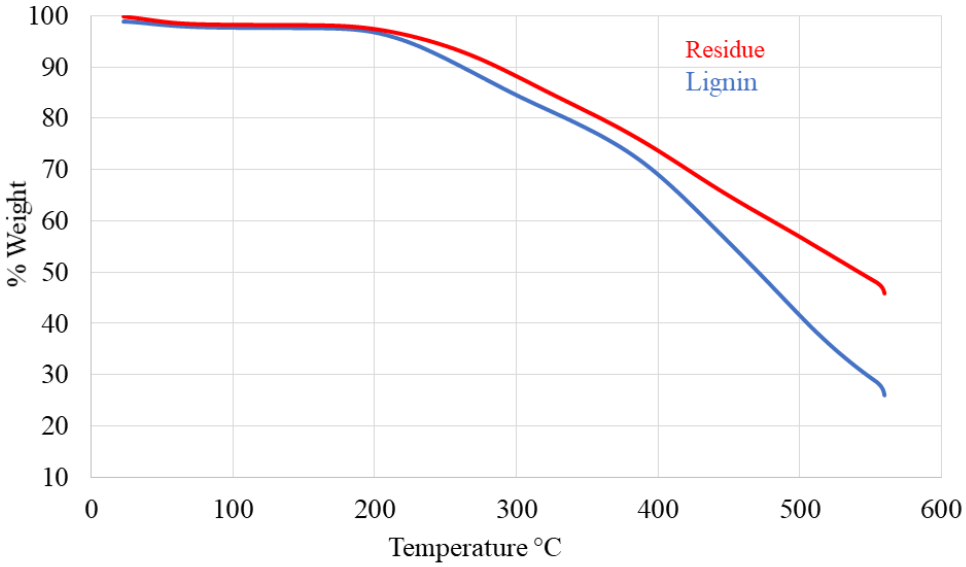


**Figure 2.1.** TG curves of lignin and its residue from room temperature to 575°C at a constant heating rate of 10 °C/min in $N_2$.

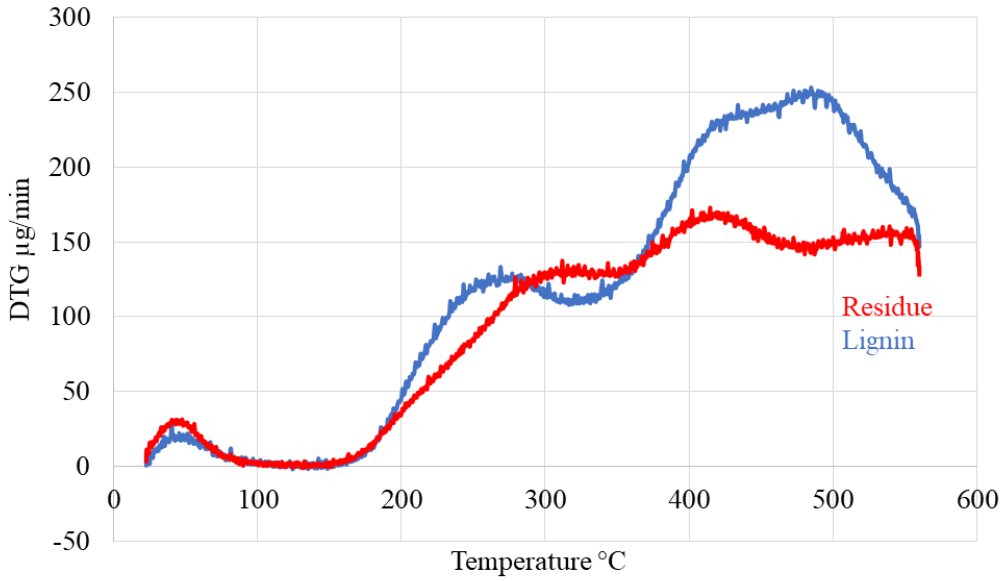


**Figure 2.2.** DTG curves of lignin and its residue from room temperature to 575°C at a constant heating rate of 10 °C/min in $N_2$.

The first stage of degradation for the lignin started at 175 °C and continues up to 320 °C while for the residue, 1st degradation started at 175 °C and continues up to 360. The weight loss during the 1st stage for lignin and its residue is 15.54% and 14.52%, respectively which indicates residue thermally behaves slightly differently compared to the lignin. In this region, the mass loss is due to the devolatilization of the functional groups present in samples[60].

Most of the weight loss occurred in the 2nd stage. Both of the samples start degrading at a higher rate due to the continued degradation of functional groups present in the samples, and breakdown of the sidechain of the samples[61]. The initial weight loss starts with the breakdown of β-O-4 linkage[62] and the formation of a monomeric phenolic compound while the cleavage begins at 250 °C and continues up to 400 °C. The

degradation is observed at a temperature range of 320-500 °C for lignin and 360-500 °C for lignin-residue with the weight loss of 40.33% and 29.24%, respectively. The highest peak or $DTG_{max}$ is observed at 480 °C and 420 °C for lignin and lignin-residue, respectively which demonstrates that, maximum weight loss is occurred at temperature 480 °C and 420 °C, respectively.

The third stage of degradation occurred at a temperature range from 500-560°C for both the samples. In this region, weight loss is due to the degradation of aromatic compounds and the formation of char[63-64]. After 560 °C the samples begin to nonvolatilized by forming char where the aromatic structures of lignin compound start to be condensed [18, 65]. At this point, most of the elemental hydrogen and oxygen are liberated as a gaseous, leaving only carbon as a residual carbon[66]. The percentages of mass remained after reaching 575 °Care 25.89% and 45.85% for the lignin and lignin residue, respectively.

**Table 2.1.** Degradation stages of the lignin in the TG and DTG curves.

| Degradation stage | Peak no | Temperature range °C | Mass loss (%) | $DTG_{max}$ | Residual C % |
|---|---|---|---|---|---|
| Loss of moisture | 1 | 22-175 | 1.35 | - | - |
| 1st | 2 | 175-320 | 15.54 | - | - |
| 2nd | 3 | 320-500 | 40.33 | 480 | - |
| 3rd | 4 | 500-560 | 15.62 | - | - |
| Residual carbon | - | After 560 | - | - | 25.89 |

**Table 2.2**. Degradation stages of the residue in the TG and DTG curves.

| Degradation stage | Peak no | Temperature range °C | Mass loss (%) | $DTG_{max}$ | Residual C (%) |
|---|---|---|---|---|---|
| Loss of moisture | 1 | 22-175 | 1.82 | - | - |
| 1st | 2 | 175-360 | 14.52 | - | - |
| 2nd | 3 | 360-500 | 29.24 | 420 | - |
| 3rd | 4 | 500-560 | 10.41 | - | - |
| Residual carbon | - | After 560 | - | - | 45.85 |

In case of the lignin residue, a higher percentage of residual carbon remained after 575 °C. This may be due to the formation of stable compound from condensation during the hydrothermal liquefaction reaction[67].

### 2.1.5. Conclusion

In this study, the thermogravimetry analysis was carried out on lignin and lignin-residue. Both of the TGA and DTG curves for the samples follow a similar pattern, although slightly different temperature ranges are showed in the degradation of each sample by the DTG curve along with a different percentage of weight loss, and the residual mass values present in the samples. Our studies are in good resemble with the studies of various lignin and biomass pyrolysis studies[60-61]. Significant weight loss occurs in three states, with the maximum weight loss occurring in the 2nd stage for both lignin and lignin-residue. The weight loss during the three stage is due to the loss of various functional group. It is also showed that weight loss of lignin is significantly higher than the lignin-residue throughout the three stages. The lower weight loss of the lignin -

residue demonstrates the condensation or formation of stable components during the hydrodeoxygenation reaction. The higher percentage of nonvolatile residual carbon left over for the lignin residue (45.85%) compare to lignin (25.89%) also agree with the previous statement that the lignin residue contains thermally stable compounds which is produced during the hydrodeoxygenation reaction. But the DTG curve shows the higher $DTG_{max}$ value for lignin (480 °C) compare to lignin-residue (420 °C). This value suggests that thermally fewer stable compounds are also produced during the hydrodeoxygenation reaction which degrades comparably at a lower temperature.

## 2.2. Differential Scanning Colorimetry

### 2.2.1. Introduction

Differential scanning calorimetry (DSC) is another type of thermo-analytical technique using to measure the necessary energy to establish a nearly zero temperature difference between a substance and an inert reference material. It is a most widely used thermal technique to determine the glass transition[24, 68], melting, decomposition, and crystallization temperature of different types of amorphous polymer e.g., lignin[24, 68]. In this process, physical and chemical changes of the substances are monitored as a function of temperature. Aluminum and platinum are used as reference material to analyze the precise heat capacity of a material. To measure the phase transition of a sample, comparably less or more heat flow requires to maintain the same temperature compared to the reference material. This difference of heat flow at different temperature permits to determine the glass transition, melting, degradation temperature of materials.

With the increase of temperature polymer materials undergoes transformation to a rubbery state from a glassy state. The temperature at which this transformation occurred is called glass transition temperature ($T_g$) which is one of the fundamental characteristics of the amorphous portion of the semi-crystalline materials like lignin[69]. In addition, DSC analysis also widely used to measure the melting, decomposition, and crystalline temperatures.

In recent years, much research has been completed to understand the thermal characteristics of lignin for efficient application. In several studies, glass transition, melting, and decomposition temperatures of bagasse lignin, steam explosion lignin, Kraft lignin, alkali lignin, grass lignin, organosolv lignin, and lignin-blended material were determined by using DSC analysis[18 70-72]. But there is not enough or no data available for the glass transition, melting, and decomposition temperature of several types of lignin-residue after hydrothermal treatment. Therefore, the main objective of our DSC analysis is to determine the glass transition, melting, and decomposition temperature of residue and compare it with lignin.

### 2.2.2. Materials

In our study alkali lignin, from Sigma-Aldrich (St. Louis, MO) and residue after catalytic hydrothermal reaction at 240 °C were used as a sample and Tzero aluminum pans from TA instruments (New Castle, DE) was used.

### 2.2.3. Method

Differential scanning calorimetry (DSC) analysis was carried out by using a DSC Q-200 differential scanning calorimeter from TA Instruments (New Castle, DE). About 7-10 mg of sample was weighted in a $T_{zero}$ aluminum pan for analysis with a reference. Nitrogen gas with a flow rate of 20 mL/min was used as a carrier gas to maintain an inert atmosphere throughout the system. To determine the obvious glass transition temperature the lignin samples were heated from room temperature to 110 °C at a heating rate of 10 °C/min to remove any moisture present in the samples and cooled down to room temperature to nullify the prior thermal history. After that, the lignin samples were heated again from room temperature to 400 °C at a constant rate of 15 °C/min. Finally, the data were analyzed with the TA-Universal Analysis 2000 software to determine the glass transition (Tg), melting, and decomposition temperature of the samples.

### 2.2.4. Results and Discussion

To study the phase transition of lignin and its residue, samples were heated from room temperature to 400 °C at a constant rate of 15 °C/min in the DSC under a nitrogen atmosphere. Phase transition of lignin and its residue are shown in **Figure 2.3.** The change of enthalpy in the form of glass transition, melting point, and decomposition temperature are shown in **Table 2.3**. The thermal curve shows three distinct endothermic peaks for residue while two distinct peaks for lignin. Endothermic peaks for lignin and residue are observed at 76.82 °C and 77.96 °C, respectively which are correspond to the glass transition temperature. In this temperature, no significant formal phase transition of the materials was occurred, rather than the amorphous material change to rubber like state from a brittle and

relatively hard state. The slightly lower glass transition temperature of residue representing residue is less brittle and harder than the lignin. The curve shows very little peak indicating the difficulty to trace the glass transition temperature for lignin and its residue, due to a higher degree of linkage and lack of proper sequence of regularly repeating units. But a very significant change is shown at high temperatures. The 2$^{nd}$ endothermic peak for residue and lignin is shown at 150.48 °C and 174.40 °C, respectively representing the melting point of residue and lignin.

**Table 2.3.** Values of glass transition, melting, and decomposition temperatures of lignin and its residue determined by DSC analysis.

| Sample | Glass transition $T_g$ / °C | Melting °C | Decomposition °C |
|---|---|---|---|
| Residue | 76.82 | 150.48 | 369.17 |
| Lignin | 77.96 | 174.40 | - |

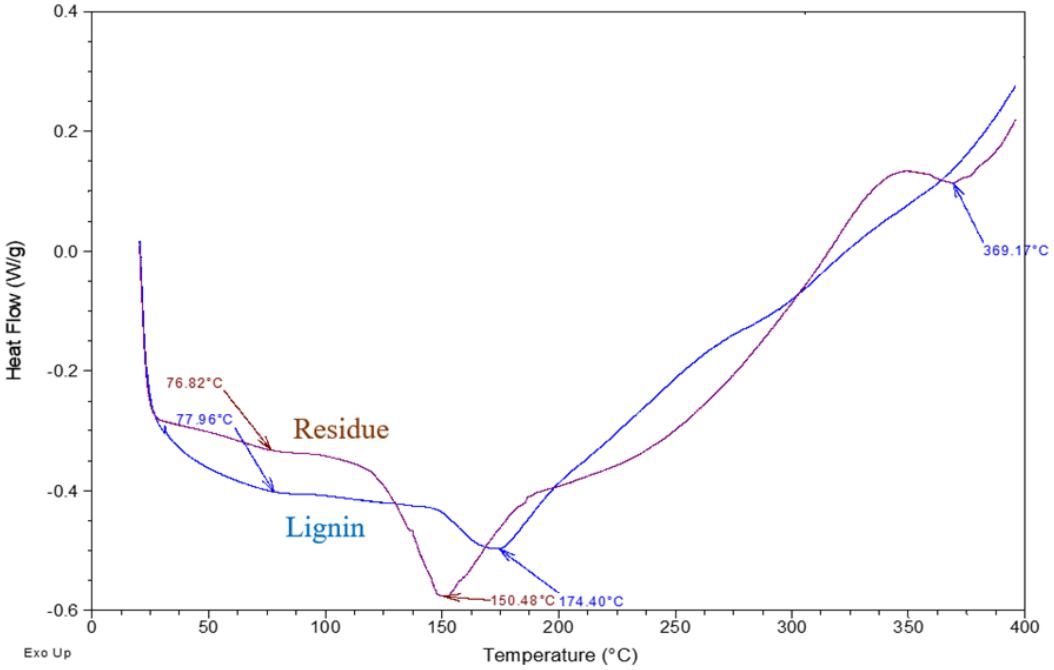


**Figure 2.3.** Comparison of DSC heating curve of lignin and its residue obtained by conducting the thermal analysis in the temperature range of 20-400°C.

Lower melting point of residue indicating the breakdown of side chain or functional groups during the hydrodeoxygenation reaction resulted in, residue converts to liquid state at lower temperature than lignin. On the other hand, residue exhibits 3$^{rd}$ endothermic peak at 369.17 °C where no significant peak for the lignin around this region. The endothermic peak at higher temperature for residue is due to the decomposition of thermally unstable compounds produced during the hydrodeoxygenation reaction.

### 2.2.5. Conclusion

The thermal behavior of lignin and its residue in a nitrogen atmosphere was examined by using differential scanning calorimetry and the glass transition, melting, and

decomposition of lignin and lignin residue was successfully determined by this technique. DSC analysis shows a slightly lower glass transition temperature compared to residue representing residue is thermally less brittle and harder than the lignin. The melting point of lignin (174.40 °C is higher than the lignin residue (150.48 °C). On the other hand, lignin residue decomposed at 369.17 °C but no significant change was observed around that temperature for lignin. Overall, lignin sample shows higher thermal behavior compared to lignin-residue. Finally, this study showed, the thermal property of lignin and lignin-residue was successfully determined by this technique.

## 2.3.Effects of Gamma Irradiation on the Thermal properties of 3D-Printed Samples of Poly Lactic Acid (PLA)

### 2.3.1. Introduction

Poly lactic Acid (PLA) is a biodegradable polymer that has unique properties like good appearance, high mechanical strengths and low toxicity[43]. Researchers have paid huge attention on poly lactic acid because of its wide range of applications in different fields[36]. At present, it has been used to produce different types of devices and electronics, building structures for exploration, medical application in space, and packaging and agricultural fields where it can be exposed by different kinds of radiation[73-74].

Food irradiation is considered as an effective technology which is used to reduce postharvest food loss and ensuring hygienic quality of foods. Gamma irradiation shows high penetration power, hence it is widely used as a cold sterilization technique[75]. During the storage period, ionizing irradiation produced by the technique passes through the food package and causes different types of physical and chemical changes of the packages[76].

Conventionally, petroleum-based plastics have been used as a food packaging material, but Petro-polymer has a bad impact on environment. Therefore, it is time to replace the Petro-polymer by a biodegradable polymer such as poly lactic acid (PLA). Biodegradability of PLA can be influenced by the irradiation levels[77-78]. It was shown that, Poly lactic acid is rapidly degraded in high humidity and temperatures above 55°C without irradiation. On the other hand, it remains stable when storage at lower temperatures and humidity[79]. Nevertheless, irradiation may facilitate alternatives to the direct disposal of PLA wastes in a landfill[80].

Thermal analysis is a very important technique, which is widely used to determine the physical and chemical properties of polymer samples. Thermogravimetry Analysis (TGA) and Differential Scanning Calorimetry (DSC) are used to analyze the physical and chemical properties of polymers like lignin and PLA where the methods observe the property change as a function of temperature.

Thermogravimetry analysis is used to measure the thermal stability, reaction mechanisms, and phase transformation with change of temperatures. This analysis shows two different types of thermogram TG and DTG. TG thermogram denotes percent of weight loss as a function of temperature, whereas the DTG thermogram denotes the rate of weight loss as a corresponding temperature which is the 1$^{st}$ derivative of TG thermogram.

DSC analysis is usually used to measure the glass transition temperatures, along with melting, decomposition, and crystallization temperatures. With the increase of temperature samples undergo transformations from a glassy state to a rubbery state. The temperature at which this transformation occurs is called glass transition temperature (Tg) and is one of the fundamental characteristics of the polymers.

The aim of this research is to study the thermal performance of poly lactic acid (PLA) after subjecting to different kiloGray of gamma radiation from a Cobalt-60 irradiator. Therefore, in order to analysis the thermal behavior of PLA, our proposed objectives for this study are : 1. To identify the glass transition, melting, decomposition, and crystallization temperatures using DSC and 2. Analysis of the range of peak temperature and percent of weight loss of sample after different gamma irradiation.

### 2.3.2. Materials

3D-printing is commonplace with thermoplastics such as PLA or ABS (acrylonitrile butadiene styrene), and it has been shown that properties like the layer thickness impact the mechanical response of such 3D-printed material and their use in additive manufacturing[81-82].

Samples were manufactured using a standard desktop 3D-printer (CTC Bizer) using Makerbot software to create the slicing profile. The printer had a nozzle diameter of 0.4 mm with a standard direct drive extruder set at an extrusion temperature of 230°C. The base plate of the printer was a sheet of glass heated to 100°C and was maintained at that temperature for the duration of the print. More than one spool of material was required to manufacture all samples, but all the spools were purchased together and came from the same batch (eSUN PLA – natural).

It has also been shown that the toolpath deposition pattern influences the overall part strength[81-84]. In this study, a general-purpose slicing profile intended to provide good part strength in all directions was chosen for all samples manufactured. This slicing profile uses two outer shells and an alternating +/- 45° fill pattern for all layers (see

**Figure 2.4**) and all layers are 0.2mm thick. Specimen were printed at 60 mm/sec which allowed enough time for each layer to cool sufficiently before the successive layer was deposited on top.

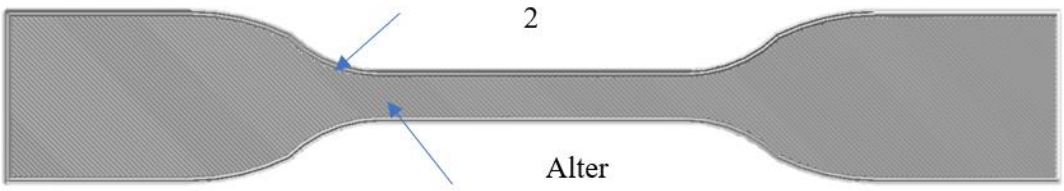


**Figure 2.4.** Slicing profile used for specimen manufacturing (shown on tensile sample).

### 2.3.3. Experimental

To determine the thermal stability of the PLA, 6 specimens were printed for each of nine doses: 0, 25, 50, 75, 100, 125, 150, 175, and 200 kiloGray of gamma radiation from a Cobalt-60 irradiator

The thermogravimetry analysis (TGA) was carried out by using TG/DTA 220 from Seiko Instruments, Japan. About 10 mg of sample were taken in a TGA pan for analysis with a reference pan. The oven was heated from room temperature to 575°C at a constant heating rate of 15 °C/min. Nitrogen gas was used as a carrier gas at a flow rate 20 mL/min to maintain an inert atmosphere and to avoid the samples to contact with the air and help to sweep the pyrolysis gas like $H_2$, $CO_2$, CO, $CH_4$, $C_2H_2$ and water vapor from the system.

The differential scanning calorimetry (DSC) analysis employed a DSC Q-200 differential scanning calorimeter from TA Instruments (New Castle, DE). About 7-10 mg of sample were weighed in a $T_{zero}$ aluminum pan for analysis with a reference pan. Nitrogen gas with a 20 mL/min flow rate was used to maintain an inert atmosphere throughout the system. To determine the glass transition temperature the samples were heated from room temperature to 110 °C at 10 °C/min to remove any moisture in the samples before cooling them down to room temperature to nullify the prior thermal history. Then the samples were heated again from room temperature to 420 °C at a constant 15 °C/min. Finally, the data was analyzed with the TA-Universal Analysis 2000 software to determine the glass transition ($T_g$), melting, and decomposition temperatures.

### 2.3.4. Results and discussion

Thermal decomposition behavior of poly lactic acid (PLA) was measured with the increase of temperature from room temperature to 575°C at a constant heating rate of 15 °C/min. **Table 2.4** shows the indication of thermal characterization of PLA at different irradiation dose. It was shown from the table and as well as from **Figure 2.5** the range of peak temperature of PLA linearly increased with the increase of gamma irradiation dose.

**Table 2.4.** Peak temperature difference, % weight loss, and residual carbon of PLA samples at different gamma irradiation dose.

| Dose of Gamma Irradiation (kGy) | Average peak temperature difference (˚C) | Average %weight loss | Average residual carbon (%) |
|---|---|---|---|
| 0 | 98.5 | 98.22 | 1.18 |
| 25 | 115.33 | 98.55 | 0.67 |
| 50 | 98.5 | 98.01 | 1.14 |
| 75 | 108 | 96.62 | 1.58 |
| 100 | 112 | 97.73 | 1.38 |
| 125 | 113 | 96.51 | 1.90 |
| 150 | 110 | 97.54 | 1.42 |
| 175 | 120 | 96.63 | 1.95 |
| 200 | 122 | 97.49 | 1.11 |

On the other hand, the weight loss was reduced shown in **Figure 2.6** as the radiation dose increased, which may be a sign of weight increases due to oxidation in air. Residual carbon in **Figure 2.7** did not show any overall linear dependence, with fractions generally between 1% and 2%.

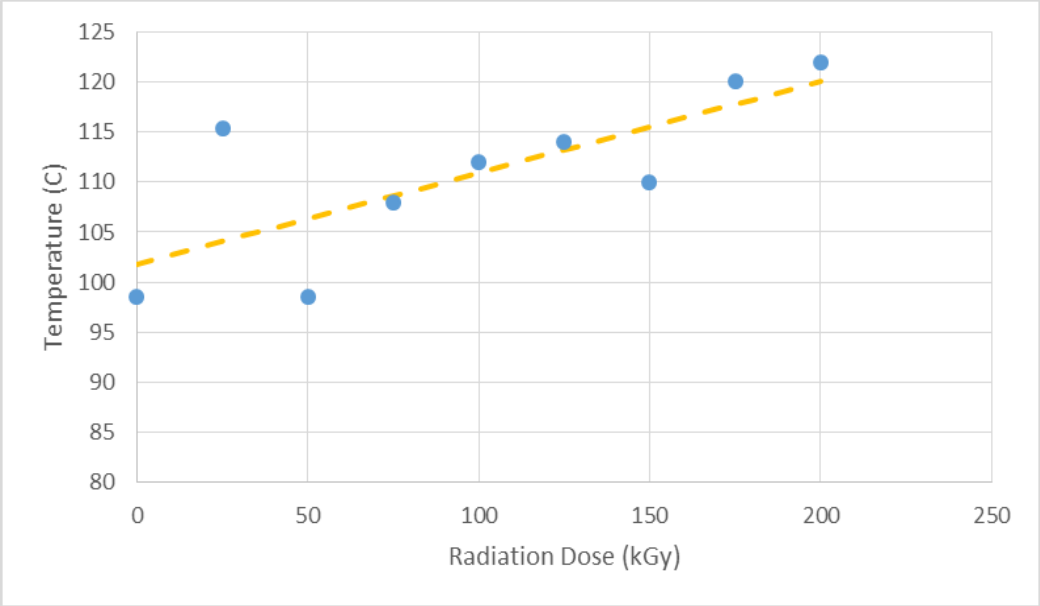


**Figure 2.5.** The difference between the peak temperatures during TGA testing increased linearly with the radiation dose applied to 3D-printed PLA samples.

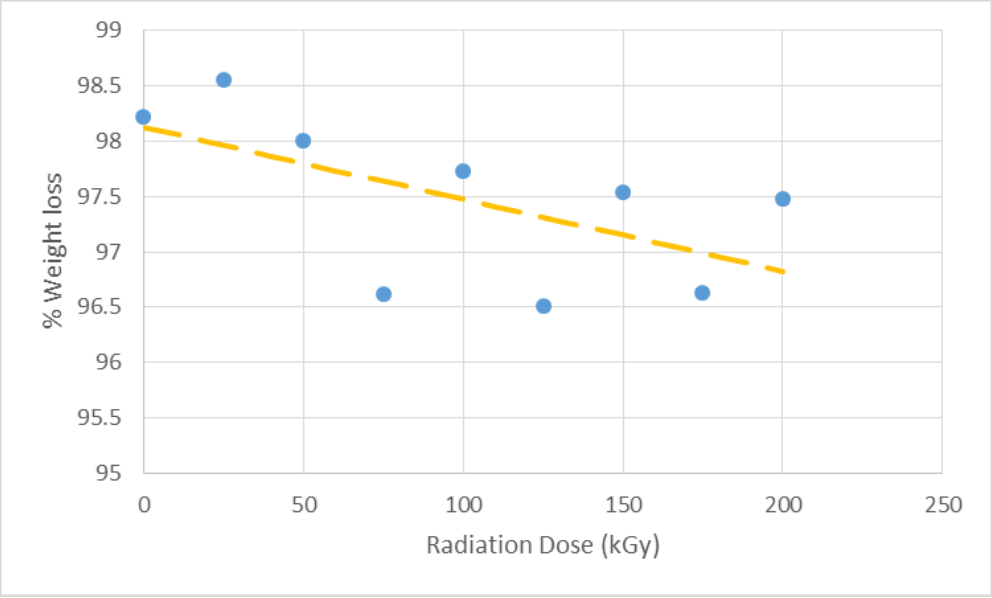


**Figure 2.6.** Weight loss decreases linearly with the radiation dose after TGA.

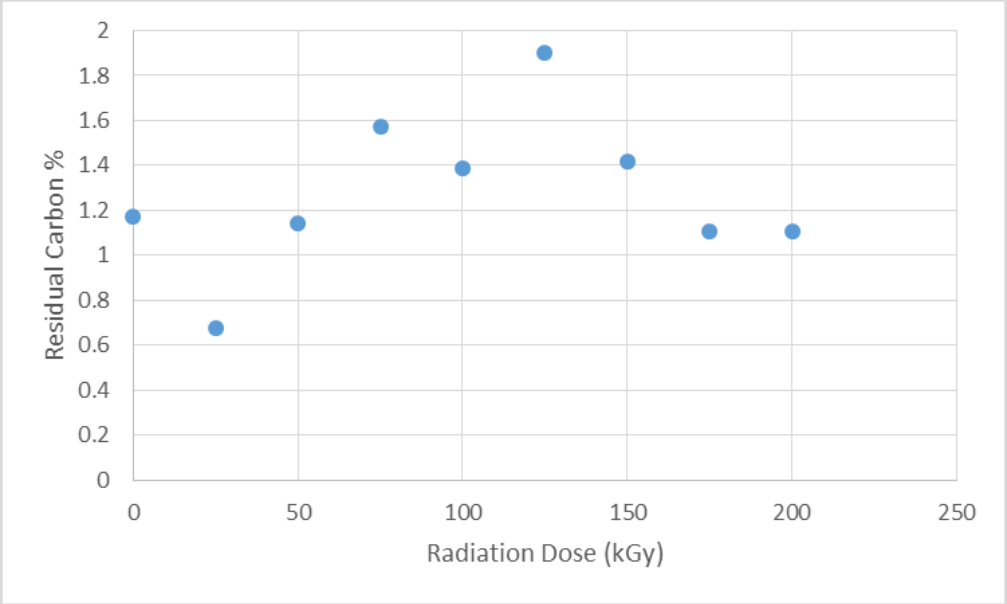


**Figure 2.7.** Residual carbon left after thermogravimetric analysis

### 2.3.5. Conclusion

Thermal study of PLA shows, the range of peak temperature increased with the increases of radiation dose. The temperature changes occurred when the mass loss is about 5% and continuous up to 75%. TGA study showed weight loss reduced with the increase of radiation doses indicating the sign of oxidation resulted in increases of weight. On the other hand, residual carbon did not show any overall linearity but just fluctuate between 1-2%.

# CHAPTER THREE

# INSTRUMENTAL ANALYSIS OF POLYMER

## 3.1. Attenuated Total Reflectance Fourier Transform Spectroscopy (ATR-FTIR)

### 3.1.1. Introduction

Different types of spectroscopic techniques are routinely used as an analytical tool to identify the chemical structure of various types of materials. The spectroscopic technique shows better performance to analyze the complete structure of a polymer rather than making assumptions from the data obtained from monomers compared to degradative techniques. Fourier transform infrared spectroscopy (FTIR) is a highly useful technique for analytical chemist as it can analyze a wide variety of solids, liquids, and gaseous materials by transmitting the infrared radiation through the materials[85-86]. Traditional FTIR is not widely used because it needs some form of sample preparation to get a good quality of spectroscopy. Nevertheless, attenuated total reflectance (ATR) in combination with traditional FTIR permits the solid and liquid sample directly analyzed without any kind of sample preparation. Additionally, ATR-FTIR is a very fast, reproducible, and highly sensitive technique and requires a small amount of sample.

This is a useful technique for the identification and fingerprinting the characteristics of absorption bands of various functional groups present in the polymer sample like lignin[87]. In previous years, many researchers have conducted many investigations to reveal the chemical structure of lignin and its different derivatives. Therefore, much literature data on FTIR studies of lignin and derivatives are available[71]. On the other hand, there is not enough data for lignin-residue after different types of reaction and no data for lignin-

residue after hydrodeoxygenation reaction. The aim of our FTIR study is to identify the chemical structure of lignin-residue and lignin based on the absorption band and find out the basic structural difference between the two.

### 3.1.2. Materials

In our study alkali lignin, from Sigma-Aldrich (St. Louis, MO) and its residue after catalytic hydrothermal reaction at 240 °C were used as a sample.

### 3.1.3. Methods

FTIR data was obtained by using a Thermo-Fisher Scientific Nicolet 380 FTIR spectrometer in the attenuated total reflectance mode. The spectra were recorded between 400 and 4000 $cm^{-1}$ with an 8 $cm^{-1}$ resolution with 100 scans where the spectra of the samples were analyzed by EZ OMNIC software.

### 3.1.4. Results and Discussion

The FTIR spectra of lignin and its residue are shown in **Figure 3.1** and **Figure 3.2**, and characteristics FTIR absorption bands assignments are shown in Table 3.1. The spectra of lignin and its residue obtained from FTIR are shown very complex as most of the bonds are produced by the imposition of various types of vibrations of different functional groups. Therefore, assignment of many bands is possible only in the approximation of the predominant contribution of certain chemical groups[88]. The absorption band at 3460-3212 $cm^{-1}$ for both samples are due to the strong O-H bond stretching which is attributed the hydroxyl groups in the aromatic and aliphatic structures. The bands around 2935 $cm^{-1}$

indicate apparent C-H stretching in methyl and methylene groups of the side chain present in samples. On the other hand, the absorption band in the range of 1685 $cm^{-1}$ are shown by lignin and its residue which can be attributed of C= O for unconjugated ketones, carbonyls, and ester groups[18, 89] along with a C=O vibration band at 1265 $cm^{-1}$. But band at 1665 $cm^{-1}$ for residue is poor than lignin represents unconjugated bonds broke down during the hydrodeoxygenation reaction. According to Faix, the absorption band at 1592 $cm^{-1}$ is shown by impurity or water association[89]. In addition, absorption (lower absorbance for residue) peaks around 1510 $cm^{-1}$ and 1424 $cm^{-1}$ for both the sample are shown by aromatic skeletal vibrations and around 1455 $cm^{-1}$ for aromatic ring vibrations. Higher % transmittance (lower absorbance) for residue indicates less aromatic in nature compared to lignin.

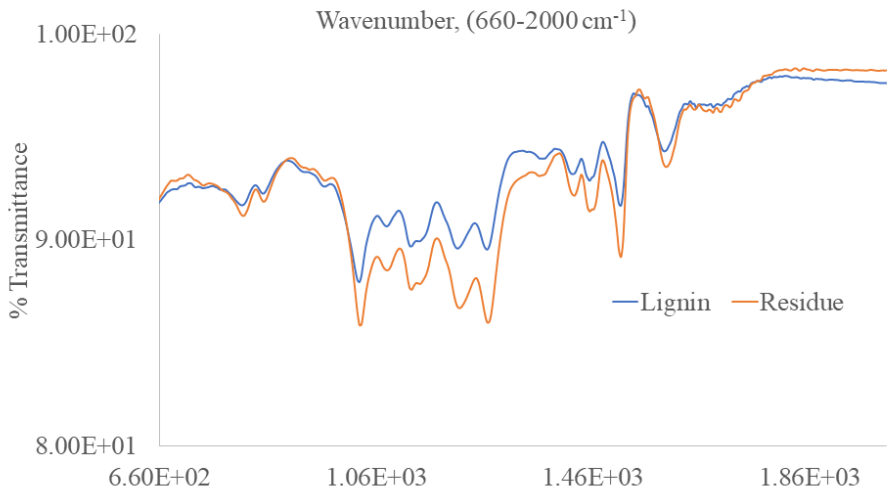


**Figure 3.1:** FTIR spectra of lignin and residue from wavenumber 660-2000, $cm^{-1}$.

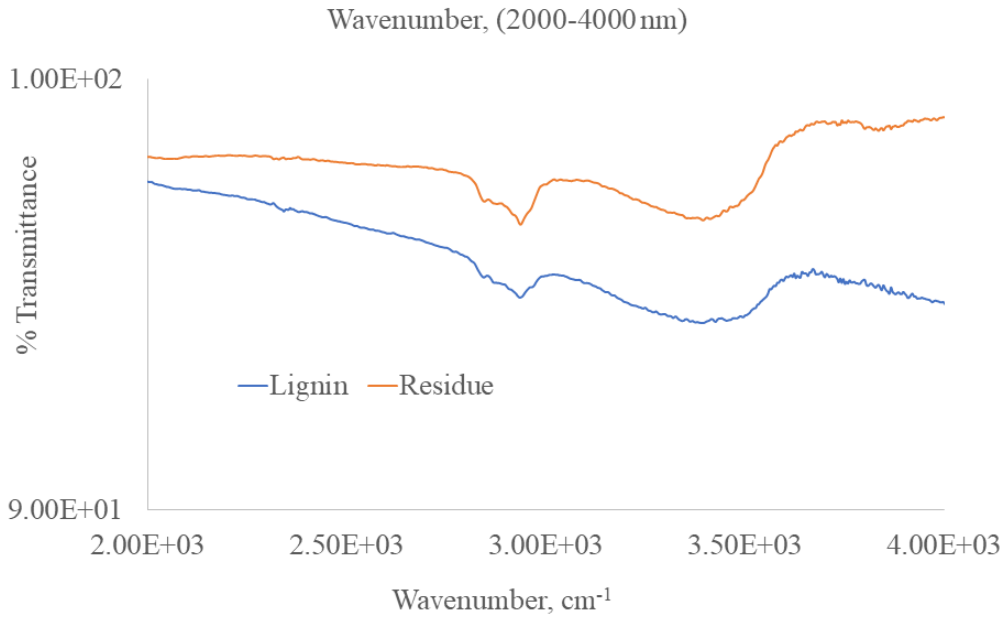


**Figure 3.2:** FTIR spectra of lignin and residue from wavenumber 2000-4000, $cm^{-1}$.

**Table 3.1:** FTIR absorption band ($cm^{-1}$) assignments for lignin and its residue.

| **Absorption band ($cm^{-1}$)** | **Functional groups** |
|---|---|
| 3460-3212 | O-H Stretching |
| 3000-2842 | C-H Stretching in methyl and methylene groups |
| 1687-1655 | C=O stretch in unconjugated ketone, carbonyl and in ester groups |
| 1610-1590 | Aromatic skeletal vibrations plus C=O Stretch |
| 1515-1505 | Aromatic Skeletal vibrations; G>S |
| 1460-1450 | C-H deformations asymmetric in methyl and methylene |
| 1430-1420 | Aromatic skeletal vibrations plus C-H in plane deformation |
| 1270-1200 | G ring plus C=O stretch |
| 1130-1120 | Aromatic C-H in plane deformation; for G moieties |
| 1080 | C-O deformations in secondary alcohols and aliphatic ethers |
| 1030 | C-H in plane deformation of guaiacol (G) units |
| 860-815 | C-H out of plane in position 2,5,6 of G units |

The absorption region below 1300 $cm^{-1}$ is considered the fingerprint region for lignin polymer. the investigation of FTIR spectra of lignin and residue are very difficult below the absorption region 1300 $cm^{-1}$ due to the involvement of different vibrational

modes comes from the same functional group. The absorption peak for lignin at 1205 $cm^{-1}$ and for the residue at 1214 $cm^{-1}$ are a characteristics absorption band for guaiacyl (G) monomer ring plus C=O stretch. But a little higher % transmittance (lower absorbance) peak for residue assuming the lower proportion of G moieties for residue compare to lignin with a breakdown of the side chain of the monomer. The aromatic C-H in plane deformation at 1130 $cm^{-1}$ and 1030 $cm^{-1}$ for both the samples are for guaiacyl (G) monomer ring[90]. Residue also shows large % transmittance (lower absorbance) peaks around 853 $cm^{-1}$ and 815 $cm^{-1}$ which are specific to for C–H out-of-plane vibrations in position 2, 5 and 6 of guaiacyl.

### 3.1.5. Conclusion

The FTIR analysis was helpful to reveal the structural information of lignin and its residue. The absorption band around 1265, 1129, 1030, 853, and 815 $cm^{-1}$ reveals G moieties present in both the samples. But no characteristics absorption bands for H and S moieties are observed in these samples. Additionally, higher % transmittance (lower absorbance) for residue at 1610, 1510, 1460, 1265, and 815 $cm^{-1}$ proves that less G moieties and Aromatic skeletal vibrations plus C=O Stretch. The softwood lignin's are mainly composed of G moieties whereas the hardwood lignin's are composed by a different proportion of S, G and H moieties[88]. Finally, the study proves that the FTIR analysis is a very important and a quick qualitative instrumental technique to characterize the chemical and functional properties of lignin and residue.

## 3.2. Nuclear Magnetic Resonance

### 3.2.1. Introduction

Nuclear magnetic resonance spectroscopy commonly known as NMR is a widely used spectroscopic technique. This spectroscopic technique is one of the important tools to obtain reliable and complete structural information of different types of polymer materials. NMR shows higher resolution and greater accuracy which makes it the most updated and advantageous technique compared to Raman, FTIR, and UV spectroscopy. NMR has different types of application, proton nuclear spectroscopy ($^1$H) is one of them which deals with the magnetic spin of hydrogen-1 nuclei to identify and estimate the different functional groups and interunit linkages present in the compounds.

$^1$H NMR spectra is a unique, well-resolved, and very powerful technique which is used to confirm the identity of the various sample. During the previous years, various studies have been done on milled-wood lignin's (MWL), dehydrogenation polymers of coniferyl alcohol, donax reed lignin and maize milled-wood lignin's to investigate the different functional groups such as phenolic, hydroxyl, methoxy and formyl groups present on it[91-92].

Although, there are enough NMR data are available on the structural characterization of lignin and its derivatives. But significant research has not been done on lignin-residue to understand the structural structure and interunit linkages after hydrodeoxygenation reaction. Therefore, the main aim of our present work is to 1. The qualitative determination of various functional groups, structural moieties (G/H/S-unit),

and different linkages between them, 2. The quantitative determination of different functional groups present in the lignin-residue and compare with the lignin.

### 3.2.2. Materials

In our study alkali lignin, from Sigma-Aldrich (St. Louis, MO) and residue after catalytic hydrodeoxygenation reaction at 240 °C were used as a sample. DMSO-$d_6$ was used as solvent and 1,3,5-trioxane used as an internal standard where both chemicals were obtained from ACROS ORGANICS, New Jersey, USA.

### 3.2.3. Method

The Proton (1H) NMR spectra of lignin and its residue were recorded on a Bruker 400 spectrometer (Bellerica, MA) equipped with a QNP 5-mm probe at 400 MHz at 295 K. In this experiment DMSO-$d_6$ was used as a solvent and 1,3,5-trioxane was used as an internal standard. About 25 mg of lignin and residue were taken with 0.044 mmol IS/0.5-mL DMSO-$d_6$. Experiment parameters for the spectra were a 90 ° pulse angle, 2-s pulse delay, and 512 scans. Quantification of the spectra was done in triplicate where each sample was balancing distinctly.

### 3.2.4. Results and discussion

The proton NMR spectrum of lignin and the residue are shown in **Figure 3.3** and extended spectrum from region 6-13 δ is shown **Figure 3.4** The chemical shift values and quantitative analysis of different functional and structural moieties are summarized in **Table 3.2** and Table **3.3** respectively. The quantitative value is shown in $mmolg^{-1}$ unit

which was measured using internal standard (IS) concentration. The NMR spectrum are obtained from both the samples are quite similar

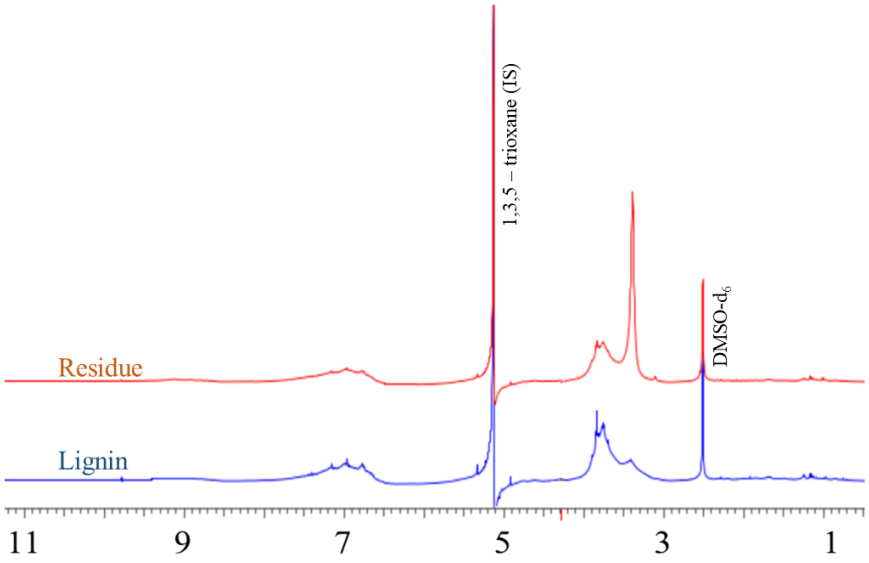


**Figure 3.3.** Proton ($^{1}$H) NMR analysis of lignin and its residue.

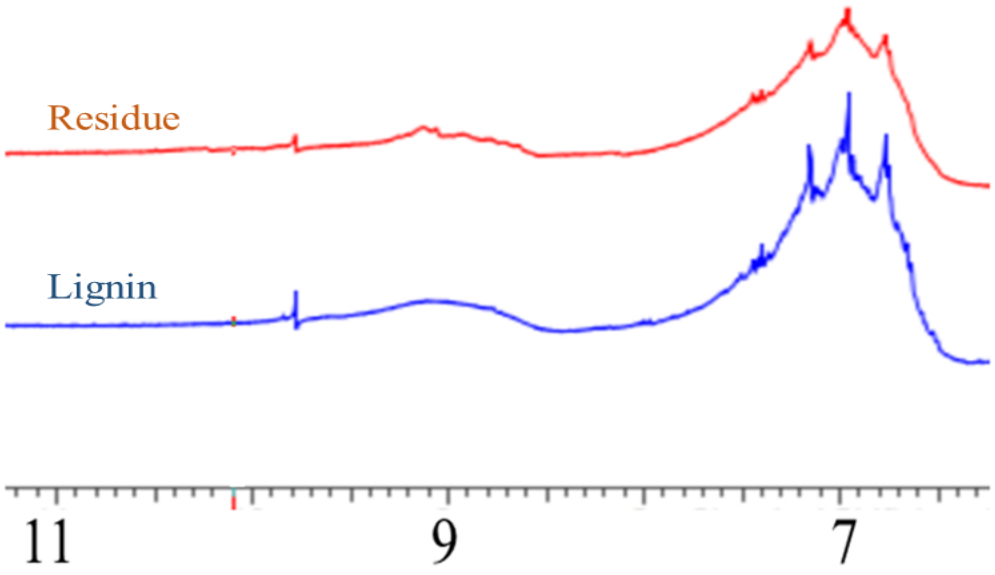


**Figure 3.4.** Expansion of aromatic, formyl, and phenolic hydroxyl regions (6-12 δ) from the $^{1}$H NMR analysis of lignin and its residue.

**Table 3.2.** Analysis of the chemical shift values of various functional groups present in lignin and the residue by $^{1}H$ NMR.

| Peak (ppm) | Functional Groups |
|---|---|
| 1.30 | Hydrocarbon contaminant |
| 2.54 | DMSO-$d_6$ solvent |
| 3.40 | Proton in Methoxyl group |
| 3.80 | Proton in Hydroxyl group |
| 4.90 | β-O-4 |
| 5.12 | 1,3,5-trioxane (IS) |
| 5.35 | β -5 |
| 7.00 | Aromatic protons |
| 9.12 | Proton in phenolic groups |
| 9.77 | Formyl protons |

**Table 3.3.** Quantitative analysis of various functional groups and structural moieties present in the lignin and the residue by $^{1}H$ NMR analysis.

| | Lignin | | Residue | |
|---|---|---|---|---|
| Functional group | Peak | $mmolg^{-1}$ | Peak | $mmolg^{-1}$ |
| DMSO-$d_6$ solvent | 2.54 | | 2.54 | |
| Proton in Methoxyl group | 3.40 | 0.082 | 3.40 | 2.365 |
| Proton in Hydroxyl group | 3.80 | 1.467 | 3.80 | 1.263 |
| 1,3,5 – trioxane (IS) | 5.12 | - | 5.12 | - |
| $Ph.H^{4}$ | 7.00 | 1.379 | 7.00 | 1.189 |
| $Ph.OH^{3}$ | 9.12 | 0.228 | 9.12 | 0.013 |
| CHO | 9.77 | 0.005 | 9.77 | 0.003 |

**i.Methoxyl groups**

The peaks centered at 3.4 ppm is due to proton of methoxyl groups present in both lignin and its residue. To determine the quantitative value of methoxyl groups the peaks are integrated from 3.17-3.54 region. The quantitative value for lignin is 0.082 and for residue is 2.365. The higher value of methoxyl group for lignin residue is suggesting the breakdown of β-O-4 linkage during the hydrodeoxygenation reaction[92-93]. In the unreacted lignin, monomer units are strongly bonded to each other. Therefore, very less amount of -$OCH_3$ are exposed but because of breakdown of β-O-4 linkage more -$OCH_3$ groups are exposed and shown in NMR spectroscopy spectra.

**ii.Aliphatic hydroxyl groups**

The spectral peaks centered at 3.80 is for aliphatic hydroxyl groups present in the samples[94]. For quantification, the peaks are integrated from 3.54-3.95 ppm. The quantity of hydroxyl group present in lignin is 1.467 mmol/g and in residue is 1.263 mmol/g. The lignin monomer containing hydroxyl groups are easily breakdown and went through the reaction mixture. Therefore, reside shows lower value of this group compared to lignin. The lower value of this group in residue also suggest the partial breakdown of side chain of lignin during catalytic hydrodeoxygenation reaction.

**iii.Aromatic protons**

The NMR figure shows a broad peak from 6.53-7.35 is due to the aromatic protons in sample. The broad peak contains three small peaks at 6.75, 7.00 and 7.15 ppm which is due to the guaiacol propane unit in the samples[92, 95]. The table shows the lignin contain 1.379 mmol/g of aromatic protons where the residue contains 1.189 mmol/g. Table 3.3

shows lignin is in rich in aromatic proton compare to its residue which again suggested the breakdown of guaiacyl unit during the catalytic hydrodeoxygenation reaction.

**iv.Phenolic Groups**

The spectral region from 8.51-9.56 centered at 9.12 is due to the proton present in phenolic hydroxyl groups. The literature data shown that the peaks from 8.51-9.56 ppm are due to conjugated carbonyl guaiacyl units of structures[96-97]. The integrated quantitative value for lignin and its residue is 0.228 and 0.013 mmol/g respectively.

**v.Formyl Groups**

The spectral peaks ranging from 9.77-9.83 ppm are due the protons present in formyl groups. The quantitative results of this formyl protons in lignin and its residue are 0.005 and 0.003 mmol/g, respectively which was calculated by integrating the region from 9.77-9.83 ppm.

**vi.Aliphatic to aromatic ratio**

Total amount of aliphatic and aromatic proton was calculated using table 3.3 which is shown on table 3.4. Total number of aliphatic and aromatic proton is found in lignin are 1.55 (mmol/g) and 1.61 (mmol/g), respectively and total number of aliphatic and aromatic proton is found in residue are 3.63 (mmol/g) and 1.20 (mmol/g), respectively. **Table 3.4** shows, the ratio of aliphatic/aromatic for residue was more than 3 times larger than lignin. This is because of the breakdown of β-O-4 bond of lignin during the hydrodeoxygenation reaction.

**Table 3.4:** Ratio of aliphatic/aromatic proton**.**

| Sample | Aliphatic Proton (mmol/g) | Aromatic proton (mmol/g) | Ratio (Aliphatic/Aromatic |
|---|---|---|---|
| Lignin | 1.55 | 1.61 | 0.96 |
| Residue | 3.63 | 1.20 | 3.03 |

### 3.2.5. Conclusion

$^{1}$H NMR is successfully able to quantify the structural and functional moieties present in lignin and its residue. The quantitative data is calculated in mmolg$^{-1}$ unit which is measured using internal standard (IS) concentration. Our experimental results show that lignin contain almost same amount of aliphatic and aromatic moieties, but residue contains more than 3 times aliphatic moieties compare to aromatic, which indicates aromatic moieties went through the reaction mixture during the hydrodeoxygenation reaction leaving the aliphatic moieties.

## 3.3. Molecular Weight Distribution Analysis of Lignin by Gel Permeation Chromatography (GPC)

### 3.3.1. Introduction

Natural lignin is undoubtfully a complex natural polymer with a structural variety across the environment and origin[23, 98]. Its tedious isolation techniques disclose the difficulty of its comprehensive structural study. Different methods have been studied for acquiring the molecular weight information of lignin such as weight-average molecular weight (Mw), and number-average molecular weight (Mn)[99-100]. Technologically advanced method e.g., NMR-based field-flow fractionation approaches has developed to overcome the inconveniences which is connected to the less reactivity of lignin[101]. However, no

better-advanced methods have been developed so far that can determine the Mw and Mn of lignin perfectly.

Previous studies showed, lignin is containing a highly polymerized structure, but some recent studies showed lignin is not that much highly polymerized as thought before. More interestingly, some studied also showed that lignin exhibits polymeric size which lies within the traditional dynamic range. Therefore, well equipment and accessible methods can determine the weight distribution of the molecular weight of lignin by gel permeation chromatography (GPC)[48, 102-103].

Gel permeation chromatography (GPC) is one of the highly used technique for the analysis of weight distribution of polymers. It is also considered the most reliable and accessible instruments for the characterization of comprehensive molecular weight distribution of polymers[102, 104]. Gel permeation chromatography is a fast and consistent method for gathering the molecular weight distribution information of polymers[105]. It separates the molecules based on the size where large molecules elute first then small molecules. But it is very important to establish a quantitative relationship between elution volume and molecular weight of polymers.

The purposes of this study are to determine the molecular weight information of lignin such as

1. Weight-average molecular weight (Mw)
2. Number-average molecular weight (Mn)

### 3.3.2. Materials

In our study alkali lignin, from Sigma-Aldrich (St. Louis, MO) and its residue after hydrodeoxygenation reaction at 240 °C were used as a sample. Polystyrene from Agilent

Technologies was used as a standard. Tetrahydrofuran and dimethyl sulfoxide were purchased from fisher scientific (Fair Lawn, NJ). All the chemicals were used without any further purification.

### 3.3.3. Sample Preparation

For the molecular weight analysis, 10 mg of sample was dissolved in 0.5 mL of dimethyl sulfoxide (DMSO). Then, 4.5 mL of 1:4 mixture of dimethyl sulfoxide and tetrahydrofuran (THF) solution was added to make a 5 mL of sock solutions for gel permeation chromatography analysis. Same procedure also followed for the preparation of blank sample.

### 3.3.4. Method

To determine the molecular weight distribution of lignin and its residue, a gel permeation chromatography (GPC) was performed by using a shimadzu high performance liquid chromatography (LC-2030C) and a KNAUER refractive index detector (RID-2300). Two analytical GPC columns were used in a series for analysis, one of them is PLgel 10μm MIXED-B (7.5 mm × 300 mm) and another one is PLgel 3μm MIXED-E (7.5 mm × 300 mm) from Agilent Technologies. HPLC grade Tetrahydrofuran (THF) from Fisher Scientific (Fair Lawn, NJ) was used as a mobile phase with a flow rate of 0.7 mL/min at 40 °C for 70 mins. An aliquot of 30 μL of filtered lignin and its residue solution was analyzed at a time. A standard calibration was performed with standards polystyrene (Agilent Technologies) with a molecular range (Mw) of 705-6375000 Da.

### 3.3.5. Results and Discussion

Molecular weight of lignin is a fundamental property that affects the recalcitrance of biomass and depolymerization of lignin into monomers. Gel permeation chromatography (GPC) is a commonly used technique to investigate the molecular weight of lignin[106]. To investigate the molecular weight of lignin and its residue, GPC study was performed using polystyrene as a standard and THF as an eluent. **Figure 3.5** shows the gel permeation chromatogram with retention time and **Figure 3.6** shows the molecular weight distribution for lignin and its residue.

**Table 3.5.** Number average, and weight average molecular weight based on % area, and % height of lignin and its residue at different retention time.

| Retention Time(min) | | Area (%) | | Height (%) | | Number-average molecular weight Mn (g/mol) | | Weight-average molecular weight Mw (g/mol) | |
|---|---|---|---|---|---|---|---|---|---|
| Lignin | Residue | Lignin | Residue | Lignin | Residue | Lignin | Residue | Lignin | Residue |
| 23.45 | 23.41 | 76.11 | 77.08 | 39.86 | 51.33 | 1157 | 1230 | 2337 | 3172 |
| 25.03 | 25.08 | 6.56 | 18.47 | 26.66 | 36.23 | 225 | 62 | 231 | 129 |
| 25.44 | - | 12.47 | - | 23.68 | - | 53 | - | 82 | - |

**Table 3.6.** Molecular weight distribution of lignin and its residue based on % area and % height.

| Sample | Number average (Mn) molecular weight distribution based on %Area | Weight average (Mw) molecular weight distribution based on %Area | Number average (Mn) molecular weight distribution based on %Height | Weight average (Mw) molecular weight distribution based on %Height | Polydispersity Area % | Polydispersity Height % |
|---|---|---|---|---|---|---|
| Lignin | 901.95 | 1804 | 553.72 | 1012.53 | 2.0 | 1.83 |
| Residue | 959.6 | 2468.80 | 653.82 | 1674.92 | 2.57 | 2.57 |

**Table 3.5** indicates three distinct chromatogram peaks for lignin and two for residue which reveals the different fundamental properties of lignin and its residue. **Table 3.6** as well as **Figure 3.5** shows the molecular weight distribution of residue is larger than lignin, as well as the higher polydispersity of residue than lignin. The relative higher polydispersity of residue is connected to the possibility of forming C-C bond during the hydrodeoxygenation reaction[107]. Ane et al. confirmed that, this type of bond is related to C5 structure in aromatic ring which is called guaiacol type units. Therefore, guaiacol units are connected to each other at elevated temperature and formed compounds with higher molecular weight[107].

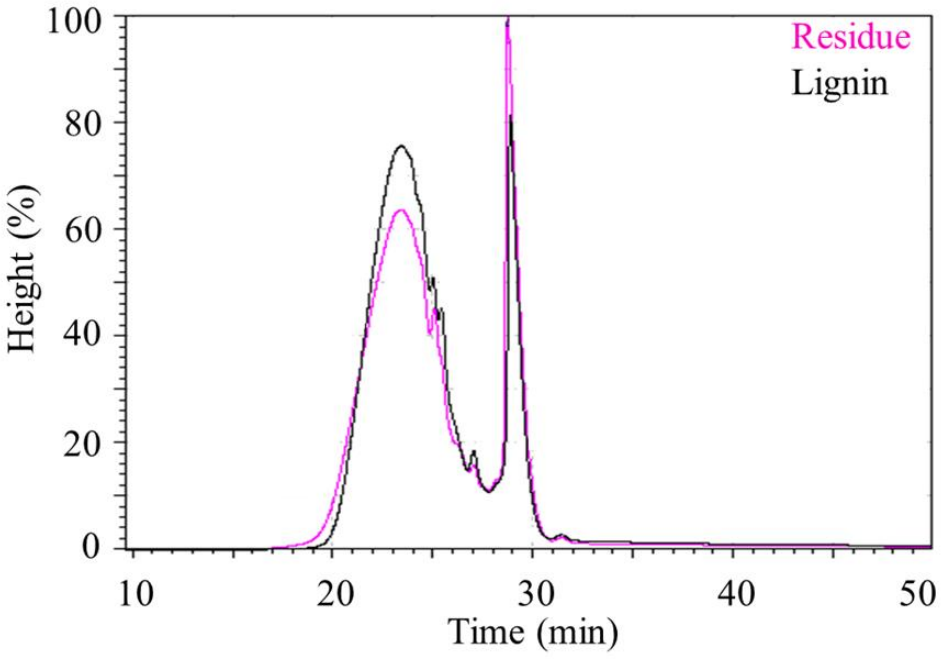


**Figure 3.5.** Chromatogram for lignin and residue

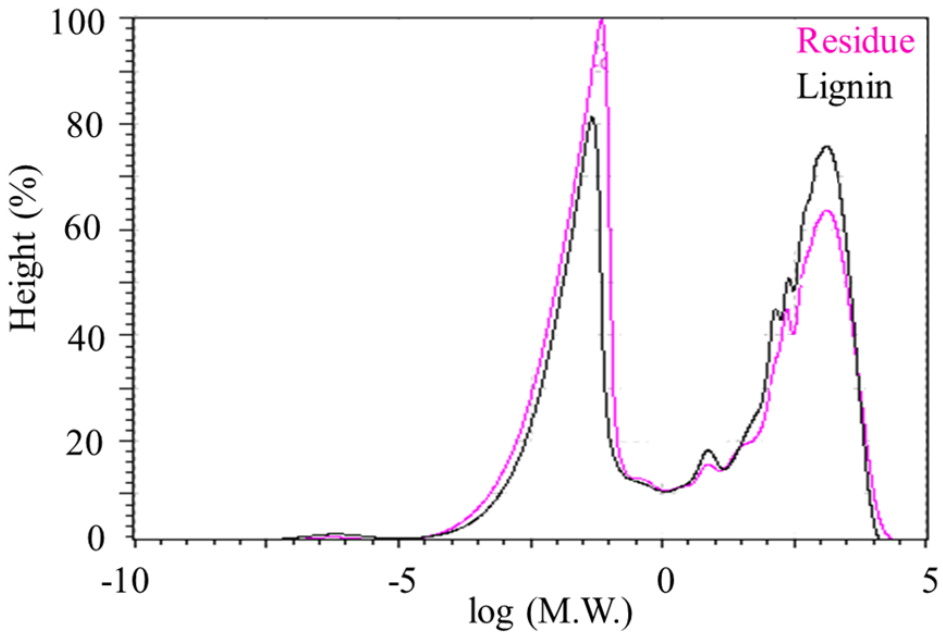


**Figure 3.6.** Molecular weight distribution for lignin and residue

### 3.3.6. Conclusion

Molecular weight distribution of lignin and its residue was successfully determined by gel permeation chromatography. The study showed three distinct peaks for lignin and two for residue. Molecular weight distribution and polydispersity were found comparability higher for residue than lignin indicating the formation of carbon-carbon condensation during the catalytical hydrodeoxygenation reaction.

# CHAPTER FOUR

# STRUCTURAL CHARACTERIZATION OF LIGNIN BY DEGRADATIVE TECHNIQUE (CuO OXIDATION)

## 4.1. Introduction

Lignin is an amorphous irregular polymer which is a major structural component of secondary cell wall of vascular plant mixed with cellulose and hemicellulos[15-17]. It is a complex polymer of hydroxylated and methoxylated monomeric units linked with irregular order to each other which makes it structural determination very difficult. In its helical structure, monomeric units are interconnected with each other with different types of ether and C-C linkages[18-19]. In order to the structural elucidation of lignin, different thermal and chemical degradation methods such as pyrolysis, oxidation, reduction, and hydrolysis has been used[17]. All these methods, selectively breakdown the lignin polymer into its corresponding monomer called p-hydroxycinnamyl alcohol (H-moiety), coniferyl alcohol (G-moiety), sinapyl alcohol (S-moiety) [13], and the structural configuration of lignin has been characterized by the relative abundance of H/G/S.

However, most the method requires noble or expensive metal catalyst[108], homogeneous catalyst (hard to separate and reuse)[109], expensive reagents[110], and solvents[111] other than inexpensive solvents such as ethanol, methanol, and water. Therefore, to develop an efficient lignin conversion with inexpensive catalyst and solvent media is still a challenging task to a better understanding of the mechanistic cleavage of lignin into phenolic monomers. In addition, the production of selective moiety such as

vanillin, syringaldehyde, and its derivatives are depending on the botanical source of lignin making it more tricky to the scientific community[17, 112].

Cleavage of β-O-4 is carried out in an aqueous or organic/aqueous solution under acidic and basic conditions. Studies showed acids (HBr, HCl, and $H_2SO_4$) are usually used in different types of organosolv process to remove lignin from biomass through the cleavage of aryl-ether linkages present in lignin[113-115]. Studies also showed acidolysis cleavage of β-O-4 bonds are start with the formation of σ-carbon cation followed by two routes (**Figure 4.1**): 1. With the loss of ϒ-carbinol group via the cleavage of β,ϒ carbon-carbon bond followed by the hydrolyze to a β-aldehyde, and 2. Through the migration of cation from σ-carbon to β-carbon to form ketone and guaiacol[116-118].

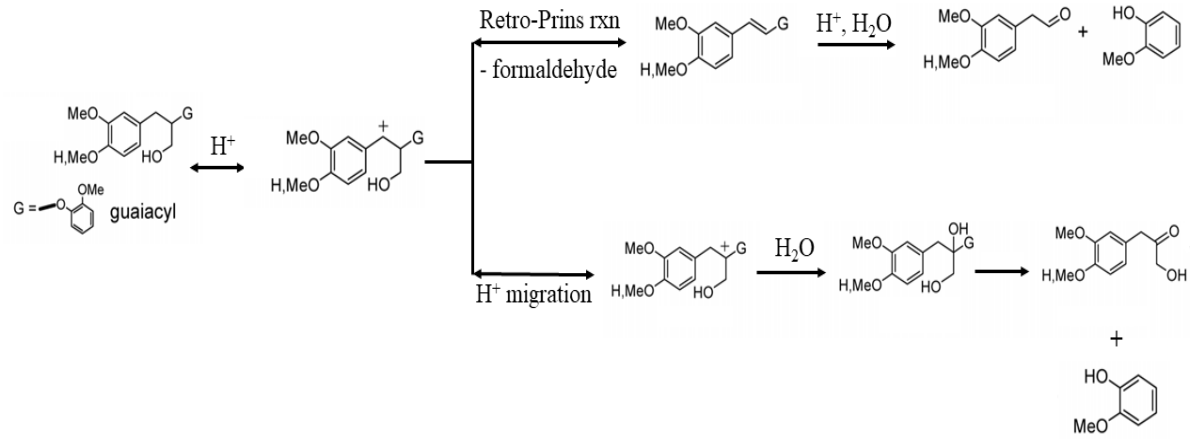


**Figure 4.1.** Acidolysis reaction mechanism for the cleavage of β-O-4 bond.

Though inorganic acids playing an important role in the field of biomass pretreatment to remove lignin, but acids are rarely used in hydrothermal treatment of solvolysis of lignin[119-120]. Several studies reported that, during hydrothermal pretreatment repolymerization/condensation are observed as well as decomposition products which

cause problem for hydrothermal treatments and requires much longer reaction times and temperatures than delignification process of biomass[113, 121]. On the other hand depolymerization of lignin has been intensely studied in the presence of a wide range of basic conditions such as NaOH, KOH along with water and water-alcohol mixture[122-124] . It has been reported that, basic medium minimizes the char formation and increase the phenolic liquid products[125-126]. It has been suggested that during the base catalyst cleavage of β-O-4 takes place through the six-membered transition state. In this reaction, both sodium and hydroxyl ion participate, where sodium ion catalyze the reaction through the formation of cation abduction with lignin and polarizing the ether bond (**Figure 4.2**). This phenomenon increased the negative charge of oxygen atom which decreases the energy required for the cleavage of ether bond. On the other hand abstraction of proton from σ-carbon atom of the ether bond by hydroxide ion resulted in the formation of syringaldehyde and water molecule[127].

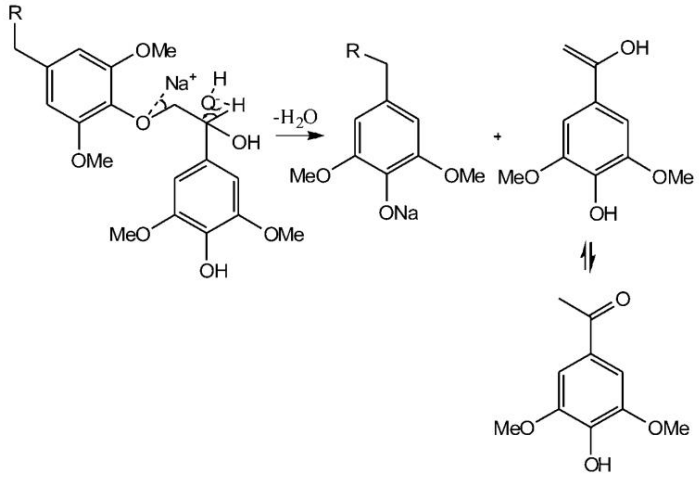


**Figure 4.2.** Basic (NaOH) reaction mechanism for the cleavage of β-O-4 bond adapted from[127].

Nowadays oxidation in the basic medium is considering one of the most promising techniques for the degradation of lignin into its corresponding phenolic monomer. But the strong oxidant such as permanganate, chlorine, chlorine dioxide, and hypochlorite are destroying the aromatic ring structure and produce low molecular weight acids rather than phenolic monomers[128-129]. On the other hand, milder oxidants e.g., cupric oxide and nitrobenzene are selectively breakdowns the ether linkages of the phenolic monomeric by keeping the aromatic ring intact and produce expected phenolic monomers. But these oxidation techniques have a limitation which is the structural information mainly attained from the chemically modified and degraded lignin moieties rather than the native lignin.

Nitrobenzene oxidation was developed by Freudenberg and his coworkers for the investigation of aromatic properties in lignin[130]. This oxidation technique is mainly used for the degradation of propane side chains (**Figure 4.3**) in uncondensed structures which primarily produce vanillin, *p*-hydroxybenzaldehyde units or its derivatives from softwood lignin's and syringaldehyde phenolic units from hardwood lignin's[131-132]. In 1942, an oxidation method was developed by Pearl to produce vanillin from lignin by using cupric sulfate[133], which was later replaced by cupric oxide and considered as a less costly method compared to other traditional methods.

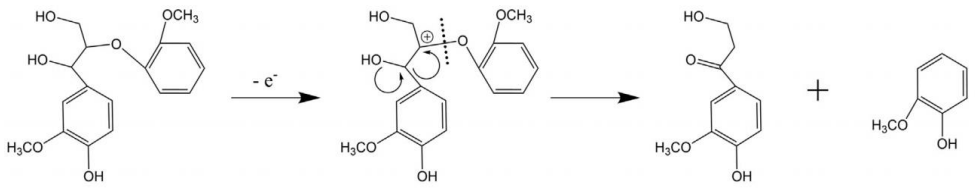


**Figure 4.3.** Oxidative reaction mechanism for the cleavage of β-O-4 bond adapted from[134].

Among these two oxidations, nitrobenzene is considered more effective compared to cupric oxidation in case of aldehyde extraction[131]. But nitrobenzene and its reduced form show very harmful effects and are required to remove from the reaction mixture which is not easy. On the other hand, cupric oxide and its reduced form are very easy to remove from the reaction mixture. Additionally, most of the cupric oxide is produced from its reduced form which makes it more beneficial over the nitrobenzene[131, 135]. In recent years, lots of oxidation analysis has been performed on lignocellulose materials and lignin-blended materials but very few analysis has been done on alkali lignin by cupric oxide oxidation[13] and till date, no data has been found on its residue after hydrodeoxygenation reaction.

Therefore, the aim of our present study is to determine the structural moieties present in the alkali lignin and its residue after hydrodeoxygenation reaction. The objectives of this study are 1. To use cupric oxide for the analysis and identification of phenolic monomers present in lignin and its residue. 2. To quantitative determination of different types of phenolic monomers present in lignin and its residue. 3. Optimize the reaction conditions for the depolymerization of lignin.

**4.2. Materials**

In this study, alkali lignin from Sigma-Aldrich (St. Louis, MO) and the residue after hydrodeoxygenation reaction of lignin at 240 °C was used as a sample. Cupric oxide and guaiacol were purchased from Acros organics (New Jersey, USA) and other standards such as vanillin, acetovanillone, and homovanillic acid were purchased from Sigma-Aldric (St. Louis, MO). O-terphenyl from Sigma-Aldrich (St. Louis, MO) was used as an internal

standard during GC-MS analysis. Methylene dichloride and sodium hydroxide were purchased from fisher scientific (Fair Lawn, New Jersey). All the chemicals were used without any further purification.

### 4.3. Preparation of standards for calibration

Standard solution of guaiacol, vanillin, acetovanillone, and homovanillic acid and internal standard O-terphenyl were made for the quantification of oxidative products. Stock solutions of both standard phenolic monomers of 1000 ppm and internal standard of 1000 ppm were prepared in DCM. The stock standard solutions of guaiacol, vanillin, acetovanillone, and homovanillic acid were diluted by DCM to prepare calibration standards of 31, 62, 125, 250, 500, and 1000 ppm. Three different sets of calibration standard were prepared where the concentration of internal standard was 50 ppm. A calibration curve was constructed by the average peak area signal ratios of standard to internal standard. The signal ratio was plotted as a function of concentration of standard solutions. The peak areas of both standard and internal standard were calculated by manual integration from baseline to baseline using Agilent ChemStation software (Santa Clara, CA, USA). Calibration behavior of standards were evaluated by the regression factor ($R^2$) which was obtained from the linear equation of $y = mx + c$.

### 4.4. Methods

#### 4.4.1. Cupric Oxide Oxidation

In this oxidation, the pearl method was used after slight modifications for the oxidation of lignin and its residue[136-137]. About 100 mg of samples along with 1 g of CuO

were taken in a 100 ml round bottom flask and mixed well with firmly stirring. After that, the flask was degassed and filled with nitrogen gas to maintain an inert atmosphere inside the flask. Then about 15 mL of 2M NaOH was added into the flask and the reaction mixtures were properly stirred at room temperature until the samples were completely dissolved. The reactions were carried out for 2.5 hours at around 175°C with water cooling and continuous stirring. After the completion of reaction, the flask was taken out and kept at room temperature for cooling and then clear reaction mixtures were transferred to other vials for further treatment. The mixtures were acidified with concentrated HCl to maintain the pH at 2-3 and filtered to remove all the insoluble particles from the reaction mixtures. Then the phenolic monomers were extracted by liquid-liquid extraction using 10 mL methylene chloride three times from the acidified reaction mixtures and extracted methylene layers were combined and evaporated by passing nitrogen gas over them under a controlled vacuum. Finally, 5 mL of methylene chloride was added into the crude oxidation mixture which was used as a stock solution for further analysis.

### 4.4.2. GC-MS Analysis

To determine the phenolic monomers present in lignin and its residue a gas chromatography mass spectroscopy was performed by using Agilent 7890A and 7890B (Wilmington, DE) system equipped with Agilent 5975C and 5977B, respectively. Both of MS were triple-axis mass detector with electron-impact ionization. An injection volume of 2 μL was used with the split-less mode for both the lignin samples and the residue along with the standards at an injection temperature of 280°C. An Agilent (30 m x 250 μm x 0.25 μm) 5%-phenyl-methylpolysiloxane capillary column was used with an initial temperature

of 50°C, held for 0 min, heating up to 200°C with heating rate of 20°C/min and held for 1 min, then heating rate at 40°C/min up to 300 °C held for 2 mins. Hydrogen was used as a carrier gas at a flow rate of 1.2 mL/min. The MS analysis was performed in full-scan mode with a range of m/z 50-600 and the Agilent Chemstation software was used to autotune the mass detector. The NIST database and authentic standards were used to identify and quantify the structural moieties present in the lignin and its residue.

## 4.5. Results and Discussion

### 4.5.1. Oxidation Result of Lignin and Residue.

#### 4.5.1.1. Chromatography and Quantification Results

The phenolic moieties present in the oxidation mixture were identified and determined using a 5%-phenyl-methylpolysiloxane capillary column with a linear temperature program. Phenolic monomers were classified into *p*-hydroxyphenyl (H), guaiacyl (G), and syringyl (S) phenolic moieties. Guaiacol (G), vanillin (G), Acetovanillone (G) and Homovanillic acid (G) standards were used for the quantification of all the respective H, G, and S moieties present and 1, 3, 5-tri-tert-butyl benzene was used as an internal standard.

**Figure 4.4** shows the calibration curve of Guaiacol, vanillin, Acetovanillone, and Homovanillic acid. Calibration curves were constructed by the average peak area signal ratios of standard to internal standard which were plotted as a function of standard concentrations. The linearity of the calibration curve was determined by the evaluation of the regression and correlation coefficient ($R^2$) factor. It was shown from the following

chromatogram that, the regression and correlation coefficient ($R^2$) > 0.99 was considered precise.

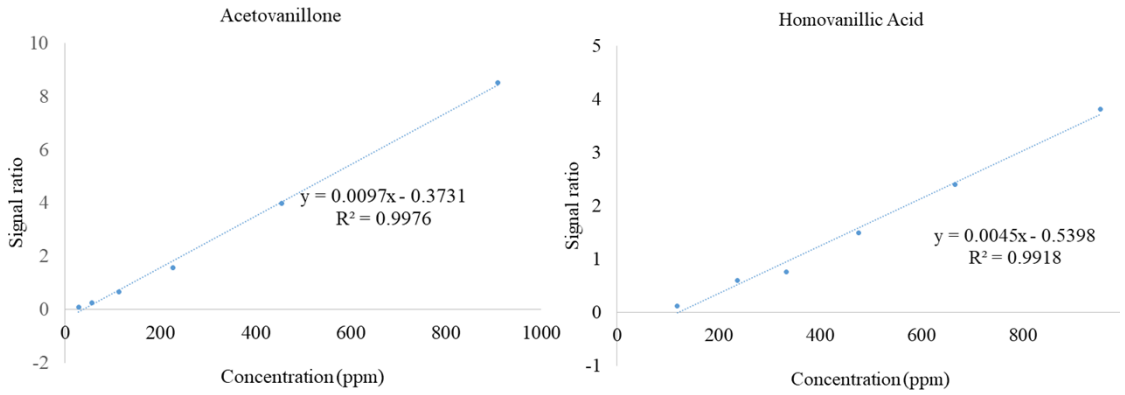


**Figure 4.4.** Calibration chromatogram for guaiacol, vanillin, acetovanillone, and homovanillic acid.

Lignin and its residue were subjected to monomeric structural characterization by cupric oxide oxidation followed by GC-MS analysis. The Chromatograms of lignin and its residue are shown in **Figure 4.5** and **Figure 4.6,** respectively. On the other hand, the quantitative results are shown in **Table 4.1** and **Table 4.2,** respectively. It is shown from **Table 4.1** that the %RSD for phenolic moieties in lignin is less than 5% and **Table 4.2** shows the %RSD is less than 6%. **Figure 4.7** shows the comparison of the oxidation products of phenolic monomers between the lignin and its residue.

**Table 4.1.** Identified phenolic moieties, type, average yield (mg/g lignin dry weight) from cupric oxide oxidation of lignin.

| No | Name of Moiety | Type | Amount (mg/g) | STD | %RSD |
|---|---|---|---|---|---|
| 1 | Guaiacol | G | 1.25 | 0.006 | 4.72 |
| 2 | Vanillin | G | 8.48 | 0.019 | 2.29 |
| 3 | Acetovanillone | G | 2.06 | 0.008 | 3.73 |
| 4 | Homovanillic | G | 4.79 | 0.013 | 2.78 |

**Table 4.2.** Identified phenolic moieties, type, average yield (mg/g lignin dry weight) from cupric oxide oxidation of residue.

| No | Name of Moiety | Type | Amount (mg/g) | STD | %RSD |
|---|---|---|---|---|---|
| 1 | Vanillin | G | 5.22 | 0.013 | 2.54 |
| 2 | Acetovanillone | G | 1.90 | 0.011 | 5.66 |

The GC-MS analysis showed lignin produced four phenolic monomers such as guaiacol (1.25±0.01 mg/g), vanillin (8.48±0.02 mg/g), acetovanillone (2.06±0.01 mg/g) and homovanillic acid (4.79±0.01 mg/g) moieties. Among that vanillin is the major product and homovanillic acid is the second major product. On the other hand, residue produced two phenolic monomers, vanillin (5.22±0.01 mg/g) and acetovanillone (1.90±0.01 mg/g) moieties. It was also shown that residue produced less amount of vanillin than lignin and no peak was found for guaiacol and homovanillic acid in residue which proved that all guaiacol and homovanillic acid along with significant amount vanillin were gone through the reaction mixture during the hydrodeoxygenation reaction. Additionally, residue contain little less amount of acetovanillone than lignin which indicates very small amount of

acetovanillone went through the reaction mixture during the hydrodeoxygenation reaction. Finally, the results showed that all the phenolic monomers are G type moieties, and no syringyl (S) of P-hydroxyphenyl (H) moiety were shown in this study.

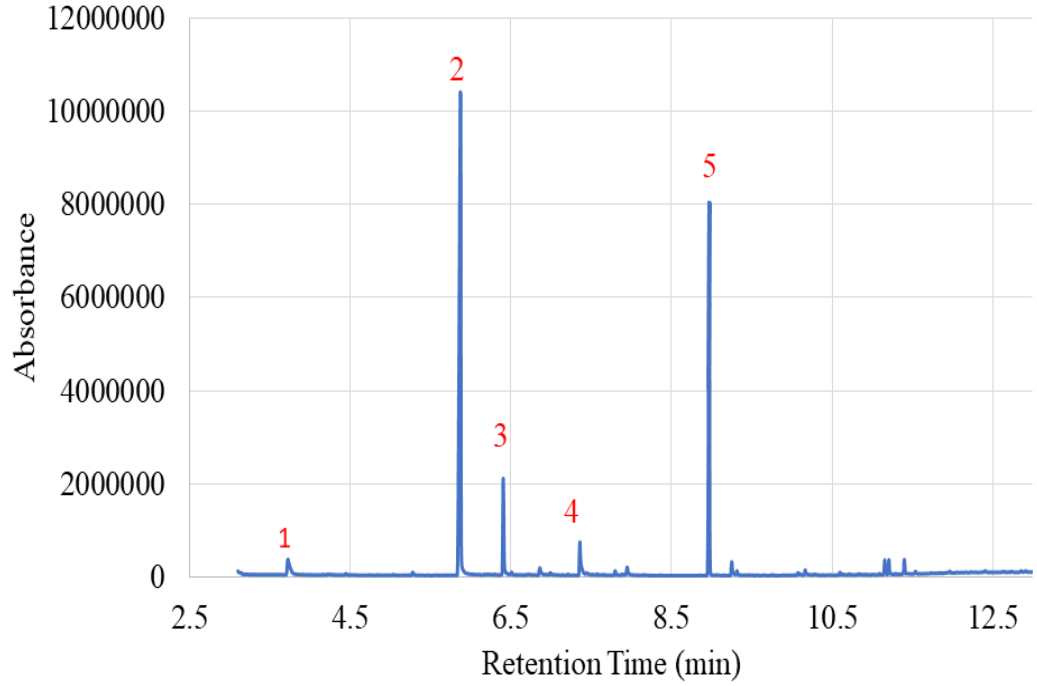


**Figure 4.5.** Chromatogram of oxidative depolymerized products of lignin.

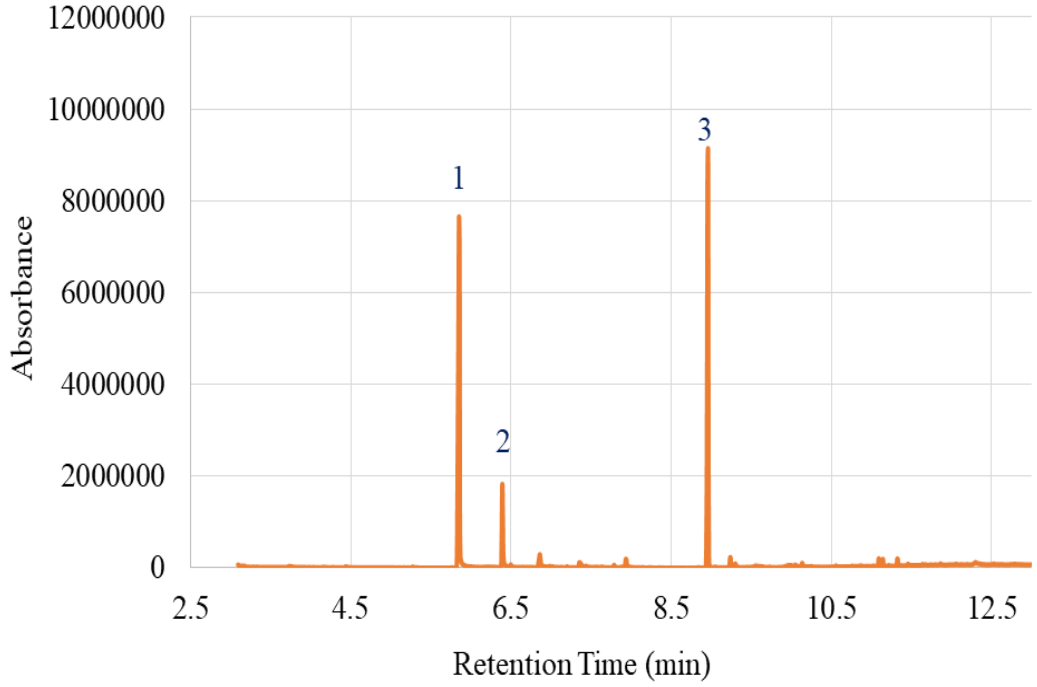


**Figure 4.6.** Chromatogram of oxidative depolymerized products of residue.

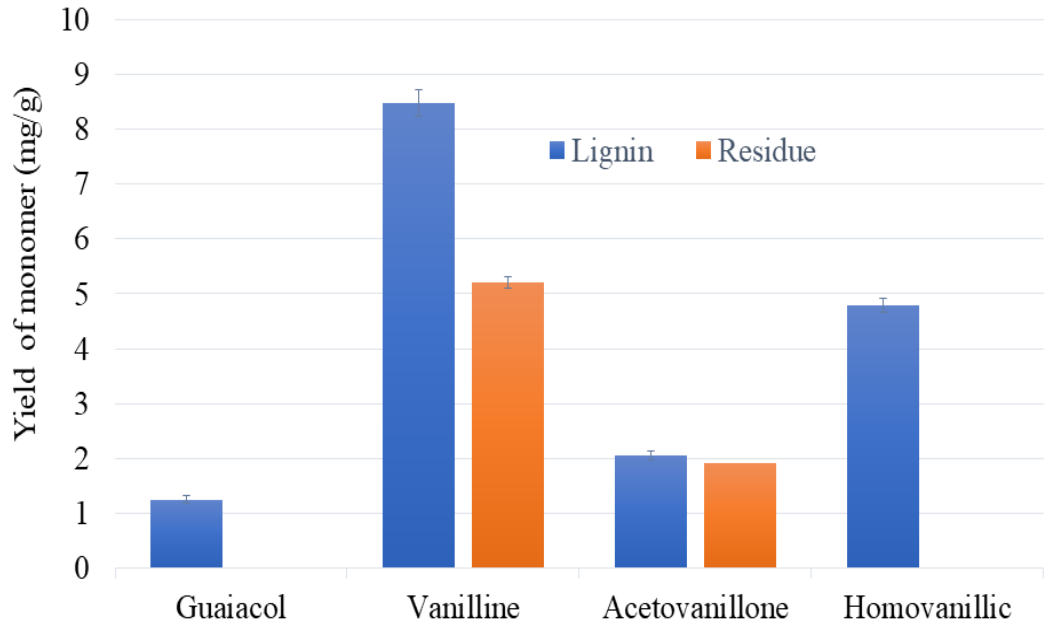


**Figure 4.7.** Comparison between depolymerized products of lignin and its residue.

#### 4.5.1.2. Conclusion

Lignin and its residue were successfully degraded into phenolic compounds by oxidative degradation and identified and quantified by GC-MS analysis. In this study, oxidant CuO cleaved the ether linkages of the compound and produced different types of phenolic compounds. Lignin produced four different phenolic compounds and residue produced two different compounds, among them vanillin was the major product. The residue does not produce guaiacol and homovanillic acid and the production of vanillin also significantly less than lignin. Therefore, our study showed significant amount of guaiacol, vanillin, and homovanillic acid were gone through the reaction mixture during the hydrodeoxygenation reaction. Our study also showed that all the aromatic monomers were G type moieties, and there was no existence of S/P types moieties present in the samples.

### 4.5.2. Oxidation Result of Alkali Lignin at different Temperatures and Times.

Alkali lignin were subjected to structural characterization by cupric oxide oxidation followed by GC-MS analysis. The chromatogram of lignin at different temperatures and times are shown in **Figure 4.8** and **Figure 4.9,** respectively. The quantitative results are shown in **Table 4.3** and **Table 4.4,** respectively. On the other hand, comparison of moieties present in lignin with standard error at different temperature and times are shown in **Figure 4.10** and **Figure 4.11**, respectively

**4.5.2.1. Effects of temperature for the oxidative degradation of lignin into Phenolic monomers.**

Oxidative degradation of lignin was carried out at three different temperatures 125 °C, 150 °C and175 °C for 2.5 hours. **Table 4.3** shows the production of guaiacol and acetovanillone slightly increased when the temperature changes from 125 °C to 150 °C and decreased at 175 °. But the production of vanillin significantly increased from 125 °C to 175 °C which is the major products of this degradation. On the other hand, homovanillic acid slightly increased up to 150 °C and then significantly decreased at temperature 175 °C. After analysis all the data, it was found that the reaction at 150 °C for 2.5 hours gives reasonably good result compare to other conditions.

**Table 4.3.** Identified phenolic moieties, type, average yield (mg/g lignin dry weight) from cupric oxide oxidation of lignin at different temperatures.

| | | | 125 °C | | 150 °C | | 175 °C | |
|---|---|---|---|---|---|---|---|---|
| No | Name of Moiety | Type | Amount (mg/g) | STD (±) | Amount (mg/g) | STD (±) | Amount (mg/g) | STD (±) |
| 1 | Guaiacol | G | 1.45 | 0.08 | 1.55 | 0.09 | 1.25 | 0.07 |
| 2 | Vanillin | G | 6.14 | 0.22 | 7.33 | 0.57 | 8.48 | 0.24 |
| 3 | Acetovanillone | G | 2.09 | 0.10 | 2.15 | 0.04 | 2.06 | 0.08 |
| 4 | Homovanillic | G | 6.42 | 0.26 | 6.46 | 0.12 | 4.79 | 0.13 |

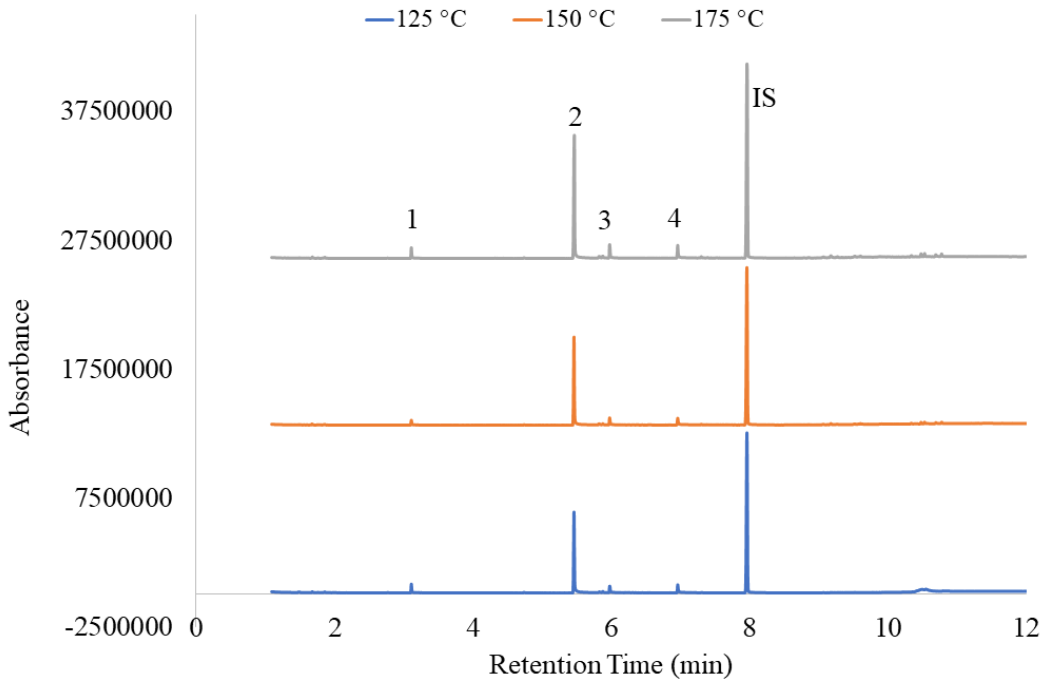


**Figure 4.8.** Chromatogram of oxidative depolymerized products of lignin at different temperatures.

### 4.5.2.2. Effects of time for the oxidative degradation of lignin into Phenolic monomers.

From the analysis of effect of temperatures, it was found that degradative reaction at 150 °C and 2.5 hours gives better conversion compared to other conditions. Therefore, in this section, degradation reaction was carried out at three different times and 150 °C to get optimized time for better conversion. After analysis, the quantitative data shows in **Table 4.4**, The production of guaiacol was stable all three temperatures. **Table 4.4** represents vanillin is a major product and its production increased with the increased of times. The production of acetovanillone and homovanillic acid also increased up to 2 hours and then decreased slightly when the time reaches at 2.5 hours.

**Table 4.4.** Identified phenolic moieties, type, average yield (mg/g lignin dry weight) from cupric oxide oxidation of lignin at different times.

| No | Name of Moiety | Type | 1.5 Hours | | 2 Hours | | 2.5 Hours | |
|---|---|---|---|---|---|---|---|---|
| | | | Amount (mg/g) | STD (±) | Amount (mg/g) | STD (±) | Amount (mg/g) | STD (±) |
| 1 | Guaiacol | G | 1.57 | 0.11 | 1.54 | 0.05 | 1.55 | 0.09 |
| 2 | Vanillin | G | 4.46 | 0.44 | 4.58 | 0.06 | 7.33 | 0.57 |
| 3 | Acetovanillone | G | 2.22 | 0.05 | 2.37 | 0.20 | 2.15 | 0.04 |
| 4 | Homovanillic | G | 6.68 | 0.09 | 6.91 | 0.27 | 6.46 | 0.12 |

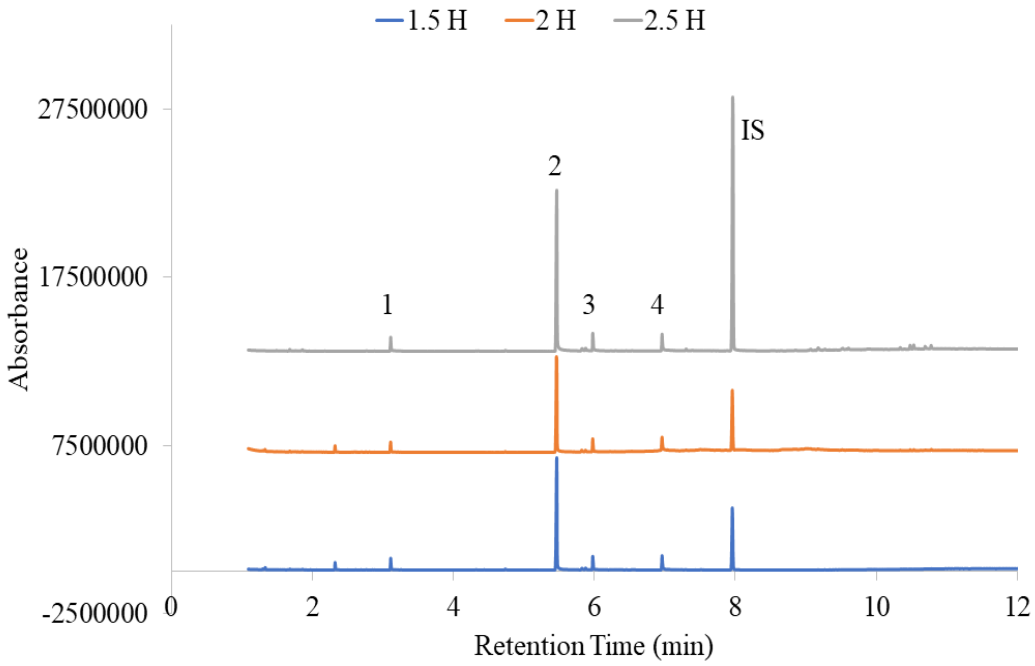


**Figure 4.9.** Chromatogram of oxidative depolymerized products of lignin at different times.

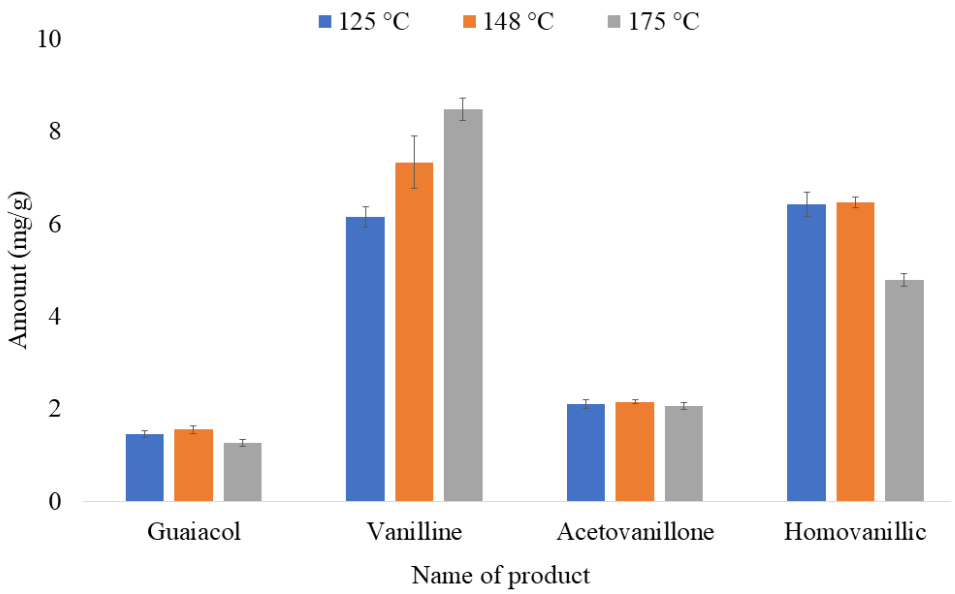


**Figure 4.10.** Comparison of depolymerized products of lignin at different temperatures.

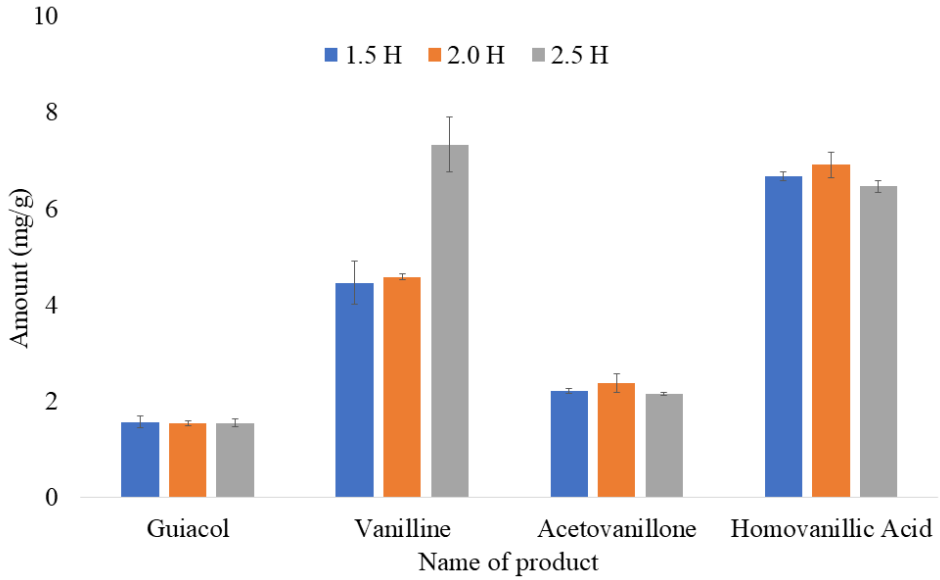


**Figure 4.11.** Comparison of depolymerized products of lignin at different times.

#### 4.5.2.3. Conclusion

In this study, oxidative degradation reactions were investigated at three different temperatures and three different times. The production of vanillin was highest at 175 °C and 2.5 hours but the production of homovanillic acid significantly decreased at 175 °C temperature. On the other hand, production of guaiacol, acetovanillone, and homovanillic acid slightly decreased when the time reaches 2.5 hours, but production of vanillin significantly increased when the time reaches 2.5 hours. Therefore, after analyzing all the quantitative data of phenolic monomers, it was found that optimization condition is 150 °C and 2.5 hours for the better production of phenolic monomers.

# CHAPTER FIVE

# EXTRACTION AND CHARACTERIZATION OF LIGNIN FROM WHEAT STRAW

## 5.1. Introduction

Lignocellulose biomass is a universally available most abundantly renewable resource, which is considered as a potential source to produce various types of chemicals and biomaterials. It is very cheap because of its availability all over the world. The main components of biomass are cellulose, hemicellulose, and lignin along with some extractives and inorganic materials. Extractives present in biomass is easily removable by solubilizing in water and ethanol because they are very soluble in water and ethanol. Inorganic materials present in biomass in form of inorganic compound and minerals which are determined as an ash content in biomass.

Lignin is the 2$^{nd}$ most abundant natural polymer after cellulose. Its proportion varies in biomass from 10% to 25% depending on the source and environment[44-45]. Lignin is considered as a building block of biomass that binds the cellulose and hemicellulose together to give a strong structure of the grass and plant. It is a three-dimensional (**Fig 5.1**)[138] crossed linked organic polymers composed of three different phenyl-propanoid units which include: coniferyl, sinapyl and p-coumaryl alcohols (**Fig 5. 2**). These alcohols units combined by enzymatic polymerization produce a giant molecule contain different types of functional groups and linkages.[139-140]

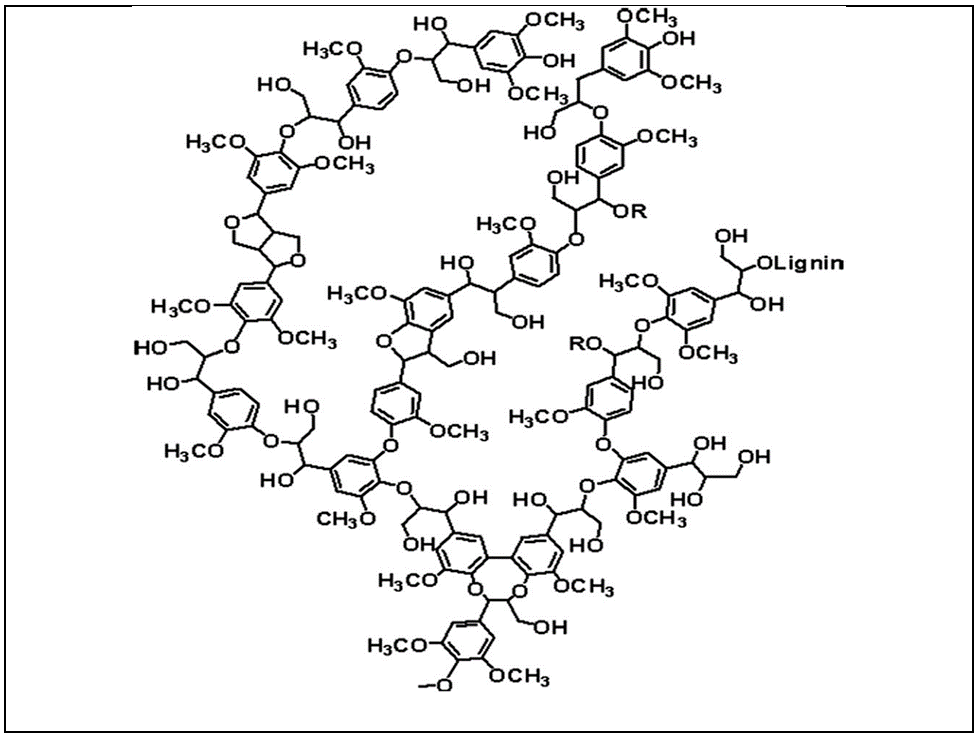


**Figure 5.1**: Three-dimensional structure of Lignin[138].

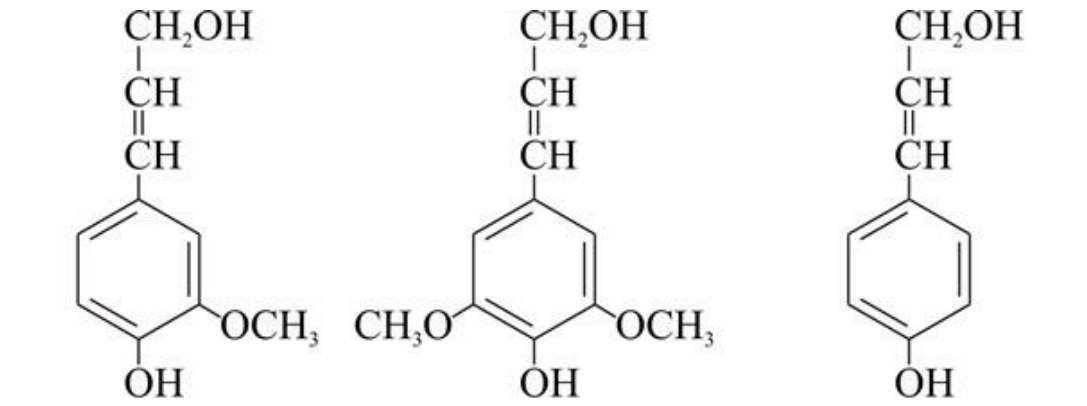


**Figure 5.2**: Monomers of Lignin.

Lignin is being isolated from numerous sources such as jute, hemp, alfalfa, cotton, wood, etc. The physical and chemical properties of lignin are varies based on their sources and extraction methods. As a result, the use of lignin in a different application could be vary based on their formulations. To isolate and determine the amount of lignin from biomass, a stepwise procedure should have followed to eliminate obstacles and bias during the analysis. In our study, The National Renewable Energy Laboratory (NREL) procedure was followed, where they developed several detailed procedures for this purpose [141]. The significance of these methods is that they describe a detailed procedure for drying, size reduction, and obtaining uniform samples and reduces obstacles and bias from analysis of total solids, ash, extractives, and lignin content.

The objectives of our present work are to provide an organosolv process to separate the lignin components from wheat straw. For this study, biomass was treated with a mixture of water-immiscible organic solvent, a water-miscible alcohol, and an acid catalyst for the pretreatment of biomass at different temperatures and times to obtain the maximum amount of lignin product. After that, the isolated lignin was studied by thermal analysis, spectrometric analysis, and sub-critical fluid extraction analysis.

## 5.2. Materials and Method

### 5.2.1. Materials

Wheat straw was obtained from a local company. The chemicals used for this study were acetone, acetonitrile, dimethyl sulfoxide, ethanol 200 proof, methylene chloride, concentrated sulfuric acid, cellulose, Hydro-matrix were obtained from Thermo Fisher Scientific. All the chemicals used for this study were analytical grade.

### 5.2.2. Solvent Mixtures and Pretreatment Conditions

Biomass samples were treated with a mixture of three different solvents e.g., methyl isobutyl ketone, ethanol 200 proof, and 0.05-0.1M sulfuric acid in the water where the ratio of solvent was 11:5:4, respectively. Sulfuric acid is used as an inorganic catalyst which helps to break down the biomass into its component and reduce the reaction times and temperatures. The reaction was carried out at three different temperatures and two acidic conditions where each reaction was carried out in triplicate.

### 5.2.3. Pretreatment process

The biomass samples were pretreated with the solvent mixture using Accelerated Solvent Extraction (Dionex model 350) equipped with a sample carrousel, 34 ml stainless steel cells, and 4×2 L bottles. About 1g of the sample was taken into the cell followed by hydromatrix to make the cell homogeneous all the way, then the cell was kept on the auto cell holder. After that biomass samples were pretreated with solvent mixtures which are passing by an automated system under the following conditions.

Preheat time: o minutes

Temperatures: 140 ºC, 170 ºC, 200 ºC

Heat time: 7, 8, 9 minutes

Pressure: 1500 psi

Static time: 60 minutes

Purge time: 300 seconds

Cycles: 1

### 5.2.4. Analysis of samples

After the end of the extraction, the reaction mixture was collected from the collection bottle. Usually, the liquid reaction mixture is homogeneous depending on the solvent mixture which was used during the extraction. The liquid reaction mixtures contain two layers organic and aqueous where aqueous or organic solvent was added for phase separation. After that, the organic phase was completely dried overnight, and the percent yield was determined. Finally, the dried solid was used for further characterization.

### 5.2.5. Thermal Analysis

The thermogravimetry analysis of extracted lignin was carried out by using TG/DTA 220 from Seiko Instruments, Japan. About 10 mg of samples were taken in a TGA pan for analysis. The oven temperature was performed from room temperature to 575°C at a constant heating rate of 10 °C/min. Nitrogen gas was used as a carrier gas at a flow rate of 20 mL/min to maintain an inert atmosphere and to avoid the samples to contact with the air. The nitrogen gas also helps to sweep the pyrolysis gas like $H_2$, $CO_2$, CO, $CH_4$, $C_2H_2$ and water vapor[59] from the system which is responsible for the vapor phase interaction with the samples.

### 5.2.6. Attenuated Total Reflectance Fourier Transform Spectroscopy (ATR-FTIR) Analysis

FTIR data was obtained by using a Thermo-Fisher Scientific Nicolet 380 FTIR spectrometer in the attenuated total reflectance mode. The spectra were recorded between

400 and 4000 $cm^{-1}$ with an 8 $cm^{-1}$ resolution with 100 scans where the spectra of the samples were analyzed by EZ OMNIC software.

### 5.2.7. High-Temperature Hydrotreatment of Extracted Lignin

Hydrothermal liquefaction reactions at high temperature were done in a stainless-steel vessel reactor of Helix$^{TM}$, a laboratory fluid process development unit which was engineered by Applied Separations (Allentown, PA). The reaction was conducted in a 24 mL reactor vessel equipped by an oven which was controlled by computer software. About 200 mg of the sample was taken in the vessel along with 20 mg of 1.7%V/$ZrO_2$ catalyst. The reaction condition was 240 °C for 10 minutes where the vessel pressure was 15-20 MPa. Catalyst amount for all the reactions was selected 10% (w/w) referenced by the lignin which was taken by the considerations of other authors[142]. The vessel was filled by 22 mL water which was pumped to the vessel with a flow rate of 22mL/min. After that, the oven temperature was set at a chosen temperature at a rate of 15 °C/min. The reaction time was counted when the temperature reached at 240 °C. Finally, the reaction mixture was collected in a vial surrounded by a condenser through an outlet channel.

### 5.2.8. GC-MS Analysis

To determine the phenolic monomers of extracted lignin, a gas chromatography mass spectroscopy (GC-MS) was performed by using an Agilent 7890B (Wilmington, DE) system equipped with an Agilent 5977B triple-axis mass detector with electron-impact ionization. An injection volume of 2 μL was used with the split-less mode for the lignin samples and the standards at an injection temperature of 300°C. An Agilent (30 m x 250

µm x 0.25 µm) 5%-phenyl-methylpolysiloxane capillary column was used with an initial temperature of 50°C and held for 0 min, then at a heating rate of 20°C/min up to 200°C and held for 1 min, and finally heating rate of 40°C/min up to 300 °C held for 2 min. Hydrogen gas was used as a carrier gas at a flow rate of 1.2 mL/min. The MS analysis was performed in full-scan mode with a range of m/z 50-600 and the Agilent Chemstation software was used to autotune the mass detector. The NIST database and authentic standards were used to identify and quantify the structural moieties present in the extracted lignin.

## 5.3. Results and Discussion

### 5.3.1. Effects of Temperatures and acid concentrations on lignin extraction from wheat straw

In our study, extraction of lignin from wheat straw biomass was carried out using the mixture of ethanol, methyl iso-butyl ketone, and sulfuric acid in water. The objective of acid is to separate the lignin compound from biomass by dissolving them in the mixture of ethanol and methyl iso-butyl ketone organic solvent. The mixture of acid/water helps to cleave the ether linkages between lignin and hemicellulose and accelerating the separation process[143].

To optimize the conditions for the isolation of lignin from wheat straw, extraction was carried out at three different temperatures and two acidic conditions for 60 minutes by accelerated solvent extraction. The quantitative percent results at 140 ºC, 170 ºC, 200 ºC are shown in **Table 5.1** at two acidic conditions.

**Table 5.1:** Percent product of extracted lignin at different conditions.

| | 140 ºC | | 170 ºC | | 200 ºC | |
|---|---|---|---|---|---|---|
| Acidic Condition (%) | Percent amount (%) | STD (±) | Percent amount (%) | STD (±) | Percent amount (%) | STD (±) |
| 0.05 | 13.89 | 0.66 | 18.92 | 0.44 | 27.80 | 0.65 |
| 0.10 | 15.97 | 0.69 | 19.39 | 0.79 | 29.16 | 1.25 |

The results showed that the production of lignin is increased with the increase of temperature. The percent of lignin extraction was 13.89 %, 18.92 %, and 27.80 % at 140 °C, 170 °C, and 200 °C, respectively at 0.05M acidic condition. On the other hand, the percent of lignin extraction was 15.97 %, 19.39 %, and 29.16 % at 140 °C, 170 °C, and 200 °C, respectively at 0.10 M acidic condition. Watkins, D., et al. reported that, the maximum amount of lignin was extracted from wheat lignin is 20.40%[144]. In their study, they pretreated the wheat biomass with formic/acidic acid followed by peroxyformic/peroxyacetic acid. Therefore, in our study, the extraction of lignin increased because of the use of ethanol. As strong solvent water can break the structure of lignin and hemicellulose, and wrapped up the cellulose for further pretreatment. But mixture of water-ethanol improves the dissolving capacity of more lignin. In addition, a mixture of water-ethanol increases the surface area of biomass and decreases the potential reticence of cellulose for further hydrolysis process[145-146].

### 5.3.2. Results of Thermal Analysis

Thermal stability and decomposition behavior of extracted lignin from wheat straw were studied with the increase of temperature from 25°C to 560°C at a rate of 15°C/min under nitrogen atmosphere. **Figure 5.3** represents the TG and DTG curves of lignin. TG

curve represents the % weight loss of the sample with the increase of temperature. On the other hand, the DTG curve represents the rate of weight loss at the corresponding temperature of the TG curve. These two thermogram describes the thermal behavior of lignin at various temperatures. **Table 5.2** shows the various degradation stages at different temperature ranges, their corresponding peak and weight loss, maximum thermal decomposition temperature, and % of residual carbon after 560 °C for extracted lignin.

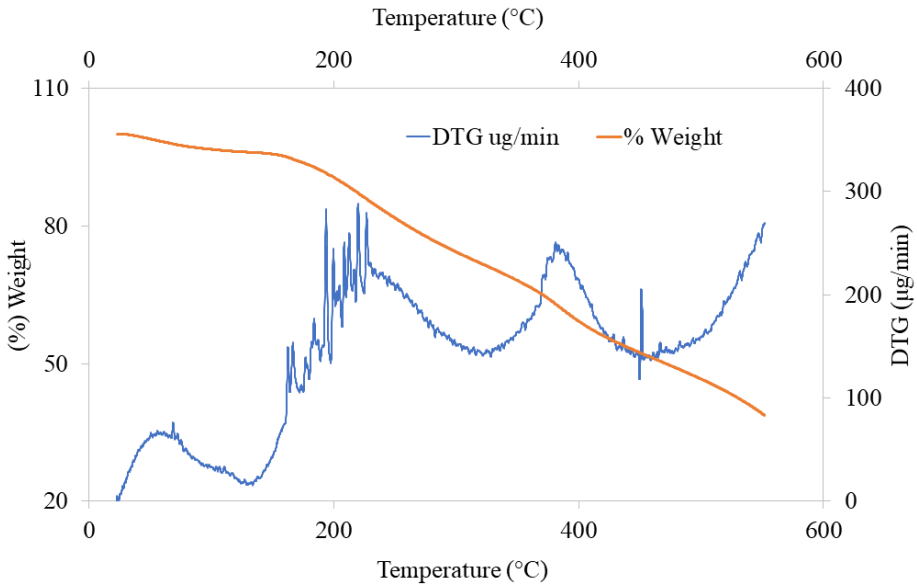


**Figure 5.3**: Pyrolysis TG and DTG curve for lignin from room temperature to 575°C at a constant heating rate of 15 °C/min under $N_2$ atmosphere.

The DTG curve shows 4 different types of peak. The small peak at temperature range 25-134˚C is mainly for the evaporation of free and bound water[14] with the sample itself. Therefore, the initial weight loss for the extracted lignin was 3.97 %. A very small DTG peak was shown in this region indicating of slow weight loss during the drying stage.

**Table 5.2:** Degradation stages of the extracted lignin in the TG and DTG curves.

| Degradation stage | Corresponding peak | Temperature range °C | % Mass loss | DTG $_{max}$ | Residual C % |
|---|---|---|---|---|---|
| Drying | 1 | 22-134 | 3.97±0.48 | - | - |
| 1$^{st}$ | 2 | 134-328 | 25.18±0.47 | - | - |
| 2$^{nd}$ | 3 | 328-453 | 22.83±0.73 | 389 | - |
| 3$^{rd}$ | 4 | 453-555 | 9.11±0.28 | - | - |
| Residual carbon | - | After 555 | - | - | 38.91 |

Degradation of lignin mainly started from the 1$^{st}$ degradation stage. During this stage, the extracted lignin lost its weight about 25.18% where the degradation started at 134 °C and continued up to 328 °C. In this region, the mass loss for the sample is devolatilization of the functional groups and side-chain present in the sample[60].

The key degradation for the sample mainly occurred at the 2$^{nd}$ stage. The sample started degrading at a higher rate due to the continued degradation of functional groups present in the samples, continuous breakdown of the side of the samples[61]. The initiate of mass loss is started with the breakdown of β-O-4 linkage[62] and formation of the monomeric phenolic compound while the cleavage of β-O-4 linkage started at 300 °C and went up to 453 °C[62]. The weight loss of lignin was observed 22.83% in the temperature range of 328-453 °C. The highest peak or $DTG_{max}$ was observed at 389 °C for lignin which represents that the lignin degraded at a higher rate at temperature 389 °C.

The third stage of degradation occurred at a temperature range from 453-555°C. This region displays apparent weight loss due to the degradation of a few aromatic

compounds and the formation of char[63-64]. After 555 °C, the samples initiated to nonvolatilized by forming char and the aromatic structures of lignin started to highly condensed[18, 65]. At this point, most of the elemental hydrogen and oxygen are liberated as a gaseous leaving only carbon as a char which called residual carbon[66]. The percentage of residue carbon remained after 575 °C is 38.91%.

### 5.3.3. Results of Spectrometric Analysis

The FTIR spectra of extracted lignin are shown in **Figure 5.4** and characteristics FTIR absorption bands are shown in **Table 5.3**. The spectra of the extracted lignin obtained from FTIR are shown very complex as most of the observed bands are produced by the imposition of various types of vibrations of different functional groups. Therefore, the assignment of many bands is possible only by the approximation of the predominant contribution of certain chemical groups[88]. The absorption band at 3400 $cm^{-1}$ is due to the strong O-H hydroxyl groups present in the aromatic and aliphatic structures of lignin. The bands around 2973 $cm^{-1}$ indicate apparent C-H stretching in methyl and methylene groups of the side chain present in the structure. The absorption band at 1703 $cm^{-1}$ is shown by lignin can be attributed of C= O for unconjugated ketones, carbonyls, and ester groups[18, 89] along with a C=O vibration band at 1225 $cm^{-1}$. The absorption band at 1600 $cm^{-1}$ represents aromatic skeletal vibrational unconjugated bonds. In addition, absorption peaks around 1506 $cm^{-1}$ and 1404 $cm^{-1}$ for the sample are shown by aromatic skeletal vibrations and around 1455 $cm^{-1}$ for aromatic ring vibrations.

**Table 5.3:** FTIR absorption band ($cm^{-1}$) assignments for extracted lignin.

| **Absorption band wavenumbers ($cm^{-1}$)** | **Functional groups** |
|---|---|
| 3400 | O-H Stretching |
| 2973 | C-H Stretching in methyl and methylene groups |
| 1703 | C=O stretch in unconjugated ketone, carbonyl and in ester groups |
| 1600 | Aromatic skeletal vibrations plus C=O Stretch |
| 1506 | Aromatic Skeletal vibrations; G>S |
| 1455 | C-H deformations asymmetric in methyl and methylene |
| 1404 | Aromatic skeletal vibrations plus C-H in plane deformation |
| 1225 | G ring plus C=O stretch |
| 1057 | C-O deformations in secondary alcohols and aliphatic ethers |
| 828 | C-H out of plane in position 2,5,6 of G units |

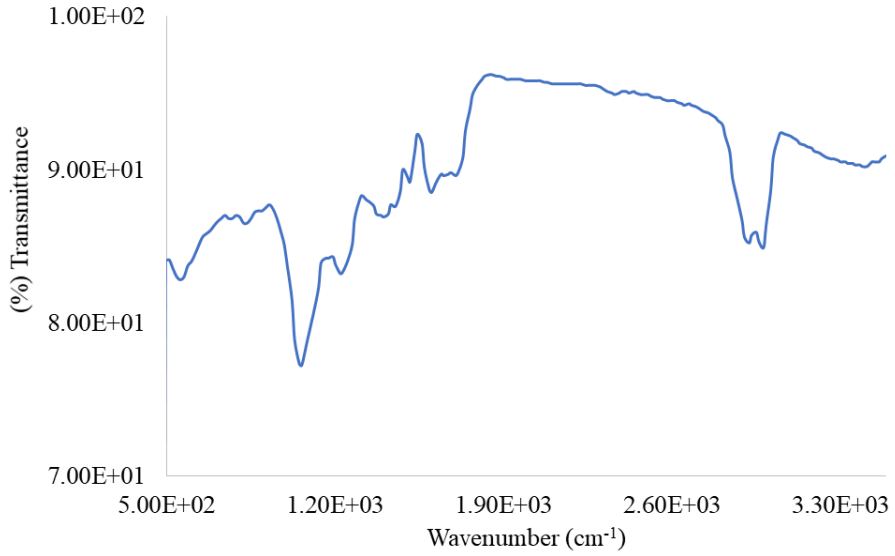


**Figure 5.4**: FTIR Spectrum of extracted lignin.

The absorption region below 1300 $cm^{-1}$ is the fingerprint region. In this region, the investigation of FTIR spectra of extracted lignin is very difficult due to the involvement of different vibrational modes comes from the same functional group. The absorption peak for lignin at 1225 $cm^{-1}$ is a characteristic absorption band for guaiacyl (G) monomer ring plus C=O stretch. The large absorption peak at 1057 $cm^{-1}$ represents the peak is not only for methylal -OH but also for aliphatic -OH[90]. On the other hand, Absorption peak at 828 $cm^{-1}$ for C–H out-of-plane vibrations in position 2, 5 and 6 of guaiacyl.

### 5.3.4. Results of Hydrotreatment of Extracted Lignin

Hydrothermal liquefaction reactions of extracted lignin were performed in a 24 ml vessel reactor using the SFE-helix system. The reaction was performed for 10 mins at 240 °C with the presence of a catalyst to observe the monomeric product yield. The chromatogram of extracted lignin is shown in **Figure 5.5** and the phenolic compounds, their retention time, types of moieties, relative percentage were shown in **Table 5.4**.

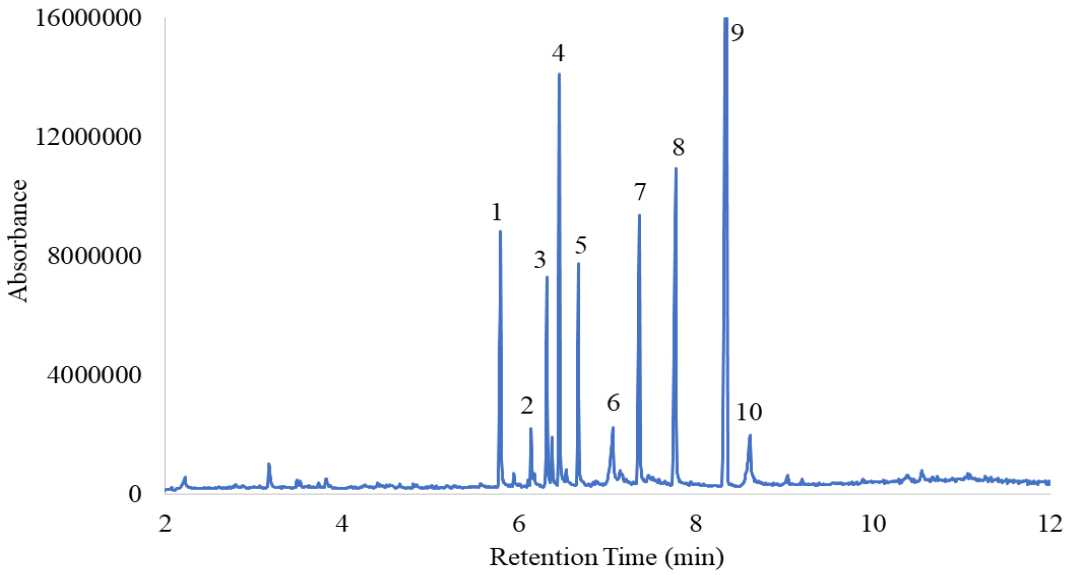


**Figure 5.5.** Chromatogram of hydrothermal liquefaction of extracted lignin at 240 °C and 10 mins in the presence of catalyst.

In this study, the depolymerization of extracted lignin from wheat straw was carried out under the subcritical fluid extraction. The reaction was taken place with the mixture of water and catalyst at 240 ºC for 10 min. Water at 240 ºC behaves like an organic solvent that can dissolve any kind of organic compound. The objective of the catalyst is to depolymerize the lignin molecule into its monomers by breaking down the ether linkages in it.

**Table 5.4:** Identified phenolic compounds, their corresponding retention time (RT), and relative amount (%) from hydrothermal liquefaction of extracted lignin.

| Peak no | RT (Min) | Name of compound | Types of moieties | Relative amount (%) | Total amount (%) |
|---|---|---|---|---|---|
| 1 | 5.796 | Vanillin | G | 11.26 | |
| 2 | 6.139 | Benzaldehyde-3- hydroxyl | H | 3.06 | |
| 3 | 6.311 | Ethanone-1-(4-hydroxyl, 3-methoxyphenol | G | 6.95 | |
| 4 | 6.454 | 1,2-Dimethoxy propyl Benzene | G | 15.73 | |

| | | | | | |
|---|---|---|---|---|---|
| 5 | 6.674 | Guiacylacetone | G | 7.29 | 86.09 |
| 6 | 7.055 | Benzoic Acid, 4-hydroxyl-3-methoxy | G | 4.59 | |
| 7 | 7.358 | Benzaldehyde, 4-hydroxy-3,5-dimethoxy | G | 12.56 | |
| 8 | 7.754 | Ethanone,1(4-hydroxy-3,5-dimethoxyphenyl | S | 18.71 | |
| 9 | 8.331 | IS (o-terphenyl) | | | |
| 10 | 8.611 | Benzoic Acid, 4-hydroxy, 3,5-dimethoxy | S | 5.93 | |

The chromatogram shows 9 different types of phenolic monomers after the hydrothermal liquefaction reaction of extracted lignin at 240 °C for 10 mins. Four major compounds are vanillin, 1,2-Dimethoxy propyl Benzene, Benzaldehyde, 4-hydroxy-3,5-dimethoxy, and Ethanone,1(4-hydroxy-3,5 dimethoxyphenyl where their relative percentage are 11.26%, 15.73%, 12.56%, and 18.71%, respectively. **Table 5.4** shows total relative percent amount of all 9 compounds are 86.09%.

## 5.4. Conclusion

Our present study includes extraction of lignin from wheat straw biomass by using acid/organic solvent through accelerated solvent extraction techniques. After that, extracted lignin was characterized by TGA, FT-IR, Subcritical Fluid Extraction, followed by GC-MS analysis. The study showed lignin was successfully extracted from the wheat straw biomass by accelerated solvent extraction. Results showed, extraction of lignin significantly increased with the increase of reaction time and reached to 27.80 % at 200 °C. On the other hand, extraction of lignin increased slightly when the concentration changed from 0.05% to 0.10 % at the corresponding temperatures. Therefore our study

indicates, the suitable concentration of acid is 0.05 % for the extraction of lignin and a further increase of acid does not affect the extraction that much.

Thermogravimetry analysis (TGA) was used to observe the degradation properties of lignin at different temperature. Thermal study indicates that the significant weight loss was observed during the $1^{st}$ and $2^{nd}$ stages. $DTG_{max}$ for extracted lignin was recorded at 389 °C indicating the maximum rate of weight loss has occurred during the $2^{nd}$ stage. The leftover after 555 °C is considered residual carbon (char). The thermal study showed that percent of residual carbon (char) is about 39% suggesting extracted lignin is stable at high temperature.

The absorption band from the FT-IR studied revealed the structural information of extracted lignin. The absorption band at 1506 $cm^{-1}$ reveals the extracted lignin contains more G moieties than S moieties where the absorption band at 1225, 1057, and 828 $cm^{-1}$ reveal the G moieties present in the lignin.

Hydrothermal liquefaction reactions followed by GC-MS analysis successfully identified and determined the structural moieties present in lignin. Total 9 moieties were determined among them 4 are major components with a total of 86% relative amount. Out of 9 moieties, 6 are G, 2 are S and 1 is H moieties. The hydrothermal liquefaction showed that the extracted lignin contains more G moieties than S which was also proved by FT-IR analysis.

# CHAPTER SIX

# CONCLUSIONS

## 6.1. Summary

Due to the extensive depletion of fossil fuel to produce different types of biochemicals and biomaterials, an alternative resource is very much needed. Because of cheap, easily availability, and sustainable renewability, lignocellulose is appealing the potential alternative for those chemicals and replacing the continuous diminishing of fossil fuels. Studies showed biochemical produced from lignocellulose is easily biodegradable and environmentally safe. Lignocellulose is a very complex biopolymer consists of cellulose, hemicellulose, and lignin. Therefore, the significant transformation of lignocellulose into value-added product is depending on the successful separation into its basic components. In recent years, several pretreatment methods such as organosolv, alkaline, oxidative, hydrothermal, torrefaction, and sub/supercritical fluid-based pretreatment methods has been developed. Among the three basic components of lignocellulose, lignin has been remaining mostly unused because of its complex and crosslinked structure. But being aromatic in nature and easily available, lignin could be a potential source to produce a wide range of biochemicals and bioproducts. Therefore the overall goal of this research is to develop a novel and green technology for the conversion of biomass-based lignin into biochemicals.

To accomplish the goal, lignin was extracted from sustainable and renewable biomass sources and transformed into phenolic monomers through a novel and green methodology. For a better understanding of the reaction mechanism of

hydrodeoxygenation reaction a comprehensive investigation of catalytic hydrodeoxygenation reaction was studied by the comparative structural characterization of lignin and its residue by thermal, spectrometric, and oxidative techniques. A comparative study reveals that hydrodeoxygenation successfully breakdown the ether and C-C linkages of lignin to convert into phenolic monomers. Spectroscopic study showed similar chemical properties, but a smaller number of β-O-4 and β-5 linkages present in residue validate the significant amount of ether and C-C bonds were cleaved during the hydrodeoxygenation reaction. Additionally, the production of phenolic monomers from the residues by cupric oxide oxidation proved that the partial breakdown was occurred in the state of a complete breakdown. On the other hand, thermal and GPC analysis showed, not only ether and C-C bonds were cleaved but also condensation or side reaction has occurred. In addition, higher amount of residual carbon, lower rate of weight loss through the thermal process, and higher polydispersity verify the side reaction or condensation reaction during the hydrodeoxygenation reaction. Higher aliphatic nature of residue compares to lignin also confirms the occurrence of the condensation reaction. Finally, our comparative structural study successfully able to investigate the reaction of catalytic hydrodeoxygenation reaction.

Depolymerization of lignin was also carried out by cupric oxide oxidation followed by GC-MS analysis at different temperatures and times. The aim of this study is to optimize the reaction conditions for better conversion of lignin into its phenolic monomers. Oxidative study found 150 °C and 2.5 hours as a optimize conditions for the better production of phenolic monomers from lignin. The production of vanillin is highest at 175 °C and 2.5 hours but the production of homovanillic acid significantly decreased at 175 °C

temperature. On the other hand, production of guaiacol, acetovanillone, and homovanillic acid slightly decreased when the time reaches 2.5 hours, but production of vanillin significantly increased when the time reaches 2.5 hours. Therefore, after analyzing all the quantitative data of phenolic monomers, it was found that optimization condition is 150 °C and 2.5 hours for the better production of phenolic monomers.

Lignin was successfully extracted from wheat straw by using acid/organic solvent through accelerated solvent extraction techniques. Extraction of lignin increased significantly with the increase of temperature, but a notable increase was not observed when concentration of acid increases. To verify the extracted product, extracted lignin was characterized by TGA, FT-IR, subcritical hydrothermal liquefaction reaction followed by GC-MS analysis. All those studies showed a similar result with the commercial lignin. TGA result showed, significant mass loss during the $1^{st}$ and $2^{nd}$ stage and the residual carbon was observed 39% after 555 °C. The thermal study showed that extracted lignin are stable at high temperature. The absorption band from the FT-IR studied revealed the structural information of extracted lignin. The absorption band at 1506 $cm^{-1}$ reveals the extracted lignin contains more G moieties than S moieties. Additionally, band at 1225, 1057, and 828 $cm^{-1}$ reveal, extracted lignin mainly contains G moieties. Hydrothermal liquefaction reactions followed by GC-MS analysis found total 9 phenolic moieties with a total 86% relative amount. Out of 9 moieties, 6 were categorized as a G, 2 are S and 1 is H moieties. The hydrothermal liquefaction results along with FT-IR analysis revealed extracted lignin contains more G moieties than S moieties.

### 6.1. Future studies and challenges

Although organosolv pretreatment showed excellent performance for the extraction of lignin from lignocellulose, but the use of corrosive chemicals and harsh reaction conditions makes this method environmentally risk. Therefore ionic liquids (ILs) and deep eutectic solvents (DESs) could be an alternative green method for the extraction of lignin. Those method does not require to use of any toxic materials and are easy to recover after the pretreatment and able to reuse at least 4 times. On the other hand, depolymerization of lignin into phenolic monomers through catalytical hydrodeoxygenation reaction and oxidation method showed very promising, green, and economically safer. But catalytic hydrodeoxygenation reaction requires costly instruments and high temperature and cupric oxidation showed lower efficiency which makes those methods costly and commercially less viable. Therefore, ionic liquid, deep eutectic solvents along with microwave-assisted method could be a potential alternative method for the depolymerization of lignin into phenolic monomers. ILs and DESs are analog to each other and its low cost and easy formulation, as well as environmentally safer properties could be making it more beneficial.

In addition, ILs and DESs not only offer promising advantages over other traditional solvents but also offer intrinsic scientific advantages like catalytic activity. As a result, green solvent-based pretreatment and depolymerization of lignin could have a favorable perspective to produce valuable products by the comprehensive study. Therefore, our firm believes that transformation of biomass-based lignin into biochemicals and biomaterials using ILs and DESs media is going to be hot topic inside our group as well as the scientific community for quite the near future.

## REFERENCES


1. Calvo-Flores, F. G.; Dobado, J. A., Lignin as renewable raw material. *ChemSusChem* **2010,** *3* (11), 1227-1235.
2. Sen, S.; Patil, S.; Argyropoulos, D. S., Thermal properties of lignin in copolymers, blends, and composites: a review. *Green Chemistry* **2015,** *17* (11), 4862-4887.
3. Petroleum, B., *BP statistical review of world energy*. British Petroleum: 2001.
4. Lee, C. R.; Yoon, J. S.; Suh, Y.-W.; Choi, J.-W.; Ha, J.-M.; Suh, D. J.; Park, Y.-K., Catalytic roles of metals and supports on hydrodeoxygenation of lignin monomer guaiacol. *Catalysis Communications* **2012,** *17*, 54-58.
5. Huber, G. W.; Iborra, S.; Corma, A., Synthesis of transportation fuels from biomass: chemistry, catalysts, and engineering. *Chemical reviews* **2006,** *106* (9), 4044-4098.
6. Koutsianitis, D.; Mitani, C.; Giagli, K.; Tsalagkas, D.; Halász, K.; Kolonics, O.; Gallis, C.; Csóka, L., Properties of ultrasound extracted bicomponent lignocellulose thin films. *Ultrasonics sonochemistry* **2015,** *23*, 148-155.
7. Roy, R.; Rahman, M. S.; Raynie, D. E., Recent Advances of Greener Pretreatment Technologies of Lignocellulose. *Current Research in Green and Sustainable Chemistry* **2020**, 100035.
8. Zhang, Y.-H. P., Reviving the carbohydrate economy via multi-product lignocellulose biorefineries. *Journal of industrial microbiology & biotechnology* **2008,** *35* (5), 367-375.
9. Menon, V.; Rao, M., Trends in bioconversion of lignocellulose: biofuels, platform chemicals & biorefinery concept. *Progress in energy and combustion science* **2012,** *38* (4), 522-550.
10. Mood, S. H.; Golfeshan, A. H.; Tabatabaei, M.; Jouzani, G. S.; Najafi, G. H.; Gholami, M.; Ardjmand, M., Lignocellulosic biomass to bioethanol, a comprehensive review with a focus on pretreatment. *Renewable and Sustainable Energy Reviews* **2013,** *27*, 77-93.
11. Fernández-Rodríguez, J.; Erdocia, X.; Sánchez, C.; Alriols, M. G.; Labidi, J., Lignin depolymerization for phenolic monomers production by sustainable processes. *Journal of energy chemistry* **2017,** *26* (4), 622-631.
12. Gosselink, R.; De Jong, E.; Guran, B.; Abächerli, A., Co-ordination network for lignin—standardisation, production and applications adapted to market requirements (EUROLIGNIN). *Industrial Crops and Products* **2004,** *20* (2), 121-129.
13. Ninomiya, K.; Ochiai, K.; Eguchi, M.; Kuroda, K.; Tsuge, Y.; Ogino, C.; Taima, T.; Takahashi, K., Oxidative depolymerization potential of biorefinery lignin obtained by ionic liquid pretreatment and subsequent enzymatic saccharification of eucalyptus. *Industrial Crops and Products* **2018,** *111*, 457-461.
14. Brebu, M.; Vasile, C., Thermal degradation of lignin—a review. *Cellulose Chemistry & Technology* **2010,** *44* (9), 353.
15. Kaiser, K.; Benner, R., Characterization of lignin by gas chromatography and mass spectrometry using a simplified CuO oxidation method. *Analytical chemistry* **2011,** *84* (1), 459-464.
16. Guo, D.; Chen, F.; Inoue, K.; Blount, J. W.; Dixon, R. A., Downregulation of caffeic acid 3-O-methyltransferase and caffeoyl CoA 3-O-methyltransferase in transgenic alfalfa: impacts on lignin structure and implications for the biosynthesis of G and S lignin. *The plant cell* **2001,** *13* (1), 73-88.
17. Chen, J. D.; Cui, C.; Li, Y. Q.; Zhou, L.; Ou, Q. D.; Li, C.; Li, Y.; Tang, J. X., Single-junction polymer solar cells exceeding 10% power conversion efficiency. *Advanced Materials* **2015,** *27* (6), 1035-1041.

18. Tejado, A.; Pena, C.; Labidi, J.; Echeverria, J.; Mondragon, I., Physico-chemical characterization of lignins from different sources for use in phenol–formaldehyde resin synthesis. *Bioresource Technology* **2007,** *98* (8), 1655-1663.
19. Chakar, F. S.; Ragauskas, A. J., Review of current and future softwood kraft lignin process chemistry. *Industrial Crops and Products* **2004,** *20* (2), 131-141.
20. Li, C.; Zhao, X.; Wang, A.; Huber, G. W.; Zhang, T., Catalytic transformation of lignin for the production of chemicals and fuels. *Chemical reviews* **2015,** *115* (21), 11559-11624.
21. Charani, P. R.; Dehghani-Firouzabadi, M.; Afra, E.; Blademo, Å.; Naderi, A.; Lindström, T., Production of microfibrillated cellulose from unbleached kraft pulp of Kenaf and Scotch Pine and its effect on the properties of hardwood kraft: microfibrillated cellulose paper. *Cellulose* **2013,** *20* (5), 2559-2567.
22. Phillips, M., The Chemistry of Lignin. *Chemical Reviews* **1934,** *14* (1), 103-170.
23. Vanholme, R.; Demedts, B.; Morreel, K.; Ralph, J.; Boerjan, W., Lignin biosynthesis and structure. *Plant physiology* **2010,** *153* (3), 895-905.
24. Hatakeyama, T.; Hatakeyama, H., *Thermal properties of green polymers and biocomposites*. Springer Science & Business Media: 2006; Vol. 4.
25. Gosselink, R. J.; van Dam, J. E.; de Jong, E.; Scott, E. L.; Sanders, J. P.; Li, J.; Gellerstedt, G., Fractionation, analysis, and PCA modeling of properties of four technical lignins for prediction of their application potential in binders. *Holzforschung* **2010,** *64* (2), 193-200.
26. Kim, Y. S. Kinetic and mechanistic studies of polyoxometalate (POM) reaction with lignin and model compounds. University of British Columbia, 2007.
27. Freudenberg, K., Lignin: its constitution and formation from p-hydroxycinnamyl alcohols. *Science* **1965,** *148* (3670), 595-600.
28. Heitner, C.; Dimmel, D.; Schmidt, J., *Lignin and lignans: advances in chemistry*. CRC press: 2016.
29. Toor, S. S.; Rosendahl, L.; Rudolf, A., Hydrothermal liquefaction of biomass: a review of subcritical water technologies. *Energy* **2011,** *36* (5), 2328-2342.
30. Zhang, B.; Huang, H.-J.; Ramaswamy, S., A kinetics study on hydrothermal liquefaction of high-diversity grassland perennials. *Energy Sources, Part A: Recovery, Utilization, and Environmental Effects* **2012,** *34* (18), 1676-1687.
31. Saravana, P. S.; Chun, B. S., Seaweed polysaccharide isolation using subcritical water hydrolysis. In *Seaweed Polysaccharides*, Elsevier: 2017; pp 47-73.
32. Holliday, R. L.; King, J. W.; List, G. R., Hydrolysis of vegetable oils in sub-and supercritical water. *Industrial & engineering chemistry research* **1997,** *36* (3), 932-935.
33. Notley, S. M.; Norgren, M., Lignin: Functional biomaterial with potential in surface chemistry and nanoscience. *The Nanoscience and Technology of Renewable Biomaterials* **2009**, 173-206.
34. Guo, D.; Liu, B.; Tang, Y.; Zhang, J.; Xia, X.; Tong, S., Catalytic Depolymerization of Alkali Lignin in Sub-and Super-critical Ethanol. *BioResources* **2017,** *12* (3), 5001-5016.
35. Martin, O.; Averous, L., Poly (lactic acid): plasticization and properties of biodegradable multiphase systems. *Polymer* **2001,** *42* (14), 6209-6219.
36. Pillin, I.; Montrelay, N.; Bourmaud, A.; Grohens, Y., Effect of thermo-mechanical cycles on the physico-chemical properties of poly (lactic acid). *Polymer Degradation and Stability* **2008,** *93* (2), 321-328.
37. Södergård, A.; Stolt, M., Industrial production of high molecular weight poly (lactic acid). *Poly (Lactic Acid) Synthesis, Structures, Properties, Processing, and Applications* **2010**, 27-41.
38. Auras, R. A.; Lim, L.-T.; Selke, S. E.; Tsuji, H., *Poly (lactic acid): synthesis, structures, properties, processing, and applications*. John Wiley & Sons: 2011; Vol. 10.

39. Di Lorenzo, M. L., Crystallization behavior of poly (L-lactic acid). *European Polymer Journal* **2005,** *41* (3), 569-575.
40. Sánchez, M. S.; Ribelles, J. G.; Sánchez, F. H.; Mano, J., On the kinetics of melting and crystallization of poly (L-lactic acid) by TMDSC. *Thermochimica acta* **2005,** *430* (1-2), 201-210.
41. Taubner, V.; Shishoo, R., Influence of processing parameters on the degradation of poly (L-lactide) during extrusion. *Journal of applied polymer science* **2001,** *79* (12), 2128-2135.
42. Södergård, A.; Stolt, M., Properties of lactic acid based polymers and their correlation with composition. *Progress in polymer science* **2002,** *27* (6), 1123-1163.
43. Jamshidian, M.; Tehrany, E. A.; Imran, M.; Jacquot, M.; Desobry, S., Poly-Lactic Acid: production, applications, nanocomposites, and release studies. *Comprehensive reviews in food science and food safety* **2010,** *9* (5), 552-571.
44. Hu, L.; Pan, H.; Zhou, Y.; Zhang, M., Methods to improve lignin's reactivity as a phenol substitute and as replacement for other phenolic compounds: A brief review. *BioResources* **2011,** *6* (3), 3515-3525.
45. Min, D.-y.; Smith, S. W.; Chang, H.-m.; Jameel, H., Influence of isolation condition on structure of milled wood lignin characterized by quantitative 13C nuclear magnetic resonance spectroscopy. *BioResources* **2013,** *8* (2), 1790-1800.
46. Galbe, M.; Zacchi, G., Pretreatment of lignocellulosic materials for efficient bioethanol production. In *Biofuels*, Springer: 2007; pp 41-65.
47. Jørgensen, H.; Kristensen, J. B.; Felby, C., Enzymatic conversion of lignocellulose into fermentable sugars: challenges and opportunities. *Biofuels, Bioproducts and Biorefining* **2007,** *1* (2), 119-134.
48. Gidh, A. V.; Decker, S. R.; Vinzant, T. B.; Himmel, M. E.; Williford, C., Determination of lignin by size exclusion chromatography using multi angle laser light scattering. *Journal of Chromatography A* **2006,** *1114* (1), 102-110.
49. West, C.; McTaggart, R.; Letcher, T.; Raynie, D.; Roy, R., Effects of Gamma Irradiation Upon the Mechanical and Chemical Properties of 3D-Printed Samples of Polylactic Acid. *Journal of Manufacturing Science and Engineering* **2019,** *141* (4).
50. Yang, H.; Yan, R.; Chin, T.; Liang, D. T.; Chen, H.; Zheng, C., Thermogravimetric analysis− Fourier transform infrared analysis of palm oil waste pyrolysis. *Energy & fuels* **2004,** *18* (6), 1814-1821.
51. Beall, F., Thermogravimetric analysis of wood lignin and hemicelluloses. *Wood and Fiber Science* **2007,** *1* (3), 215-226.
52. Ramiah, M., Thermogravimetric and differential thermal analysis of cellulose, hemicellulose, and lignin. *Journal of Applied Polymer Science* **1970,** *14* (5), 1323-1337.
53. De Chirico, A.; Audisio, G.; Provasoli, F.; Schieroni, A. G.; Focher, B.; Grossi, B., Differential scanning calorimetry and thermal gravimetric analysis of lignin blended with triglycidyl isocyanurate. *Die Angewandte Makromolekulare Chemie* **1995,** *228* (1), 51-58.
54. Rodrigues, P. C.; Muraro, M.; Garcia, C. M.; Souza, G. P.; Abbate, M.; Schreiner, W. H.; Gomes, M. A., Polyaniline/lignin blends: thermal analysis and XPS. *European Polymer Journal* **2001,** *37* (11), 2217-2223.
55. Vasile, C.; Downey, M.; Wong, B.; Macoveanu, M.; Pascu, M.; Choi, J.; Sung, C.; Baker, W., Polyolefins/lignosulfonates blends. II. Isotactic polypropylene/epoxy-modified lignin blends. *Cellulose Chemistry and Technology* **1998,** *32* (1-2), 61-88.
56. Singh, K.; Risse, M.; Das, K.; Worley, J., Determination of composition of cellulose and lignin mixtures using thermogravimetric analysis. *Journal of Energy Resources Technology* **2009,** *131* (2), 022201.

57. Abdullah, S.; Yusup, S.; Ahmad, M. M.; Ramli, A.; Ismail, L., Thermogravimetry study on pyrolysis of various lignocellulosic biomass for potential hydrogen production. *Cellulose* **2010,** *20* (30.40), 42.20.
58. Cozzani, V.; Lucchesi, A.; Stoppato, G.; Maschio, G., A new method to determine the composition of biomass by thermogravimetric analysis. *Canadian journal of chemical engineering* **1997,** *75* (1), 127-133.
59. Klass, D. L., *Biomass for renewable energy, fuels, and chemicals*. Academic press: 1998.
60. Murugan, P.; Mahinpey, N.; Johnson, K. E.; Wilson, M., Kinetics of the pyrolysis of lignin using thermogravimetric and differential scanning calorimetry methods. *Energy & Fuels* **2008,** *22* (4), 2720-2724.
61. Chen, G.; Leung, D., Experimental investigation of biomass waste,(rice straw, cotton stalk, and pine sawdust), pyrolysis characteristics. *Energy Sources* **2003,** *25* (4), 331-337.
62. Chu, S.; Subrahmanyam, A. V.; Huber, G. W., The pyrolysis chemistry of a β-O-4 type oligomeric lignin model compound. *Green chemistry* **2013,** *15* (1), 125-136.
63. Sun, R.; Tomkinson, J.; Jones, G. L., Fractional characterization of ash-AQ lignin by successive extraction with organic solvents from oil palm EFB fibre. *Polymer Degradation and Stability* **2000,** *68* (1), 111-119.
64. El-Saied, H.; Nada, A.-A. M., The thermal behaviour of lignins from wasted black pulping liquors. *Polymer Degradation and Stability* **1993,** *40* (3), 417-421.
65. Gabilondo, N. Diseño de la conducta final de matrices fenólicas de tipo resol, en función de los productos de partida y de las características reocinéticas del curado'. Ph. D. Thesis, Euskal Herriko Unibertsitatea/Universidad del País Vasco, Donostia-San Sebastián, España, 2004.
66. Ház, A.; Jablonský, M.; Orságová, A.; Šurina, I. In *Determination of temperature regions in thermal degradation of lignin*, 4 th International Conference on renewable energy source, High Tatras, Slovak Republic, 2013.
67. Moya, R.; Rodríguez-Zúñiga, A.; Puente-Urbina, A., Thermogravimetric and devolatilisation analysis for five plantation species: Effect of extractives, ash compositions, chemical compositions and energy parameters. *Thermochimica Acta* **2017,** *647*, 36-46.
68. Glasser, W., Classification of lignin according to chemical and molecular structure. *Lignin: historical, biological, and materials perspectives* **2000,** *742*, 216-238.
69. Van Krevelen, D. W.; Te Nijenhuis, K., *Properties of polymers: their correlation with chemical structure; their numerical estimation and prediction from additive group contributions*. Elsevier: 2009.
70. Vallejos, M. E.; Felissia, F. E.; Cruvelo, A. A.; Zambon, M. D.; Ramos, L.; Area, M. C., Chemical and physico-chemical characterization of lignins obtained from ethanol-water fractionation of bagasse. *BioResources* **2011,** *6* (2), 1158-1171.
71. Lisperguer, J.; Perez, P.; Urizar, S., Structure and thermal properties of lignins: characterization by infrared spectroscopy and differential scanning calorimetry. *Journal of the Chilean Chemical Society* **2009,** *54* (4), 460-463.
72. Papatheofanous, M.; Billa, E.; Koullas, D.; Monties, B.; Koukios, E., Two-stage acid-catalyzed fractionation of lignocellulosic biomass in aqueous ethanol systems at low temperatures. *Bioresource Technology* **1995,** *54* (3), 305-310.
73. Jakus, A. E.; Koube, K. D.; Geisendorfer, N. R.; Shah, R. N., Robust and elastic lunar and martian structures from 3D-printed regolith inks. *Scientific reports* **2017,** *7*, 44931.
74. Rankouhi, B.; Delfanian, F.; McTaggart, R.; Letcher, T. In *An Experimental Investigation of the Effects of Gamma Radiation on 3D Printed ABS for In-Space Manufacturing Purposes*, ASME 2016 International Mechanical Engineering Congress and Exposition, American Society of Mechanical Engineers: 2016; pp V001T03A042-V001T03A042.

75. George, J.; Kumar, R.; Sajeevkumar, V.; Sabapathy, S.; Vaijapurkar, S.; Kumar, D.; Kchawahha, A.; Bawa, A., Effect of γ-irradiation on commercial polypropylene based mono and multi-layered retortable food packaging materials. *Radiation Physics and Chemistry* **2007,** *76* (7), 1205-1212.
76. Madera-Santana, T. J.; Meléndrez, R.; González-García, G.; Quintana-Owen, P.; Pillai, S. D., Effect of gamma irradiation on physicochemical properties of commercial poly (lactic acid) clamshell for food packaging. *Radiation Physics and Chemistry* **2016,** *123*, 6-13.
77. Garrison, T.; Murawski, A.; Quirino, R., Bio-based polymers with potential for biodegradability. *Polymers* **2016,** *8* (7), 262.
78. Benyathiar, P.; Selke, S.; Auras, R., The effect of gamma and electron beam irradiation on the biodegradability of PLA films. *Journal of Polymers and the Environment* **2016,** *24* (3), 230-240.
79. Lunt, J., Large-scale production, properties and commercial applications of polylactic acid polymers. *Polymer degradation and stability* **1998,** *59* (1-3), 145-152.
80. Lin, H.-Y.; Tsai, S.-Y.; Yu, H.-T.; Lin, C.-P., Degradation of Polylactic Acid by Irradiation. *Journal of Polymers and the Environment* **2018,** *26* (1), 122-131.
81. Letcher, T.; Waytashek, M. In *Material property testing of 3D-printed specimen in PLA on an entry-level 3D printer*, ASME 2014 international mechanical engineering congress and exposition, American Society of Mechanical Engineers: 2014; pp V02AT02A014-V02AT02A014.
82. Rankouhi, B.; Javadpour, S.; Delfanian, F.; Letcher, T., Failure analysis and mechanical characterization of 3D printed ABS with respect to layer thickness and orientation. *Journal of Failure Analysis and Prevention* **2016,** *16* (3), 467-481.
83. Tymrak, B.; Kreiger, M.; Pearce, J. M., Mechanical properties of components fabricated with open-source 3-D printers under realistic environmental conditions. *Materials & Design* **2014,** *58*, 242-246.
84. Torrado, A. R.; Roberson, D. A., Failure analysis and anisotropy evaluation of 3D-printed tensile test specimens of different geometries and print raster patterns. *Journal of Failure Analysis and Prevention* **2016,** *16* (1), 154-164.
85. Sun, X.-F.; Sun, R.; Fowler, P.; Baird, M. S., Extraction and characterization of original lignin and hemicelluloses from wheat straw. *Journal of Agricultural and Food Chemistry* **2005,** *53* (4), 860-870.
86. Saha, M.; Rahman, M. S.; Hossain, M. N.; Raynie, D. E.; Halim, M. A., Molecular and Spectroscopic Insights of a Choline Chloride Based Therapeutic Deep Eutectic Solvent. *The Journal of Physical Chemistry A* **2020**.
87. Sene, C. F.; McCann, M. C.; Wilson, R. H.; Grinter, R., Fourier-transform Raman and Fourier-transform infrared spectroscopy (an investigation of five higher plant cell walls and their components). *Plant Physiology* **1994,** *106* (4), 1623-1631.
88. Boeriu, C. G.; Bravo, D.; Gosselink, R. J.; van Dam, J. E., Characterisation of structure-dependent functional properties of lignin with infrared spectroscopy. *Industrial crops and products* **2004,** *20* (2), 205-218.
89. Faix, O., Classification of lignins from different botanical origins by FT-IR spectroscopy. *Holzforschung-International Journal of the Biology, Chemistry, Physics and Technology of Wood* **1991,** *45* (s1), 21-28.
90. Zhang, W.; Ma, Y.; Wang, C.; Li, S.; Zhang, M.; Chu, F., Preparation and properties of lignin–phenol–formaldehyde resins based on different biorefinery residues of agricultural biomass. *Industrial Crops and Products* **2013,** *43*, 326-333.
91. Li, S.; Lundquist, K., Analysis of hydroxyl groups in lignins by H-1 NMR spectrometry. *Nordic Pulp & Paper Research Journal* **2001,** *16* (1), 63-67.

92. Seca, A. M.; Cavaleiro, J. A.; Domingues, F. M.; Silvestre, A. J.; Evtuguin, D.; Neto, C. P., Structural characterization of the lignin from the nodes and internodes of Arundo donax reed. *Journal of agricultural and food chemistry* **2000,** *48* (3), 817-824.
93. Xia, Z.; Akim, L. G.; Argyropoulos, D. S., Quantitative 13C NMR analysis of lignins with internal standards. *Journal of agricultural and food chemistry* **2001,** *49* (8), 3573-3578.
94. Crestini, C.; Argyropoulos, D. S., Structural analysis of wheat straw lignin by quantitative 31P and 2D NMR spectroscopy. The occurrence of ester bonds and α-O-4 substructures. *Journal of agricultural and food chemistry* **1997,** *45* (4), 1212-1219.
95. Xu, F.; Sun, J.-X.; Sun, R.; Fowler, P.; Baird, M. S., Comparative study of organosolv lignins from wheat straw. *Industrial crops and products* **2006,** *23* (2), 180-193.
96. Pandey, M. P.; Kim, C. S., Lignin depolymerization and conversion: a review of thermochemical methods. *Chemical Engineering & Technology* **2011,** *34* (1), 29-41.
97. Li, S.; Lundquist, K., A new method for the analysis of phenolic groups in lignins by 1H NMR spectroscopy. *Nordic Pulp & Paper Research Journal* **1994,** *9* (3), 191-195.
98. Agrimi, G.; Alexopoulou, E.; Bartzoka, E. D.; Buonerba, A.; Cavani, F.; Christou, M.; Colucci, A.; Couturier, J.-L.; Crestini, C.; Dubois, J.-L., *Biorefineries: an introduction*. Walter de Gruyter GmbH & Co KG: 2015.
99. Richel, A.; Vanderghem, C.; Simon, M.; Wathelet, B.; Paquot, M., Evaluation of matrix-assisted laser desorption/ionization mass spectrometry for second-generation lignin analysis. *Analytical chemistry insights* **2012,** *7*, ACI. S10799.
100. El Mansouri, N.-E.; Salvadó, J., Analytical methods for determining functional groups in various technical lignins. *Industrial Crops and Products* **2007,** *26* (2), 116-124.
101. Sulaeva, I.; Sumerskii, I.; Bacher, M.; Zinovyev, G.; Henniges, U.; Rosenau, T.; Potthast, A. In *Comparing Different Approaches to Measure Molar Mass of Lignin: SEC, DOSY and AsFlFFF*, ABSTRACTS OF PAPERS OF THE AMERICAN CHEMICAL SOCIETY, AMER CHEMICAL SOC 1155 16TH ST, NW, WASHINGTON, DC 20036 USA: 2015.
102. Ringena, O.; Lebioda, S.; Lehnen, R.; Saake, B., Size-exclusion chromatography of technical lignins in dimethyl sulfoxide/water and dimethylacetamide. *Journal of Chromatography A* **2006,** *1102* (1-2), 154-163.
103. Fredheim, G. E.; Braaten, S. M.; Christensen, B. E., Molecular weight determination of lignosulfonates by size-exclusion chromatography and multi-angle laser light scattering. *Journal of Chromatography A* **2002,** *942* (1-2), 191-199.
104. Cathala, B.; Saake, B.; Faix, O.; Monties, B., Association behaviour of lignins and lignin model compounds studied by multidetector size-exclusion chromatography. *Journal of Chromatography A* **2003,** *1020* (2), 229-239.
105. Kennedy, J. A.; Taylor, A. W., Analysis of proanthocyanidins by high-performance gel permeation chromatography. *Journal of Chromatography A* **2003,** *995* (1-2), 99-107.
106. Tolbert, A.; Akinosho, H.; Khunsupat, R.; Naskar, A. K.; Ragauskas, A. J., Characterization and analysis of the molecular weight of lignin for biorefining studies. *Biofuels, Bioproducts and Biorefining* **2014,** *8* (6), 836-856.
107. Sequeiros, A.; Serrano, L.; Briones, R.; Labidi, J., Lignin liquefaction under microwave heating. *Journal of Applied Polymer Science* **2013,** *130* (5), 3292-3298.
108. Nguyen, J. D.; Matsuura, B. S.; Stephenson, C. R., A photochemical strategy for lignin degradation at room temperature. *Journal of the American Chemical Society* **2014,** *136* (4), 1218-1221.
109. Sedai, B.; Diaz-Urrutia, C.; Baker, R. T.; Wu, R.; Silks, L. P.; Hanson, S. K., Comparison of copper and vanadium homogeneous catalysts for aerobic oxidation of lignin models. *ACS Catalysis* **2011,** *1* (7), 794-804.

110. Son, S.; Toste, F. D., Non-Oxidative Vanadium-Catalyzed C□ O Bond Cleavage: Application to Degradation of Lignin Model Compounds. *Angewandte Chemie International Edition* **2010,** *49* (22), 3791-3794.
111. Harms, R. G.; Markovits, I. I.; Drees, M.; Herrmann, h. m. W. A.; Cokoja, M.; Kuehn, F. E., Cleavage of C□ O Bonds in Lignin Model Compounds Catalyzed by Methyldioxorhenium in Homogeneous Phase. *ChemSusChem* **2014,** *7* (2), 429-434.
112. Zakzeski, J.; Bruijnincx, P. C.; Jongerius, A. L.; Weckhuysen, B. M., The catalytic valorization of lignin for the production of renewable chemicals. *Chemical reviews* **2010,** *110* (6), 3552-3599.
113. Azadi, P.; Inderwildi, O. R.; Farnood, R.; King, D. A., Liquid fuels, hydrogen and chemicals from lignin: A critical review. *Renewable and Sustainable Energy Reviews* **2013,** *21*, 506-523.
114. Erdocia, X.; Prado, R.; Corcuera, M. A.; Labidi, J., Effect of different organosolv treatments on the structure and properties of olive tree pruning lignin. *Journal of Industrial and Engineering Chemistry* **2014,** *20* (3), 1103-1108.
115. Bauer, S.; Sorek, H.; Mitchell, V. D.; Ibáñez, A. B.; Wemmer, D. E., Characterization of Miscanthus giganteus lignin isolated by ethanol organosolv process under reflux condition. *Journal of agricultural and food chemistry* **2012,** *60* (33), 8203-8212.
116. Hauteville, M.; Lundquist, K.; von Unge, S., NMR studies of lignins. 7. 1H NMR spectroscopic investigation of the distribution of erythro and threo forms of beta-O-4 structures in lignins. *Acta Chemica Scandinavica* **1986**, 31-35.
117. Sturgeon, M. R.; Kim, S.; Lawrence, K.; Paton, R. S.; Chmely, S. C.; Nimlos, M.; Foust, T. D.; Beckham, G. T., A mechanistic investigation of acid-catalyzed cleavage of aryl-ether linkages: implications for lignin depolymerization in acidic environments. *ACS Sustainable Chemistry & Engineering* **2014,** *2* (3), 472-485.
118. Nagel, E.; Zhang, C., Hydrothermal Decomposition of a Lignin Dimer under Neutral and Basic Conditions: A Mechanism Study. *Industrial & Engineering Chemistry Research* **2019,** *58* (40), 18866-18880.
119. Ibbett, R.; Gaddipati, S.; Davies, S.; Hill, S.; Tucker, G., The mechanisms of hydrothermal deconstruction of lignocellulose: new insights from thermal–analytical and complementary studies. *Bioresource technology* **2011,** *102* (19), 9272-9278.
120. Zakzeski, J.; Weckhuysen, B. M., Lignin solubilization and aqueous phase reforming for the production of aromatic chemicals and hydrogen. *ChemSusChem* **2011,** *4* (3), 369-378.
121. Kobayashi, T.; Kohn, B.; Holmes, L.; Faulkner, R.; Davis, M.; Maciel, G. E., Molecular-level consequences of biomass pretreatment by dilute sulfuric acid at various temperatures. *Energy & Fuels* **2011,** *25* (4), 1790-1797.
122. Toledano, A.; Serrano, L.; Labidi, J., Improving base catalyzed lignin depolymerization by avoiding lignin repolymerization. *Fuel* **2014,** *116*, 617-624.
123. Krutov, S. M.; Evtuguin, D. V.; Ipatova, E. V.; Santos, S. A.; Sazanov, Y. N., Modification of acid hydrolysis lignin for value-added applications by micronization followed by hydrothermal alkaline treatment. *Holzforschung* **2015,** *69* (6), 761-768.
124. Yuan, Z.; Cheng, S.; Leitch, M.; Xu, C. C., Hydrolytic degradation of alkaline lignin in hot-compressed water and ethanol. *Bioresource technology* **2010,** *101* (23), 9308-9313.
125. Karagöz, S.; Bhaskar, T.; Muto, A.; Sakata, Y.; Uddin, M. A., Low-temperature hydrothermal treatment of biomass: effect of reaction parameters on products and boiling point distributions. *Energy & fuels* **2004,** *18* (1), 234-241.
126. Xu, C.; Lad, N., Production of heavy oils with high caloric values by direct liquefaction of woody biomass in sub/near-critical water. *Energy & Fuels* **2008,** *22* (1), 635-642.

127. Roberts, V. M.; Stein, V.; Reiner, T.; Lemonidou, A.; Li, X.; Lercher, J. A., Towards quantitative catalytic lignin depolymerization. *Chemistry–A European Journal* **2011,** *17* (21), 5939-5948.
128. Knill, C. J.; Kennedy, J. F., Degradation of cellulose under alkaline conditions. *Carbohydrate Polymers* **2003,** *51* (3), 281-300.
129. Wu, G.; Heitz, M., Catalytic mechanism of Cu2+ and Fe3+ in alkaline O2 oxidation of lignin. *Journal of wood chemistry and technology* **1995,** *15* (2), 189-202.
130. Scheibe, G.; Schöntag, A.; Katheder, F., Fluoreszenz und Energiefortleitung bei reversibel polymerisierten Farbstoffen. *Naturwissenschaften* **1939,** *27* (29), 499-501.
131. Villar, J.; Caperos, A.; Garcia-Ochoa, F., Oxidation of hardwood kraft-lignin to phenolic derivatives with oxygen as oxidant. *Wood Science and Technology* **2001,** *35* (3), 245-255.
132. Rodrigues Pinto, P. C.; Borges da Silva, E. A.; Rodrigues, A. r. E. d., Insights into oxidative conversion of lignin to high-added-value phenolic aldehydes. *Industrial & Engineering Chemistry Research* **2010,** *50* (2), 741-748.
133. Pearl, I. A., Vanillin from lignin materials. *Journal of the American Chemical Society* **1942,** *64* (6), 1429-1431.
134. Chio, C.; Sain, M.; Qin, W., Lignin utilization: a review of lignin depolymerization from various aspects. *Renewable and Sustainable Energy Reviews* **2019,** *107*, 232-249.
135. Villar, J.; Caperos, A.; Garcia-Ochoa, F., Oxidation of hardwood kraft-lignin to phenolic derivatives. Nitrobenzene and copper oxide as oxidants. *Journal of wood chemistry and technology* **1997,** *17* (3), 259-285.
136. Pearl, I. A.; Beyer, D. L., Studies on lignin and related products. *Tappi* **1950,** *33*, 544-548.
137. Rudie, A. W.; Hart, P. W., Catalysis: A Potential Alternative to Kraft Pulping. *TAPPI JOURNAL* **2014,** *13* (10), 13-20.
138. Prieur, B.; Meub, M.; Wittemann, M.; Klein, R.; Bellayer, S.; Fontaine, G.; Bourbigot, S., Phosphorylation of lignin: characterization and investigation of the thermal decomposition. *RSC Advances* **2017,** *7* (27), 16866-16877.
139. Lee, S. H.; Doherty, T. V.; Linhardt, R. J.; Dordick, J. S., Ionic liquid-mediated selective extraction of lignin from wood leading to enhanced enzymatic cellulose hydrolysis. *Biotechnology and bioengineering* **2009,** *102* (5), 1368-1376.
140. Brosse, N.; Mohamad Ibrahim, M. N.; Abdul Rahim, A., Biomass to bioethanol: Initiatives of the future for lignin. *ISRN Materials Science* **2011,** *2011*.
141. Sluiter, A.; Hames, B.; Ruiz, R.; Scarlata, C.; Sluiter, J.; Templeton, D.; Crocker, D., Determination of structural carbohydrates and lignin in biomass. *Laboratory analytical procedure* **2008,** *1617*, 1-16.
142. Toledano, E. R., *The ottoman slave trade and its suppression: 1840-1890*. Princeton University Press: 2014.
143. Nuruddin, M.; Chowdhury, A.; Haque, S.; Rahman, M.; Farhad, S.; Jahan, M. S.; Quaiyyum, A., Extraction and characterization of cellulose microfibrils from agricultural wastes in an integrated biorefinery initiative. *biomaterials* **2011,** *3*, 5-6.
144. Watkins, D.; Nuruddin, M.; Hosur, M.; Tcherbi-Narteh, A.; Jeelani, S., Extraction and characterization of lignin from different biomass resources. *Journal of Materials Research and Technology* **2015,** *4* (1), 26-32.
145. Liu, Y.; Luo, P.; Xu, Q.-Q.; Wang, E.-J.; Yin, J.-Z., Investigation of the effect of supercritical carbon dioxide pretreatment on reducing sugar yield of lignocellulose hydrolysis. *Cellulose Chemistry and Technology* **2014,** *48*, 89-95.

146. Silveira, M. H. L.; Vanelli, B. A.; Corazza, M. L.; Ramos, L. P., Supercritical carbon dioxide combined with 1-butyl-3-methylimidazolium acetate and ethanol for the pretreatment and enzymatic hydrolysis of sugarcane bagasse. *Bioresource Technology* **2015,** *192*, 389-396.